

Control of an offshore Bipole with AC interlink un- der dedicated metallic re- turn fault to improve avail- ability

Smit Shukla

Technische Universiteit Delft



Control of an offshore Bipole with AC interlink under dedicated metallic return fault to improve availability

by

Smit Shukla

in partial fulfilment of the requirements for the degree of

Master of Science

in Electrical Engineering - Electrical Power Engineering

at the Delft University of Technology,

to be defended publicly on July 29, 2020 at 15:00

Student Number: 4921550

Project Duration: November 18, 2019 to July 29, 2020

Supervisor:	Prof. ir. P. (Peter) Vaessen	TU Delft
	Dr. T. Batista Soeiro	TU Delft
	Dr. Cornelis Plet	DNV GL

Thesis Committee:	Prof. ir. P. (Peter) Vaessen	DCES, TU Delft
	Dr. T. Batista Soeiro	DCES, TU Delft
	Dr. ir. J.L. (Jose) Rueda Torres	IEPG, TU Delft

An electronic version of this dissertation is available at <http://repository.tudelft.nl/>.

Abstract

Total wind energy generation all over the world has grown exponentially in the last few decades. In modern days, a significant share of the wind power plants is offshore in Northern Europe, which are usually connected via Symmetrical Monopole. However, future connections are likely to be Bipole with metallic return based HVDC-link due to the benefits in redundancy and availability. The availability of a similar Bipole point-to-point link can be further improved by coupling the two offshore aggregated wind power plants with a common AC interlink. Thus, enabling equal loading of the two offshore poles in case the dedicated metallic return cable undergoes a fault. The AC-interlink based power balance control technique can also be utilized in case of a Multi-terminal Bipole connection when the high voltage cable undergoes a fault.

This thesis researches about the benefits of an offshore AC-interlink, in a Bipolar HVDC point-to-point link. Two power control strategies, Power set point control and Droop control, are designed to be tested under various possible dynamic scenarios. The primary aspect of this research is focused on the capability of offshore converters to maintain equal power loading and stable operation with the help of the AC-interlink, under the two control strategies. Tested scenarios include black-start, real-life wind fluctuations, sudden loss in power, controlled shut-down and faults in the AC submarine cable.

The simulation model of the point-to-point HVDC-link is designed as a Rigid Bipole, grounded onshore side and an AC-interlink between offshore poles. The simulations are performed in the PSCAD 4.6.3 software. These simulation models are designed to observe large AC/DC transients and the dynamics of the control schemes. Converters are modelled as Type 4 level according to the Cigre *TB604* standard. The dynamics of the wind power plant are not included, and they are modelled as ideal current sources. The offshore AC voltage and frequency are controlled entirely by the offshore grid-forming converters.

The simulation results indicate that the converters can handle the power variations and usual operation scenarios of the offshore wind power plants such as black start and controlled shut down. The possible amplitude levels and time period of the perturbations in the controlled parameters are recorded for both of the control strategies. Based on the bandwidth tuning and level of power variations, converters can keep the current and voltage deviations within the acceptable limits of the equipment. Operation of the Bipole HVDC link with the AC-interlink along with the designed control strategies is beneficial, and it will increase the Levelized cost of operation.

Contents

Abstract	i
List of Figures	v
List of Tables	1
1 Introduction	3
2 Background Research	9
2.1 Literature Review	9
2.2 MMC-VSC Technology	9
2.3 HVDC Topology	10
2.4 Bipole	10
2.5 Rigid Bipole	11
2.6 Converter control modes	14
2.6.1 Grid Forming converters	14
2.6.2 Grid Feeding/Following converters	15
2.7 Secondary Control methods	15
2.8 VSC Converter Tuning	16
2.9 Converter Modelling methods	17
3 Modelling of control strategies and HVDC point to point link	19
3.1 Power balance control strategies under DMR fault	19
3.1.1 Power set points control	20
3.1.2 Droop characteristic control	20
3.2 HVDC link modelling	22
3.2.1 Cables	22
3.2.2 Converter	24
3.2.3 AC side equipment	26
3.2.4 On-shore Strong Grid	27
3.3 Offshore Wind Power Plant modelling	29
3.3.1 Aggregated synchronized power controlled current source	29
3.3.2 OWPP structure and Reactive Power	30
4 Analysis of point to point link	33
4.1 Energization of array cables	33
4.1.1 Power set points control	34
4.1.2 Droop control	35
4.2 Wind generation fluctuations	37
4.2.1 Power set points control	38
4.2.2 Droop control	39

4.3	Controlled ramp down of wind turbine and string of the OWPP	40
4.3.1	Power set points control	40
4.3.2	Droop control.	42
4.4	Loss of wind turbine and string of the OWPP	43
4.4.1	Power set points control	43
4.4.2	Droop control.	45
4.5	Fault in the cable connecting wind farm and converter.	46
4.5.1	Power set points control	47
4.5.2	Droop control.	48
5	Results and discussion	49
5.1	Steady-state performance	49
5.2	Dynamic state performance.	50
5.3	Maximum mismatch and Fault	51
5.4	Power set point control vs Droop control strategy.	52
6	Conclusion	53
6.1	Scope of future work	54
7	Appendix	55
7.1	Appendix A	55
7.1.1	HVDC point to point link ratings	55
7.1.2	PSCAD model HVDC point to point link	56
7.2	Appendix B	57
7.2.1	Results: Energization of array cables	57
7.2.2	Results: wind fluctuations	59
7.2.3	Results: Controlled ramp down of wind turbines	63
7.2.4	Results: Loss of wind turbines	67
7.2.5	Results: Fault in the cable connecting wind farm and converter	71
	Bibliography	77

List of Figures

1.1	Schematic of offshore wind power plant Bipole with DMR export link	4
1.3	Multiterminal connection between Norflok (UK) and IJmuiden Ver (NL) OWPPs. . .	4
1.2	Schematic of point-to-point HVDC network and its operation under DMR fault with and without the AC interlink	5
1.4	Schematic of multi-terminal HVDC network and its operation under HV cable fault with and without the AC interlink	6
2.1	Various possible Bipole configurations and their implications	12
2.2	General configurations of connection between Rigid Bipole and different AC components	13
2.3	General Pac/Vdc and Qac/Vac control scheme diagram	14
2.4	Island mode control scheme with Pac and Qac Droop characteristics	15
2.5	Virtual Impedance based current limitation added to the Island mode control scheme	15
2.6	Various control methods employed in an AC side connection between converters . .	16
3.1	MMC based HVDC Rigid Bipole model	19
3.2	HVDC system operation under DMR fault with Power set-point control	20
3.3	Power reference control strategy for active and reactive power set-points in PSCAD .	20
3.4	HVDC system operation under DMR fault with droop characteristic control	21
3.5	P/f droop control strategy implementation in PSCAD	21
3.6	Cigre PSCAD four-terminal reference model	22
3.7	PSCAD Tennet Promotion model library cable dimensions and properties.	23
3.8	Simplified half-bridge MMC sub-module	24
3.9	MMC single-phase leg operation	25
3.10	Onshore AC side connection and equipment	26
3.11	Onshore AC side breaker and pre-insertion Resistance	27
3.12	On-shore grid connection from Tennet Promotion PSCAD model power source library.	28
3.13	Voltage-controlled 3 phase current source modelled in PSCAD	29
3.14	PLL block and synchronized voltage reference generation.	30
3.15	OWPPs architecture: Radial connection of wind turbines to the 66 kV substation . .	31
4.1	Step-energization (reactive power loading) of top and bottom OWPP	34
4.2	Active power losses of the equipment and DC voltages of offshore poles under power set points control while cable energization	35
4.3	Active power losses of both equipment and DC voltages of offshore poles under droop control while cable energization	36
4.4	OWPP power generation references with wind fluctuations	37
4.5	Active power loading of both OWPP and converters under power set points control with wind fluctuations	38
4.6	Active power loading of both OWPP and converters under droop control with wind fluctuations	39
4.7	Slow ramp down of turbines and active power loading of top and bottom OWPP . . .	40
4.8	Active power loading of both OWPP and converters under power set points control with controlled ramp down of wind turbines	41

4.9	Active power loading of both OWPP and converters under droop control with controlled ramp down of wind turbines	42
4.10	Active power loading of top and bottom OWPP under loss of wind turbines	43
4.11	Active power loading of both OWPPs and converters with power set points control under loss of wind turbines	44
4.12	Active power loading of both OWPPs and converters with droop control under loss of wind turbines	45
4.13	Active power loading of top and bottom OWPP under fault in the cable connecting top OWPP and converter	46
4.14	Three phase AC voltage and current of offshore Terminal 1 (top) with power set point control under fault in the cable connecting top OWPP and converter	47
4.15	Three phase AC voltage and current of offshore Terminal 1 (top) with droop control under fault in the cable connecting top OWPP and converter	48
7.1	Designed PSCAD simulation model of the HVDC point to point link	56
7.2	HVDC-link characteristics under energization of array cables with power set points control	57
7.3	HVDC-link characteristics under energization of array cables with droop control	58
7.4	HVDC-link characteristics under wind fluctuations with power set points control	59
7.4	HVDC-link characteristics under wind fluctuations with power set points control	60
7.5	HVDC-link characteristics under wind fluctuations with droop control	61
7.5	HVDC-link characteristics under wind fluctuations with droop control	62
7.6	HVDC-link characteristics under controlled ramp down of wind turbines with power set points control	63
7.6	HVDC-link characteristics under controlled ramp down of wind turbines with power set points control	64
7.7	HVDC-link characteristics under controlled ramp down of wind turbines with droop control	65
7.7	HVDC-link characteristics under controlled ramp down of wind turbines with droop control	66
7.8	HVDC-link characteristics under loss of wind turbines with power set points control	67
7.8	HVDC-link characteristics under loss of wind turbines with power set points control	68
7.9	HVDC-link characteristics under loss of wind turbines with droop control	69
7.9	HVDC-link characteristics under loss of wind turbines with droop control	70
7.10	HVDC-link characteristics under fault in the cable connecting top OWPP and converter with power set points control	71
7.10	HVDC-link characteristics under fault in the cable connecting top OWPP and converter with power set points control	72
7.10	HVDC-link characteristics under fault in the cable connecting top OWPP and converter with power set points control	73
7.11	HVDC-link characteristics under fault in the cable connecting top OWPP and converter with droop control	74
7.11	HVDC-link characteristics under fault in the cable connecting top OWPP and converter with droop control	75
7.11	HVDC-link characteristics under fault in the cable connecting top OWPP and converter with droop control	76

List of Tables

- 2.1 Summary of the tuning criteria employed to calculate PI gains of different controllers. 17
- 2.2 Summary of different model types of VSC 18
- 4.1 Sequence of operations for controlled ramp-down of OWPP wind turbine and string. 40
- 4.2 Sequence of operations to simulate loss of wind turbines 43
- 4.3 Sequence of operations to simulate fault in the cable connecting top OWPP and converter 46
- 5.1 Summary of performance of the control strategies under steady-state operation. . . 50
- 5.2 Summary of performance of the control strategies under dynamic operation. . . . 50
- 7.1 Ratings of the equipment used in the HVDC link modelling 55

1

Introduction

The modern power system supports a high degree of penetration of Renewable Energy Sources (RES). Wind power generation is one of the clean and readily available RES. Globally the wind power generation capacity has grown exponentially from 24 GW in 2001 to 792 GW in 2020. Certain European countries have a relatively high degree of penetration of wind power plants to fulfill their energy demands as given in [1].

Offshore wind power plants (OWPPs) are one of the primary RES in Northern Europe but often require a High Voltage DC (HVDC) connection to transfer the produced energy to the onshore power systems efficiently over long distances. Such an HVDC connection requires a point-to-point link between offshore and onshore HVDC converters.

Depending on the required redundancy, power ratings and onshore grid constraints, HVDC converters can be connected in Monopole or Bipole configurations. Most of the modern HVDC connections will have Bipole with dedicated metallic return (DMR) configuration due to the improved availability and hence increased Levelized cost of operation.

Usually, the two aggregated OWPPs are connected to an offshore pole separately via an AC bus and submarine cables. Under normal operating conditions, each of the wind turbine converters follows the grid-forming offshore converter and injects the produced power into the AC bus. Both offshore converters of the Bipole work under grid-forming mode to provide the AC voltage magnitude, frequency and theta angle reference for the OWPPs.

Due to the natural variations in the offshore wind speeds, the variations in power generated by the two OWPPs are inevitable. This also results in an unbalance between the power loading of the two poles. Under normal conditions, the unbalance in active power (DC current) between the two poles is transferred via the DMR, as shown in Figure 1.1.

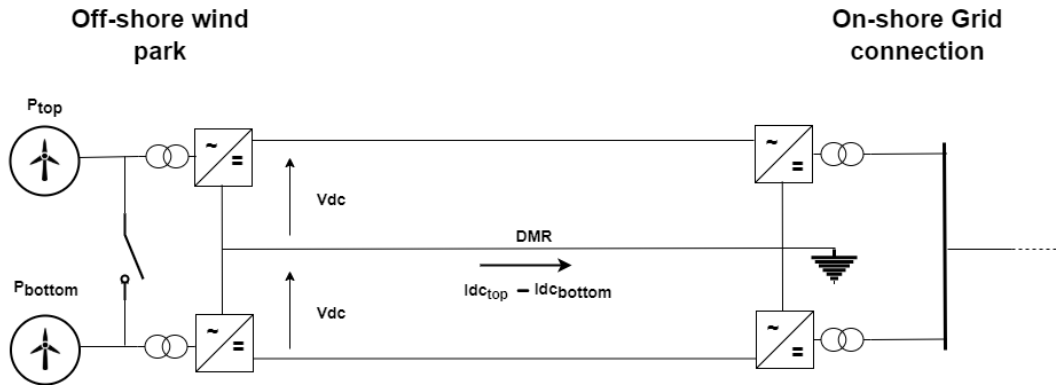


Figure 1.1: Schematic of offshore wind power plant Bipole with DMR export link

For the HVDC network, as shown in Figure 1.1, it is desirable that the OWPP can continue production in case of a DMR fault.

Under DMR fault operation, the unbalance current path is interrupted, and the HV pole currents must be equal and opposite, so slight unbalance between the OWPPs will result in unequal DC voltage of the two poles as shown in Figure 1.2a. Unbalance in the top and bottom pole DC voltages is not desired for the stable operation of the overall HVDC system components. If these voltage variations are higher or lower than the over-voltage and under-voltage limits of the HVDC system components, the cables and converters may undergo faults.

One possible way to handle differences in the generation between the OWPPs, yet ensure equal loading of the converter poles, is by distributing the combined OWPPs power equally through an AC connection (interlink) between the poles as shown in Figure 1.2b.

A similar control scheme can also be extended under the case of HV cable fault in a multiterminal connection between multiple OWPPs, as given in Figure 1.3. This figure shows an 1800 MW multiterminal connection between two OWPPs in the North Sea connecting, UK to the Netherlands.

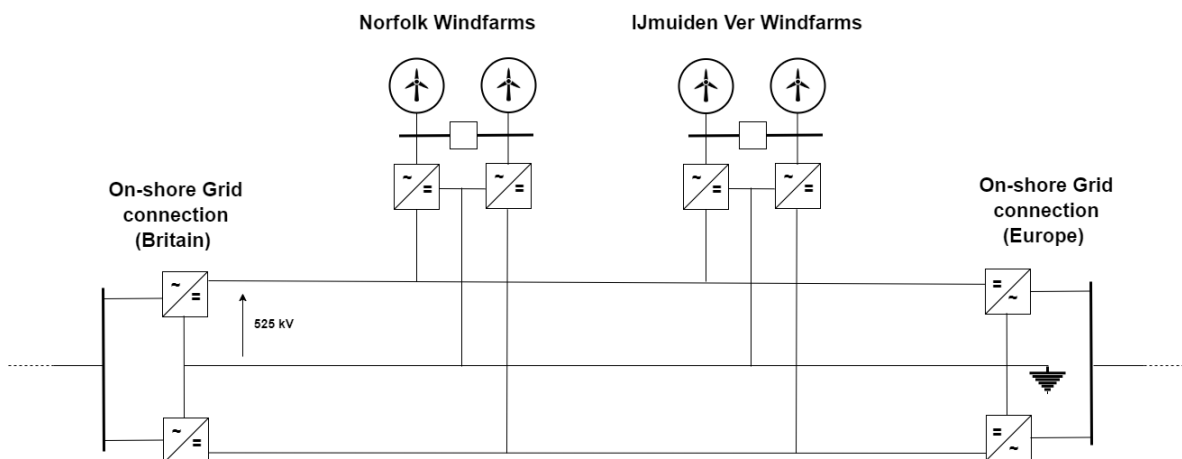


Figure 1.3: Multiterminal connection between Norfolk (UK) and IJmuiden Ver (NL) OWPPs.

In the case where an HV cable of a Bipole with DMR goes through a fault, the other HV cable and

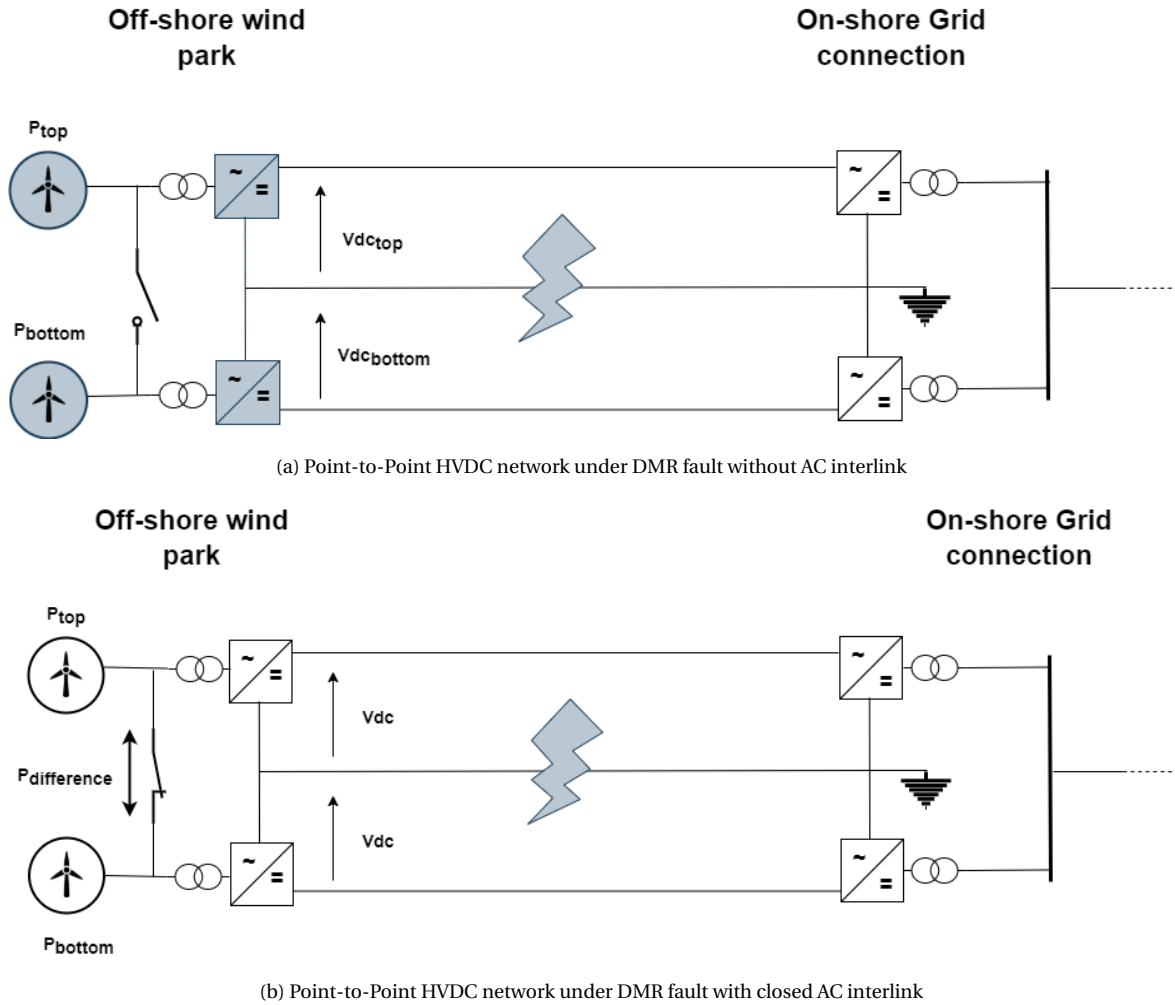


Figure 1.2: Schematic of point-to-point HVDC network and its operation under DMR fault with and without the AC interlink

DMR can be utilized as an asymmetric Monopole connection, as shown in Figure 1.4b. However, the DMR current rating must remain the same as the HV cable current rating. The pole connected to the faulted cable can still export power via the multi-terminal connection to the Netherlands. However, the amount of power is limited due to the priority access to the onshore converter capacity in the Netherlands by the IJmuiden Ver windfarms. In this situation, the AC interlink can transfer power from one OWPP bus connected to the faulted HV pole to the other pole.

This technique increases the availability of power as both of the OWPPs can be producing power up to the converter rating. Otherwise, one of the OWPP, i.e. connected to the faulted cable connected pole, has to be shut down or curtail its power export, as shown in Figure 1.4a.

This thesis focuses on the benefit of being able to operate the offshore converter station with the AC interlink closed, connecting both OWPP to one AC Point of Common Coupling (PCC).

In the case of a point-to-point HVDC connection, this functionality can improve availability dur-

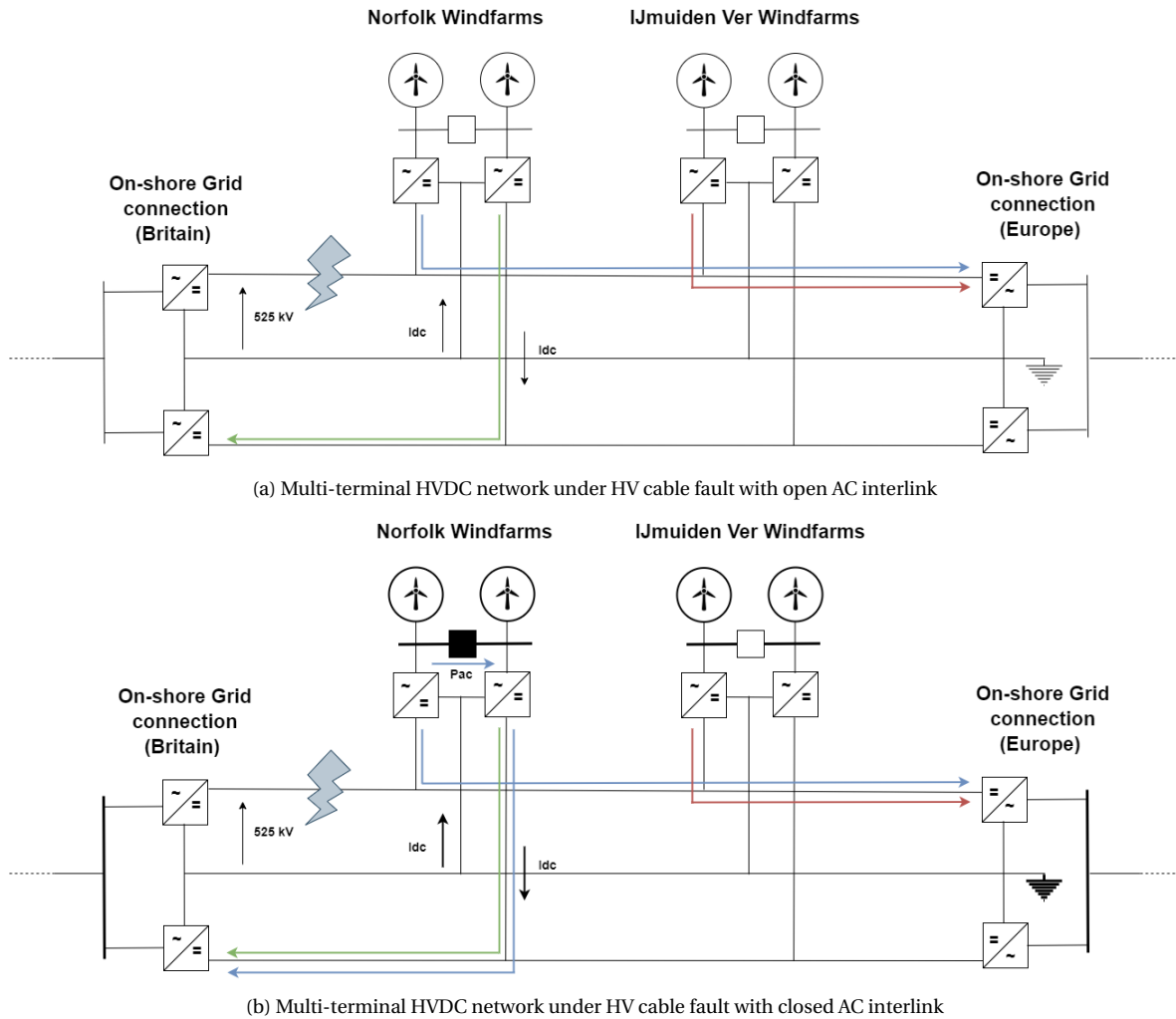


Figure 1.4: Schematic of multi-terminal HVDC network and its operation under HV cable fault with and without the AC interlink

ing a DMR fault. While in the case where offshore wind power plant is connected to an HVDC link or multi-terminal network, the functionality can improve availability in case of an HV pole fault. Overall, an inter-connected PCC can serve as a power exchange point to balance or to transfer power between the top and bottom offshore poles.

In this thesis, an OWPP with two aggregated generating OWPPs (each of 900 MW) is considered, which is connected to the onshore grid through a point-to-point Bipole link. Each OWPP is separately connected to one pole of the Bipole connection with an array voltage of 66 kV . Complex control strategies are required for the poles attached to the OWPPs and AC interlink to function under DMR fault. By designing a PSCAD simulation model that includes the whole system under consideration, the performance of the HVDC connection with the designed control strategies can be tested. After developing the model, it is to be tested under different scenarios such as steady-state operation, faults and dynamic changes in the generation. Finally, through the above analysis, the impact of such a control strategy on the equipment rating can be assessed.

The remainder of this thesis has the following structure. Chapter 2 presents the previous research work, HVDC system background and brief description of the guidelines considered to develop the simulation model for this thesis.

Chapter 3 give details about the control scheme and PSCAD modelling of the point-to-point HVDC network as shown in Figure 1.2b.

Chapter 4 presents the various possible scenarios and records the performance of the control strategies under each scenario. The impact of the control strategies over the HVDC-link and its equipment is recorded based upon the simulation results. After analysis of the system under different scenarios, the results and discussion are presented in Chapter 5.

2

Background Research

2.1. Literature Review

Multiple offshore HVDC connections are under planning and development to transfer power over long distances with a Bipole configuration due to its multiple benefits [2]. But, under DMR fault the Bipole (Rigid Bipole) will suffer from divergence in the converter sub modules energy and voltage under unbalance of power between the top and bottom poles.

The unbalance will lead to either an increase or decrease from the normal operating voltage. An increase will lead to additional stress on equipment and premature ageing. Costly additional insulation strength would be required to enable this. While, a decrease will lead to a loss of controllability; lower DC voltage will reduce the Q control capability on the AC side. Moreover, if the DC voltage is less than the AC voltage, the converter valve will become an uncontrolled diode rectifier.

Rigid Bipole configuration based HVDC links are scarce. Nordlink [3] is planned to connect Norway and Germany grids via a point-to-point Rigid Bipolar link. Such a connection is only possible between two onshore grids where the power-flow on each pole can be easily balanced as they are both connected to the same strong AC grid, without an AC side inter-connection at the PCC.

Article [4] presents a control strategy for Rigid Bipole by regulating power input at the point of common coupling (PCC) of the two AC side connections of the converters via real-time communication strategies in a point-to-point HVDC link between two onshore grids. However, in the case of OWPPs, control of power transfer is not possible at the PCC as the two OWPPs are isolated from each other. Hence an AC side interlink is added between the two converters which will serve to balance power, which can be controlled via the converters.

2.2. MMC-VSC Technology

In order to develop efficient and robust HVDC connections, Modular Multi-level Converter-Voltage Source Converter (MMC-VSC) technology has been developed, which has higher controllability than existing Line-Commutated Converter (LCC) based stations [5]. The ability to create an AC voltage offshore, i.e. grid-forming functionality, means that VSCs are the technology of choice to connect the OWPP. Half Bridge VSCs are able to operate under the opposite current direction and hence facilitate power exchangeability between two point-to-point connections. Thus, offshore converters can inject initial power to energize the HVDC cable and converter capacitors.

MMC-VSC technology enables independent control of active and reactive power at the PCC. Switching frequency losses of power electronics switches are also reduced by using insertion and bypass-based switching of the sub-modules in MMC.

2.3. HVDC Topology

Different converter configurations exist for HVDC connections between an offshore wind park and the onshore electric grid [6, 7].

- **Asymmetrical monopole with ground return:** One terminal of the converter is attached to the HV cable while the other is grounded, and hence this configuration is characterized by the continuous ground current.
- **Asymmetrical monopole with metallic return:** Both positive and neutral terminal of the converter are connected through a metallic cable of the same current rating. The return cable requires lower voltage rating compared to the HV cable. A ground connection is added at the offshore site (generally) to the return cable only.
- **Symmetrical Monopole:** This topology has two similar positive and negative HV cables. However, the DC side of the converters is grounded at the midpoint. Different methods of creating such a midpoint exist such as capacitive divider, earthing transformer or converter transformer midpoint
- **Bipole:** A pair of HV cables are used to connect a cascaded connection between two converters.
- **Multiterminal:** It is used to connect converters at different locations to the same set of terminals via cables.

The Bipole with DMR can continue to transfer half of the power as per the rated capacity via one pole when the other pole or HV cable is not operating due to maintenance or fault [8]. This can be done by using bypass switches across the pole under fault condition. Thus, Bipole has 50% redundancy which is a significant advantage over the Monopole connection which has no redundancy. The Bipole HVDC connection also has lower stress over the AC equipment as the power to be transferred is shared among the two poles compared to one pole as in the case of a Monopole connection.

In addition to the above-mentioned characteristics of symmetric and asymmetric HVDC connections, the symmetric poles have two HV cables working at opposite voltage polarity. Therefore, there is no DC stress on the converter transformer. On the other hand, as the asymmetric poles are connected to a HV and a MV cable there is a DC stress on the converter transformer, equal to half of the DC voltage.

2.4. Bipole

All OWPP HVDC connections to date have been implemented as symmetrical monopoles, but future projects, such as IJmuiden Ver, will have a Bipole configuration.

However, Bipole connections have a more complex control mechanism and higher construction cost.

Based upon the return connection, Bipole can be characterized into three categories:

- **Rigid Bipole:** A Bipole with no return path, such a connection requires power balance between both the poles, otherwise the DC voltage of the poles will get unbalanced. Rigid Bipole is usually operated between grid to grid HVDC connections. The neutral bus between the DC side of the two converters of one terminal is floating [4].
- **Bipole with ground return:** In case of power unbalance between the poles the ground current is present. Due to environmental damage caused by the ground current and set regulations by the governments, this method must be avoided. Additionally, to create a ground offshore, an electrode is required, which will undergo corrosion as it functions. A separate electrode will require regular maintenance and will also be expensive.
- **Bipole with DMR:** Due to the presence of DMR the poles can operate under unbalanced loading conditions. Such a connection can be utilized to connect an OWPPs as the pole loading is not controllable.

Figure 2.1 shows multiple Bipole point-to-point and multiterminal configurations being used and the major implications of each of them [6, 9].

2.5. Rigid Bipole

Rigid Bipole configuration, as shown in Figure 2.1, has no return path and works with only two HV cables, positive and negative. This project focuses on Bipole with DMR, but where the DMR experiences a fault. Hence the Bipole has to function as Rigid Bipole while being connected to the OWPPs. As mentioned in Figure 2.1, Rigid Bipole poles cannot function in case of a slight power imbalance without varying the DC side pole voltages. Figure 2.2 shows various configurations of connections between different AC grids (grid supporting or grid following) and the Rigid Bipole HVDC poles and it summarizes the basic operating principles for the link to work.

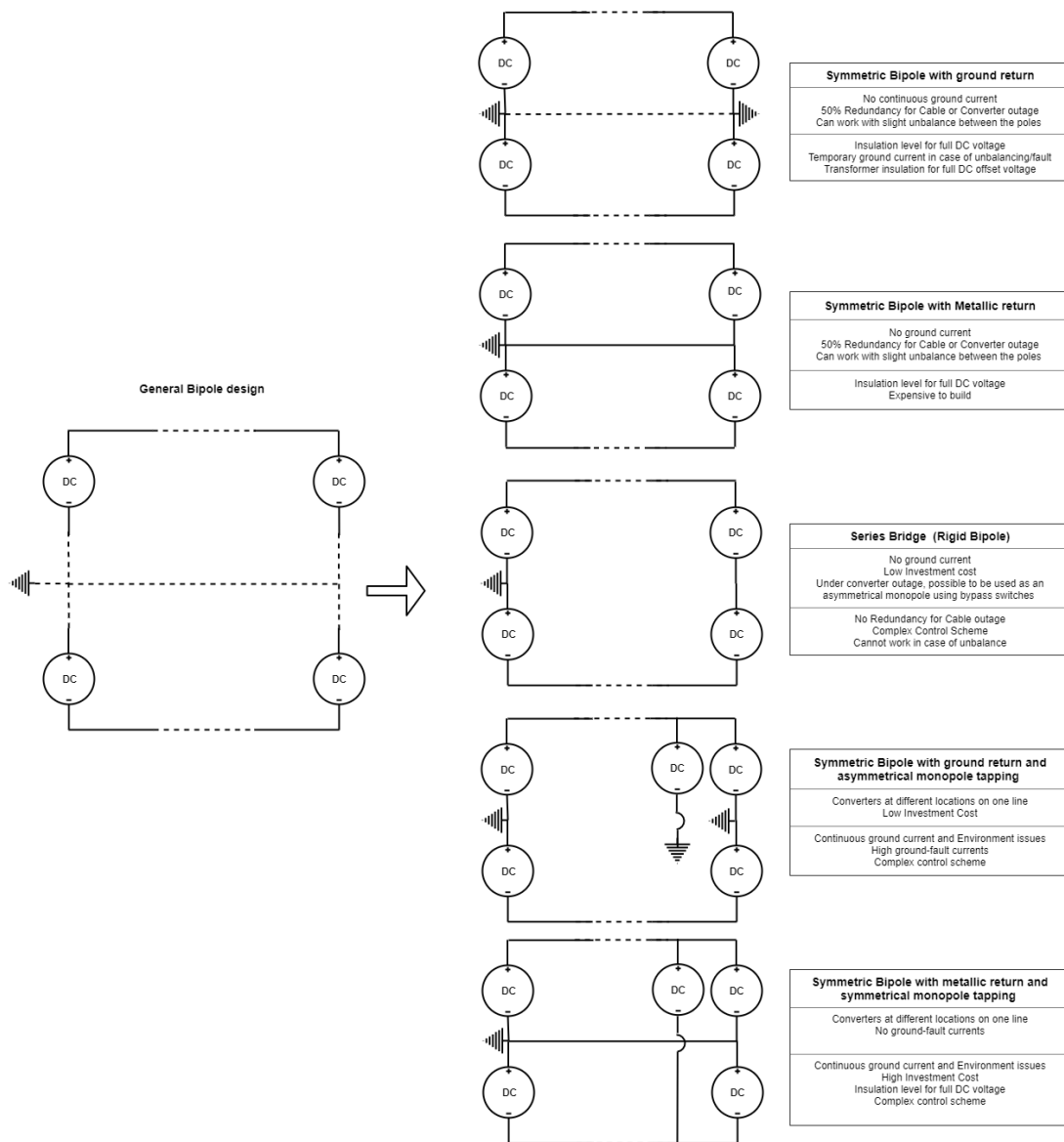


Figure 2.1: Various possible Bipole configurations and their implications

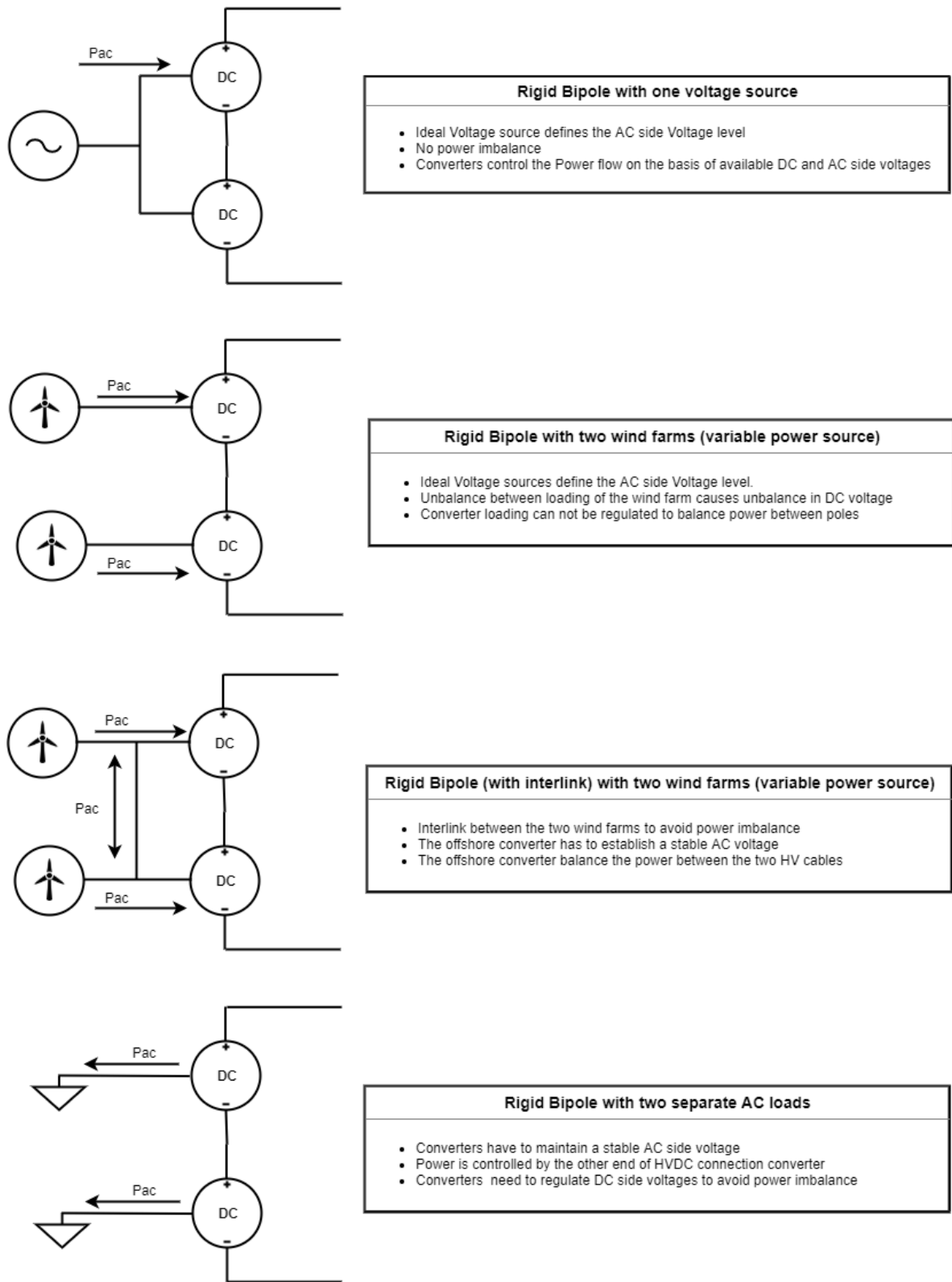


Figure 2.2: General configurations of connection between Rigid Bipole and different AC components

2.6. Converter control modes

The VSC converters used in HVDC connected OWPP can work in two major control modes, i.e. grid forming or grid following. Each mode employs a similar outer (Voltage control) and inner (Current control) loop strategy. However, the parameters being controlled, and the references in each mode are different. The Phase Locked Loop (PLL) output θ is shifted by $\pi/2$ so that the D axis current (I_d) can regulate the DC voltage (V_{dc}) or the Active Power (P_{ac}), and the Q axis current (I_q) can regulate the Reactive power (Q_{ac}) or the AC voltage (V_{ac}). While the inner control defines the pulses given to the internal power electronic switches. The current reference signals for the inner controller are generated by the outer control loop. As shown in Figure 2.3, the outer control loop generates the references of I_d and I_q , based upon the controlled parameters, for the inner control loop [5].

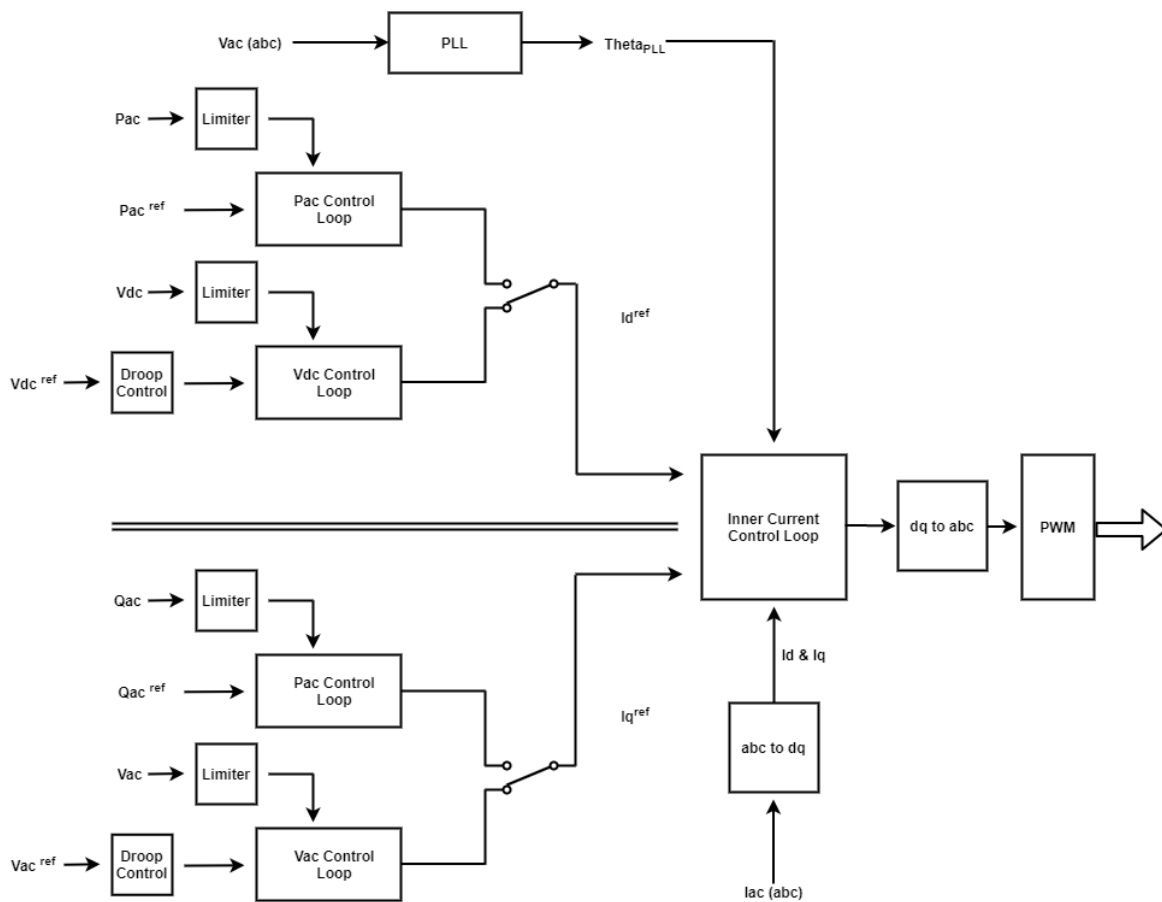


Figure 2.3: General Pac/Vdc and Qac/Vac control scheme diagram

2.6.1. Grid Forming converters

In general, the offshore converters are operated under this mode to maintain the AC voltage and frequency at the offshore AC bus. Usually, grid forming converters work under island mode. The OWPP generates power while being synchronized to the AC voltage. The offshore converter controls the D axis current, and Q axis current together to maintain the frequency and AC voltage of the offshore AC grid [10].

Under Island mode of operation, the offshore converter has to Black start, which is an additional

benefit of the VSC implementation as LCC configuration does not have this capability [11]. This mode is employed when the wind power plant is not connected to an onshore grid directly [12]. Hence the converter has to establish and maintain the AC side voltage, frequency and power-angle (theta) based upon its reference values, as shown in Figure 2.4.

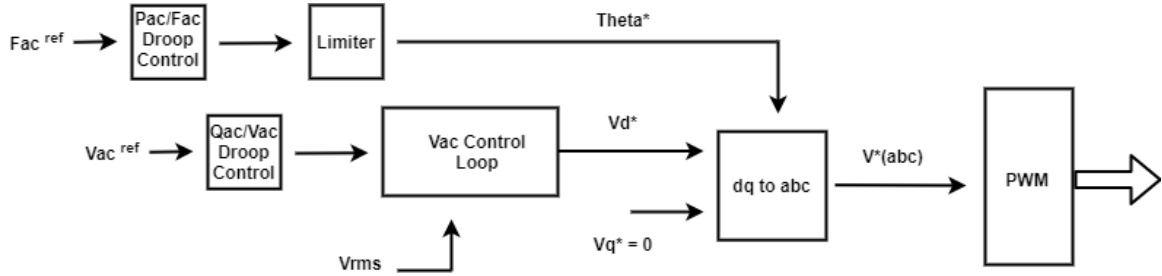


Figure 2.4: Island mode control scheme with Pac and Qac Droop characteristics

The control scheme shown in Figure 2.4, has no current control (limit) loops as it is designed to have fast control over the AC voltage and frequency directly. However, in the case of transient and fault situations, to avoid overcurrents additional current limiting methods such as DQ component limitation, vector amplitude limitation and virtual impedance-based limitation need to be utilized [13]. In this thesis, a virtual impedance-based current limitation method is used. A virtual resistance is added to the model, the virtual resistance remains zero in usual operation ($I_{ac} < I_{threshold}$) and tuned value in case of overcurrent situations, as shown in Figure 2.5.

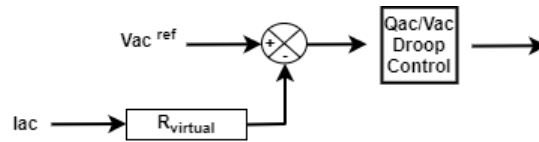


Figure 2.5: Virtual Impedance based current limitation added to the Island mode control scheme

2.6.2. Grid Feeding/Following converters

Typically, the Onshore converters and converters within the wind turbines are operated under this mode as they are responsible for feeding power produced by the wind turbines into the connected power system without regulating the AC side voltage. Grid feeding converters require a connection with a grid forming converter that maintains a stable AC voltage. In this mode, the D and Q axis currents both control the injected active and reactive power, respectively [10].

2.7. Secondary Control methods

Upper or Outer level control is related to the voltage/power (output) of the system. The secondary loop controller works to maintain system-level stability without communication between different terminals and regulating the outer-loop reference parameters. This control is done via droop control of electrical parameters around the pre-defined set points. Droop control is not a control mode, but it is a control scheme which regulates the reference parameters in order to balance the available and demand power to maintain a stable operation of the power system[14].

Power-Frequency (Pac-Freq) droop control methods [15],[16]:

- **Droop Control:** Droop control specifies a linear characteristic between the parameters being controlled (Pac and Freq). Each converter in a multi-terminal connection may have its own droop characteristics and work together to maintain system frequency and to balance the active power.
- **Dead band control:** In this control method, a combination of voltage margin and droop control strategy is applied. The converter works on a constant power for a specific range of frequency and follows a droop characteristic outside this range [15].
- **Undead band control:** Undead band control utilizes a combination of different linear droop characteristics with different slopes for steady-state and unbalanced operation [17].

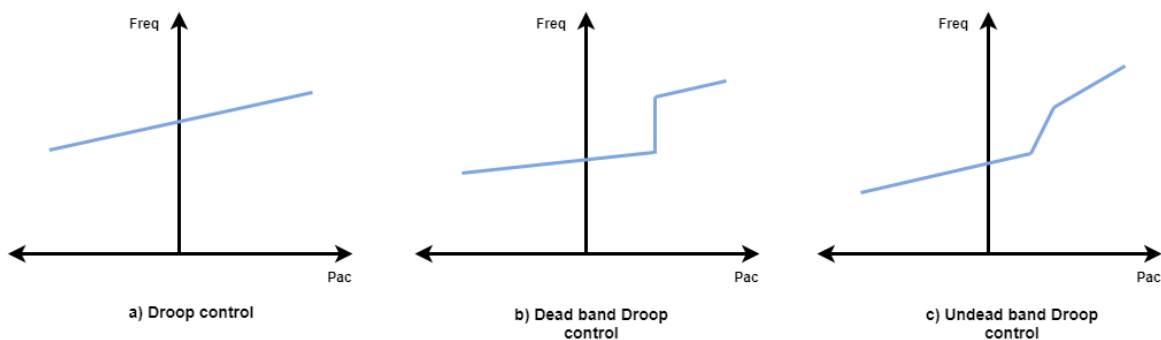


Figure 2.6: Various control methods employed in an AC side connection between converters

Figure 2.6 shows various control methods being utilized in the AC inter-connected converters. A standard operation set-point is selected by the cross-section of the characteristic of each converter, and all the converters follow this set-point to feed in or fetch power out of the system.

In addition to the Pac-Freq droop, a similar reactive power-AC voltage (Qac-Vac) curve is also required to balance the reactive power loading of the converters. To achieve, better and faster control a Power-DC voltage (P-Vdc) droop characteristic can also be added to the DC voltage controlling converter[17].

2.8. VSC Converter Tuning

Most of the control loops employed in the modern Power systems are based on simple Proportional and Integral (PI) gain controllers with Anti-windup functionality. The major drawback of the PI controller is its inherent inability to track a sinusoidal signal due to its non-unity gain while tracking a non-zero frequency signal. Therefore, a Proportional and Resonant filter (PR) gain-based controllers are used in order to track a sinusoidal signal in the control loops.

However, as the focus of this thesis is over high-level control rather than the transient and unbalanced operation of the system, the PSCAD HVDC link model is based on a balanced 3-phase operation (without negative sequence currents) and uses D-Q axis-based control loops. The control loops are always tracking a linear (zero-frequency) signal, and hence they are based on simple and efficient PI controllers.

PI controllers in the VSC are tuned by using the phenomenon of modulus optimum and symmetrical optimum. Table 2.1 summarizes the tuning criteria of the PI gains used in different controllers in the HVDC link model. The modulus optimum works by finding and cancelling the dominant time constant within the controlled system with other minor time constants. Such a scheme is used for the inner-control loops to attain fast response from the control loops.

While for the outer control loops, the symmetrical optimum based optimized and stable approach is used. Symmetrical optimum maximizes the phase margin of the system so that system can tolerate more delays. Outer-loops are supposed to work to reject disturbances and to control the system in an optimized manner. The PI controller bandwidth and gains are calculated based on the equations mentioned in [18] and [5].

Secondary-loop based droop controller gains are calculated by complex system-level analysis. Complete mathematical modelling of the HVDC link is tedious and not a priority for this thesis, and hence droop gains are calculated heuristically.

Controller	PI tuning criteria
Current controller (Inner loop)	Modulus optimum: fast response
AC voltage controller	Symmetrical optimum: optimum regulation
DC voltage controller	Symmetrical optimum: optimum regulation
Active and Reactive power controller	Symmetrical optimum: optimum regulation
Droop controller	Heuristic approach

Table 2.1: Summary of the tuning criteria employed to calculate PI gains of different controllers.

2.9. Converter Modelling methods

According to Cigre TB604 document, different levels of modelling methods can be employed to form a PSCAD converter model [19].

Types of models:

- Type 1: Full physics-based model: These models contain mathematical differential equations for each component. These models are too complex to simulate and hence should be avoided for a full power system-based model.
- Type 2: Full Detailed model: In this kind of modelling, the nonlinear behavior of switches is considered for each stage of switching.
- Type 3: Models based on simplified switchable resistances: All the switches and diodes are replaced by a corresponding on and off resistances.
- Type 4: Detailed equivalent circuit model: These models use equivalent circuit techniques to represent a large number of nodes and hence contain a Thevenin/Norton equivalent of the converter by using resistances values of Type 3.
- Type 5: Average value Models based on switching functions: both AC and DC side component attributes are modelled as controlled current or voltage sources with some harmonics present due to the switching procedure. However, the inner balancing of the capacitors and other controls are assumed to be completely accurate.

- Type 6: Simplified average value model: The AC/DC sides component's attributes are modelled as controlled voltage and current sources but without any non-ideal behavior (harmonics). The phasor domain can be used to implement such simulations. Hence it is suitable for a vast AC/DC grid.
- Type 7: RMS Load-Flow models: These models use the steady-state output values of the converters to implement load flow analysis. Transient behaviors of a system cannot be studied via these models.

Table 2.2 summarizes the above definitions into an objective format. Knowledge of these modelling techniques is essential to decide the most suitable model for a given application.

Table 2.2: Summary of different model types of VSC

Type	Use
1	<ul style="list-style-type: none"> • Individual circuit/converter sub-module design analysis • Not suitable for Power systems
2	<ul style="list-style-type: none"> • IGBTs replaced by an ideal switch with non-ideal diodes (series and anti-parallel), but the protective circuit for freewheeling diodes are missing. • Accurate analysis of current and switching but not losses within switches • Used to validate a simplified model or to see the abnormal operation of Sub-module
3	<ul style="list-style-type: none"> • Same no. of nodes and components as in Type 2 • Switches represented by on/off resistances. • Not suitable for semiconductor transients
4	<ul style="list-style-type: none"> • Represent diodes & IGBTs as two-state resistance (depending upon gate signal and current direction) • Reduction of nodes via equivalent circuit • Used for EMT studies (AC/DC sides) § Design or tune low-level control § Validate Avg value models
5	<ul style="list-style-type: none"> • Avg Value models include voltage/current controlled source replicating average response of components • Includes modulation techniques • Large transients on AC sides • High-level control (Low-level control considered ideally working)
6	<ul style="list-style-type: none"> • Large time scale approximation (steady-state) • Phasor models (no harmonics and sinusoidal)
7	<ul style="list-style-type: none"> • Load flow analysis

3

Modelling of control strategies and HVDC point to point link

3.1. Power balance control strategies under DMR fault

This section centers on system-level control methods. Figure 3.1 shows an example of an MMC converters based Rigid Bipole HVDC link. Terminal 1 and 3 are situated on the offshore side. Terminal 2 denotes the onshore grid connection.

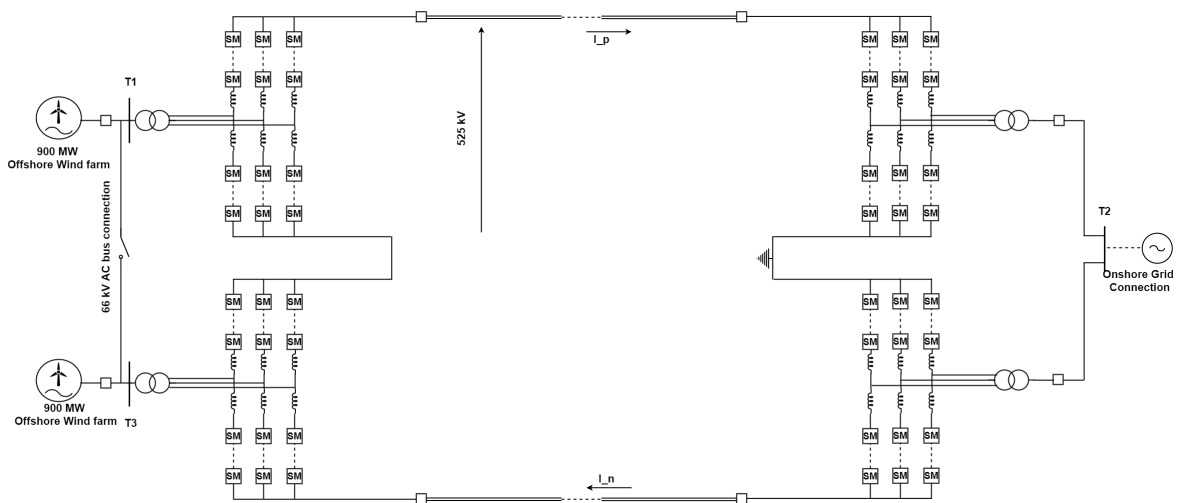


Figure 3.1: MMC based HVDC Rigid Bipole model

Due to the absence of DMR, the Rigid Bipole power flow control scheme requires a fast response to handle the power variance dynamically. Under the dynamic wind conditions, the power supplied from the two similar OWPPs cannot be identical. Slight power variations will influence the HV cable currents, and the control scheme must adjust the control parameters according to this variation.

It should be noted that the control strategies, as mentioned below, are only active under unbalanced conditions. As unbalance between the power produced by the OWPPs is depending upon the wind conditions and hence is not temporary. However, via the control schemes, the unbalance in converter loading can be adjusted by changing the AC interlink loading. Therefore, in steady-

state, the converter loading is automatically balanced as per the new power unbalance between the two OWPPs.

3.1.1. Power set points control

One of the offshore converters works in P/Q control mode while the other works in island mode, as described in section 2.6. The power set-points of the P/Q control mode converter are altered, and the extra power flows through the AC interlink between the converters. This technique ensures equal loading of the converters by transferring the difference in the OWPPs generated power through the AC interlink, as shown in Figure 3.2.

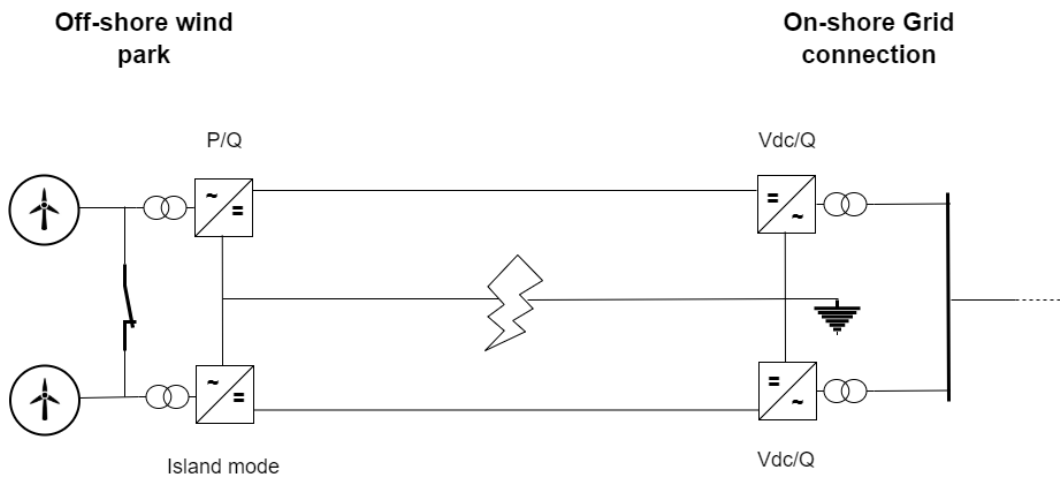


Figure 3.2: HVDC system operation under DMR fault with Power set-point control

Power set-points control varies the reference power levels given to the offshore converters. A multi-meter monitors power flow due to the wind generation in terminal 1 ($T1$) and terminal 3 ($T3$). A new set point is generated by calculating the mean of the generated power references from $T1$ and $T3$. Figure 3.3 presents a simple PSCAD implementation strategy for this technique.

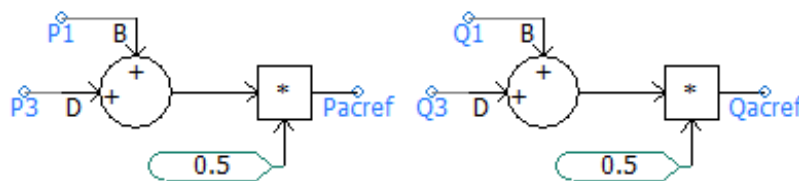


Figure 3.3: Power reference control strategy for active and reactive power set-points in PSCAD

3.1.2. Droop characteristic control

Both offshore converters work as grid forming converters (island mode) with droop characteristic control to balance the voltage and power, as shown in Figure 3.4. Power/frequency (P/f) Droop characteristic is added to the control scheme of the converters while they both work as a slack bus, i.e. grid forming converters. Under island mode, the reference frequency to the voltage-controlled

oscillator (VCO) is altered as per the loading of the converter [20],[21].

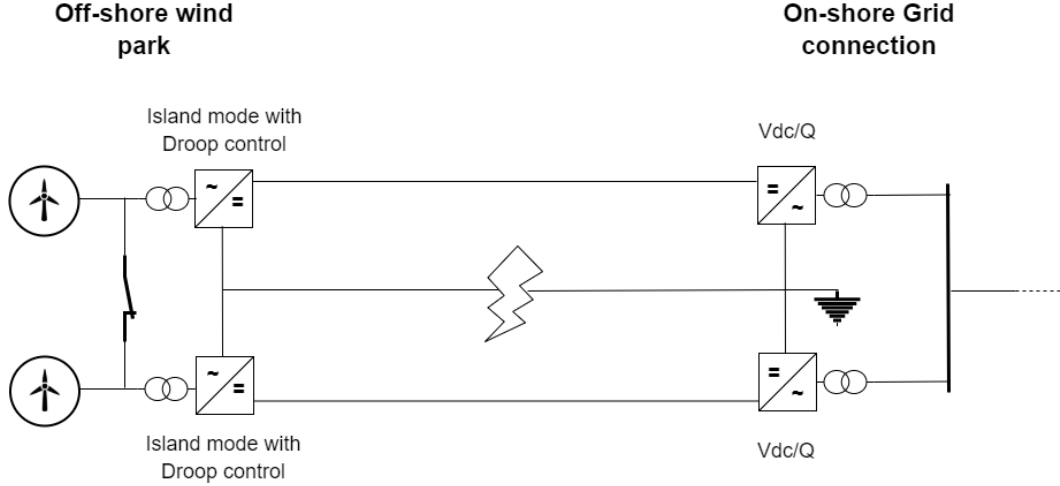


Figure 3.4: HVDC system operation under DMR fault with droop characteristic control

The converter loading is balanced based upon the stiffness of the P/f relationship or droop characteristic. The frequency reference is decreased as the Power reference increases and vice versa. The VCO creates a theta angle of the slack bus, with droop control this angle is adjusted such that the AC voltage vector lags when the converter loading decreases as given in equation 3.1 from [20]. Thus, power flows through the interlink between the converters on the basis of voltage vector, from leading to lagging voltage vector converter. Depending upon converter ratings, the droop constant can be adjusted, the converter with larger droop constant carries lower power as given in equation 3.2. However, here as the objective is to balance power between two parallel converters, the droop constant is set to be equal. Figure 3.5 shows the implementation model of the droop control strategy in PSCAD.

$$f_{ref} = f_0 - drp * (P_{ref} - P_{pu}) \quad (3.1)$$

$$P_{loading} = drp_1 * P_1 = drp_2 * P_2 \quad (3.2)$$

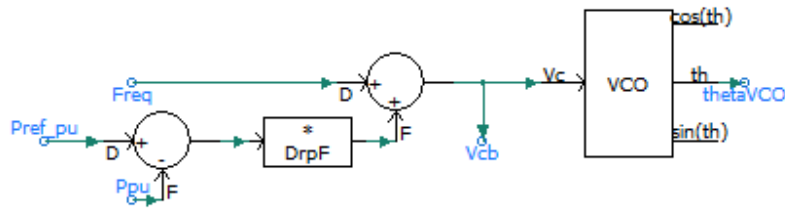


Figure 3.5: P/f droop control strategy implementation in PSCAD

3.2. HVDC link modelling

Cigre PSCAD 4-terminal example model, as shown in Figure 3.6, is selected as a base reference model. The prime reason for selecting this model is that it is open-source and based on Type 4 modelling, which is ideal for AC/DC side large transient analysis, as mentioned in table 2.2. The selected model is composed of two converter stations, either side of the HVDC transmission lines connected via a Bipole configuration.

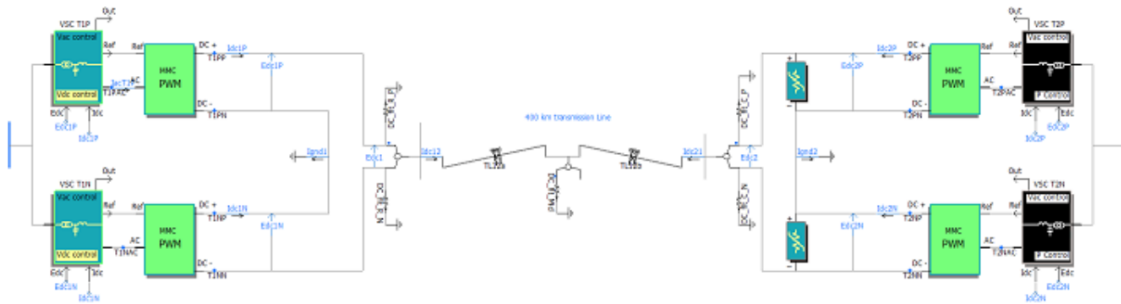


Figure 3.6: Cigre PSCAD four-terminal reference model

The four-terminal HVDC network is composed of two 900 MW OWPP on the offshore converter stations, which are connected to a Rigid Bipole configuration. As described in section 2.5, since the network is considering a particular case of a fault in the DMR cable, there are only two HV DC cables, and the DMR cable is not considered. In Bipole, converters are connected to the onshore AC grid with a 250/66 kV transformer, AC filter and AC breaker. The DC network work at the voltage of 525 kV, transferring power from the OWPPs to the onshore grid network via 200 km long DC cables. Refer to table 7.1 for the summary of the ratings of the equipment used in the HVDC link.

3.2.1. Cables

The 400 km long three-conductor DC transmission line, as shown in Figure 3.6 is replaced with two-conductor (HV) DC cables. The cables are derived from the Tennet Promotion Project PSCAD Library. This cable configuration consists of three conducting and three insulating layers. A brief description and main functions of the layers are provided below, as given in [22].

- The central conductor transfers the electrical power and consists of multiple conducting strands. The current carrying capacity, in general, is directly proportional to its cross-sectional area.
- The first Insulating layer is added to avoid the flow of electric charges from the conductor surface to the ground or neighboring cable conductor. The conductor surface not being uniform may result in irregular charge accumulation on it. Two semi-conducting screens are added to cover either side of the first insulation layer to avoid partial discharge between the conductor and the insulating layer.
- The second conducting layer or sheath protects the internal insulation from any physical damage at the same time it carries the ground current in case of faults and usually grounded at one point of the cable length. It also works as a metallic shield from outside disturbance. For safety reasons, it's always grounded at least at one point in the entire cable length.

- Sheath jacket or outer sheath is a non-conducting covering of the sheath. It also serves as protection of inside cable against external physical forces and chemical reactions.
- The metallic Armor layer is added as the cable is employed under sub-marine conditions. Usually, non- magnetic materials are used for its construction to avoid magnetic losses in the AC conductor cables. The resistance of the armor is in parallel to the sheath conductor, and hence its resistance is adjusted (while choosing the material) accordingly to the sheath resistance required to reduce the losses. However, in the case of DC cables, there are no actual magnetic losses.
- The outer covering layer provides increased thermal resistance to the cable and reduces heat transfer from the conductor. This technique helps to reduce the conductor rating, and material for the outer covering is selected based on its thermal resistance required.

Figure 3.7 shows the radial cross-section and dimensions of the components selected cable in detail. A horizontal distance of 0.5m is placed between the two negative and positive cables.

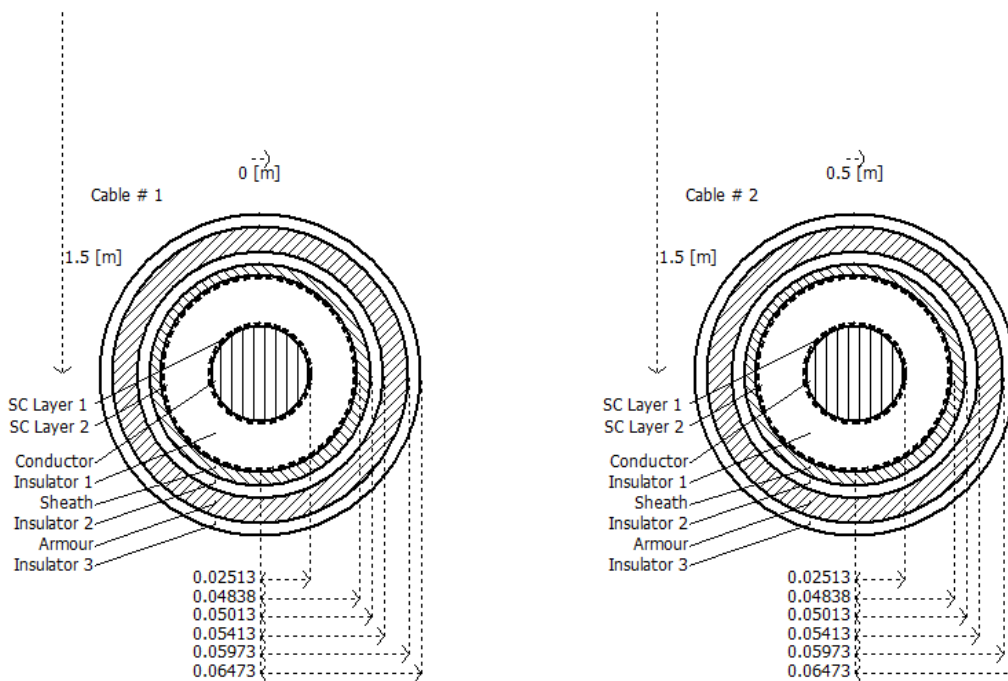


Figure 3.7: PSCAD Tennet Promotion model library cable dimensions and properties.

3.2.2. Converter

Half-bridge MMC based VSCs are used across the HVDC link to transfer power between aggregated OWPPs and onshore grid. The MMC uses general configuration composing of sub-modules, arm inductance in two top and bottom arms, which together compose a leg, as shown in Figure 3.9. Three such legs are required for a three-phase AC network connection.

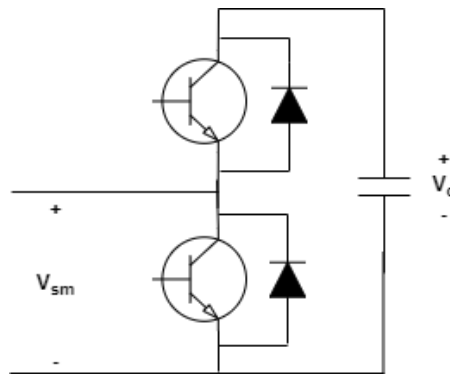


Figure 3.8: Simplified half-bridge MMC sub-module

Each half-bridge sub-module composes of a capacitor and two switches (IGBTs), which work to bypass (Off state) and insert (On state) the capacitor as in Figure 3.8. In case the capacitor is inserted, the direction of current passing through the capacitor defines whether the capacitor is charging or discharging. Current in the direction of capacitor charge orientation discharges the capacitor and, in the opposite direction, charges it.

Since there are multiple existing sub-modules and capacitors in a high voltage converter, a balancing technique is employed to ensure there exists a similar state of charge in each of the capacitors. Sub-modules in the upper and lower arm are controlled via insertion indices to be bypassed or inserted.

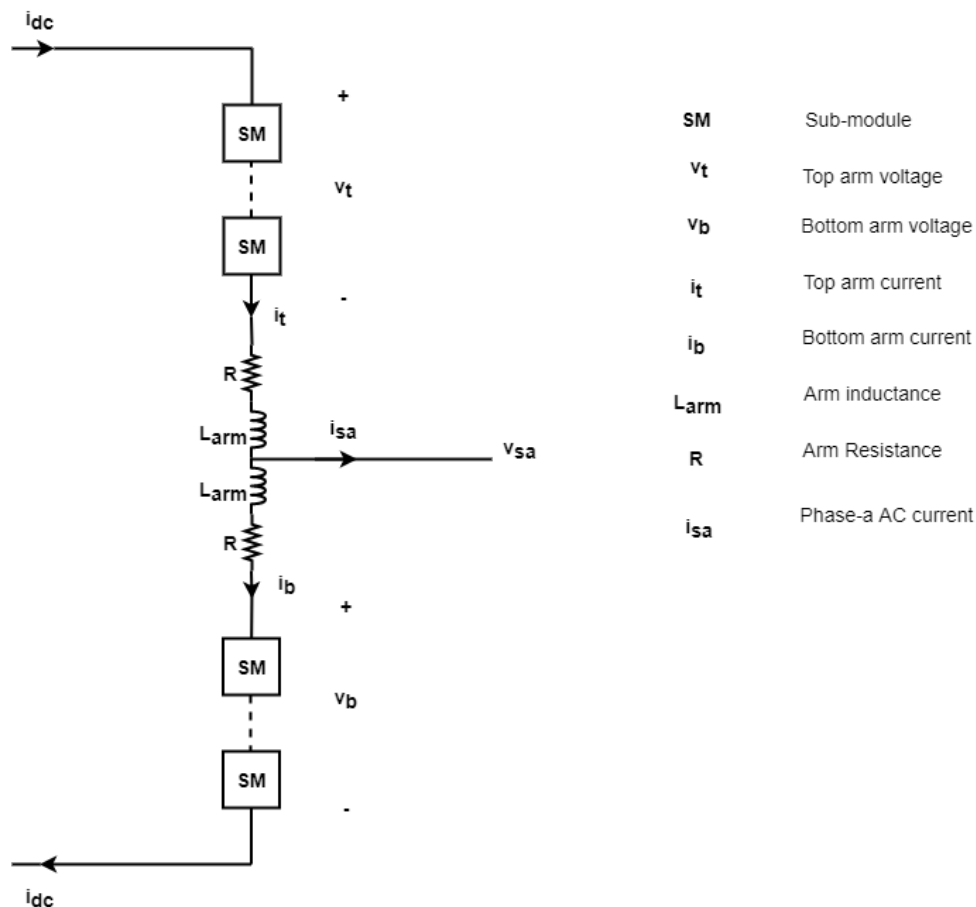


Figure 3.9: MMC single-phase leg operation

MMC produces the required reference voltage via the wave-shaping and carrier-based modulation technique. Mainly, three approaches are used to create a sinusoidal waveform, Nearest level control (NLC), Level shifted carrier (LSC), and Phase shifted carrier (PSC) wave control.

In NLC, no carrier wave is used, and the insertion indices are calculated via finding the nearest approximate value of the reference voltage to the possible output voltage within the MMC as per the given number of cells. This method is more straightforward in terms of calculation but requires further control techniques to balance the charge in all the sub-module capacitors, which requires more computation. Sorting and selecting algorithms are involved to avoid divergence in capacitor voltages.

LSC applies different carrier waveforms for individual control (cell) level. The amplitude of the reference voltage is divided by the number of cells, and each part is assigned by a carrier waveform. This method of PWM also suffers from the unbalancing of capacitors since some cells (depending upon their position) are inserted more frequently. Similar to the NLC method, LSC requires additional balancing algorithms and computation.

PSC method works by assigning different carrier waves for each cell, which differ in phase to each other, but unlike LSC, the amplitude remains the same. This way, each sub-module is inserted at

a similar frequency and hence maintain a balance in terms of capacitor voltage level. Balancing is slower as it is natural and does not employ any external control algorithms, but it is simple to operate. MMCs in this PSCAD model employs the PSC PWM technique due to fewer computation requirements.

$$i_s = i_t - i_b \quad (3.3)$$

$$i_c = \frac{i_t + i_b}{2} \quad (3.4)$$

$$v_s = \frac{v_t - v_b}{2} \quad (3.5)$$

$$v_c = \frac{v_t + v_b}{2} \quad (3.6)$$

In order to control the circulating currents, an offset voltage equal to the circulating voltage (v_c), which is an imaginary control parameter, is added and subtracted to the upper and lower arm voltage references, respectively. Since the circulating currents producing circulating voltage is half of the sum of the upper and lower arm as in equation 3.6 voltages, this action puts v_c to zero. The circulating currents are calculated for each phase via the relation, as given in equation 3.4. Then v_c is calculated for the individual phase by multiplying i_c with controlled gain (PI controller). This mechanism is employed to ensure that the circulating currents are minimum and balanced in all three-phases. Three phase i_c , if balanced, are cancelled out at the artificial neutral point present at the top and bottom nodes of the MMC leg of each phase. This point carries voltage and non-zero conducting currents while serving as a neutral point for the circulating currents.

3.2.3. AC side equipment

Offshore and onshore converters are connected to the OWPPs and onshore grid respectively via AC line and control/safety equipment. Figure 3.10 displays an overview of connected equipment between each OWPP and converter.

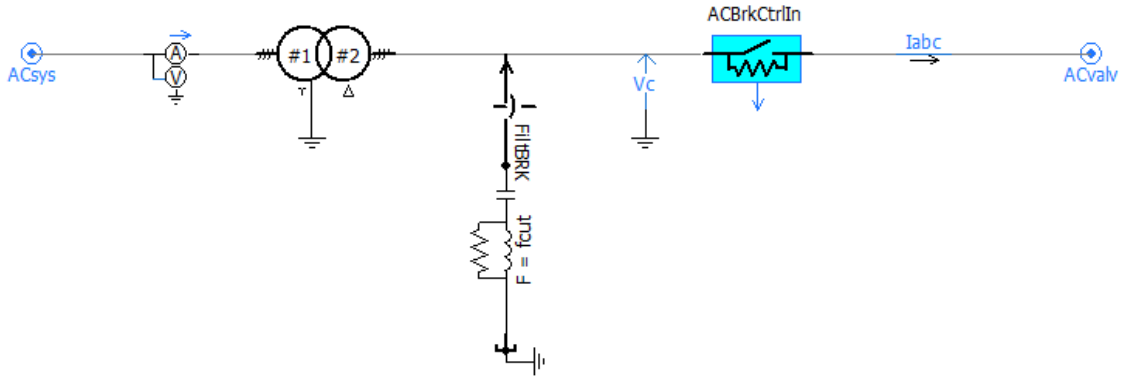


Figure 3.10: Onshore AC side connection and equipment

A star-delta transformer is used to convert the AC voltage level to the compatible AC voltage of the converters. The star side serves as a grounding connection. Lower harmonics are also cancelled due to the star-delta phase shift. Depending upon the higher voltage level and hence the insulation level required, the star-delta side is chosen to reduce the cost of the transformer winding. The insulation level and number of turns in the transformer required for the delta side is higher.

A multimeter is connected to analyze the real-time power transfer and voltage levels, which are also required for the converter control schemes. An AC filter is connected in parallel to cut-out the specific frequency voltage components present in the AC line. Disturbance in load or input power or voltage control errors can cause non-sinusoidal voltages in the AC line.

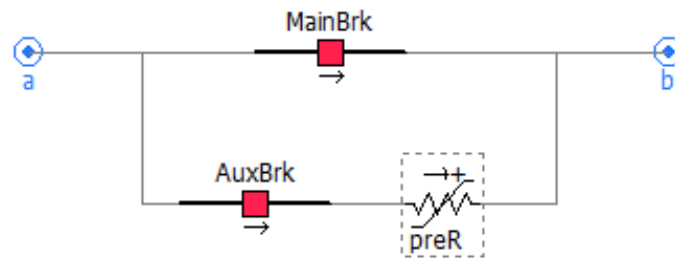


Figure 3.11: Onshore AC side breaker and pre-insertion Resistance

A master breaker is connected in series to the AC line, which works to cut-off the series connection between the converter and AC equipment under sudden fault or non-operational conditions. A parallel branch containing series-connected auxiliary AC breaker and pre-insertion resistance is added to avoid in-rush current when the system is suddenly put into operation. Pre-insertion resistor avoids large inrush currents that run to charge the converter-capacitors and other equipment as the converters are not performing any control operations. Later, after the initial high amplitude transient is passed, the master breaker is closed, and the auxiliary breaker is turned open. This way, power flow is shifted from the auxiliary to the master breaker. However, the parallel line containing auxiliary breaker and pre-insertion resistance is not required on the offshore side as the wind power plants are steadily ramped up after the cable and converter capacitance are charged, and a stable DC voltage is established.

3.2.4. On-shore Strong Grid

Onshore converters, shown in Figure 3.1, are not controlling or influencing the grid side AC voltage. The D-axis control mode is maintaining the DC pole voltages while the Q-axis control mode is controlling the flow of reactive power. A high and robust inertia grid connection is required to ensure stability under unbalanced or transient conditions.

Faults or even transient variations in supplied power can influence the onshore grid AC bus voltage and frequency. Therefore, a high capacity voltage source is attached to the onshore AC bus. A modelled strong grid is taken from the PSCAD Tnet Promotion project power source library. This model contains multiple different capacities (strong, moderate, weak and custom) based voltage sources, as shown in Figure 3.12. It is also possible to simulate the system with a different grid capacity to view the effects of grid capacity on the control scheme.

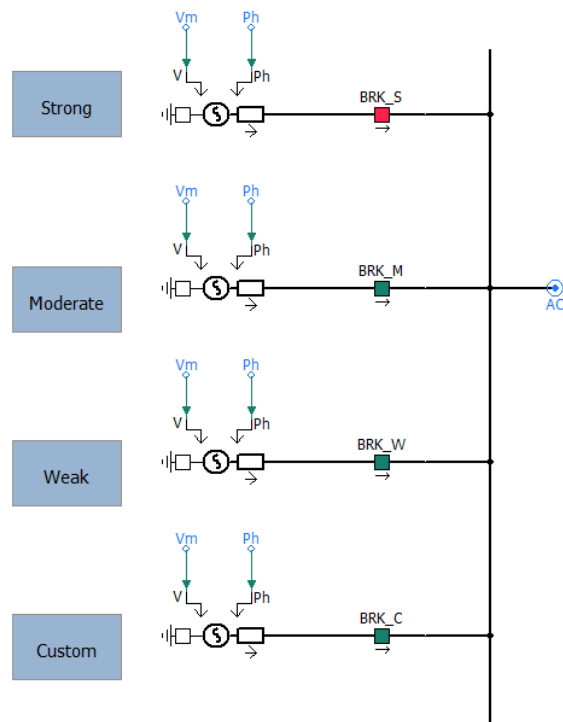


Figure 3.12: On-shore grid connection from Tennet Promotion PSCAD model power source library.

3.3. Offshore Wind Power Plant modelling

In simple words, OWPP convert the wind energy into electrical energy via large turbine blades that rotate the generators. They can be modelled as wind dependent power source.

The 3-phase generators present in the PSCAD main library are all voltage source which supplies specific power depending upon the line impedance. However, this project requires a current source alike power source, which does not influence the AC voltage at the offshore AC bus. Voltage is instead controlled and maintained via an island mode operating offshore converter. Another voltage source in series to the bus will cause control issues if not synchronized.

A conventional but sophisticated way to model OWPP is to connect wind energy-dependent voltage source to another VSC HVDC network, which is synchronized with the AC bus voltage. The converters can also be controlled to feed-in the set reference power to the offshore AC bus. Nevertheless, this method is complicated and increases the simulation computation time. Since the aim of this research is focused on the HVDC system and converter control scheme rather than the dynamics of OWPP, this elaborate modelling scheme can be replaced by a more straightforward and faster model. A voltage-controlled instantaneous 3-phase current source is used to model OWPP, as shown in Figure 3.13.

3.3.1. Aggregated synchronized power controlled current source

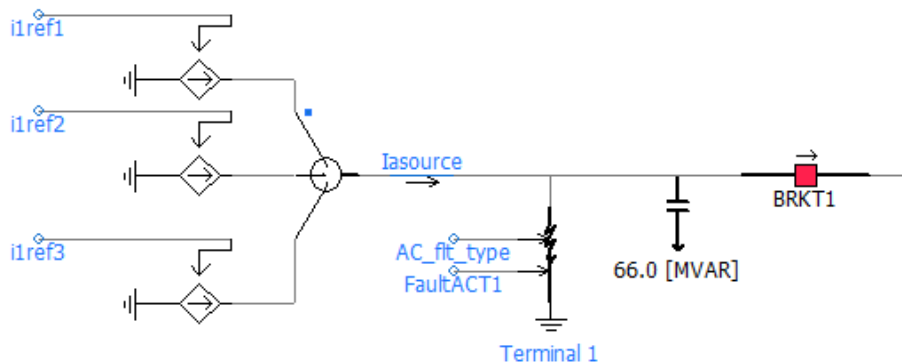


Figure 3.13: Voltage-controlled 3 phase current source modelled in PSCAD

Current references given to the two OWPPs, as given in Figure 3.1 are controlled separately to model unbalance in wind power generation.

Current sources must be synchronized to the offshore AC bus voltage to avoid excess reactive power inserted into the system. The phase-locked loop (PLL) mechanism is employed to ensure synchronous operation. PLL block generates a reference angle θ_{thetapll} . θ_{thetapll} is utilized to generate synchronized voltage references in the ABC to DQ axis and its inverse block. To ensure stable operation of the system, the current sources are only ramped up to the set magnitude after a stable AC voltage is established by the grid forming offshore converter. Figure 3.14 shows the modelling of the blocks, as mentioned above in PSCAD.

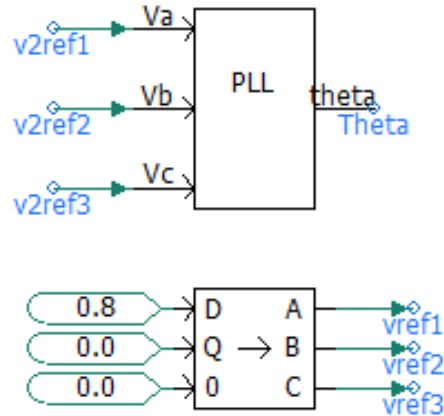


Figure 3.14: PLL block and synchronized voltage reference generation.

At last, using equation 3.7, this voltage reference is multiplied by a gain specific to each OWPP to get current references, as shown in Figure 3.13.

$$i_{ref} = Mag_{wf1} * v_{ref} \quad (3.7)$$

3.3.2. OWPP structure and Reactive Power

The reactive power demand of an OWPP depends over the cable length and cable capacitance per unit length, which is used to connect all the wind turbines together to the offshore substation. As given in [23], multiple configurations are possible to connect the wind turbines via cables such as radial, multiple ring or star. Radial architecture-based connection of wind turbines is as an optimized yet simple solution for such a connection.

This thesis assumes a radial connection for both of the 900MW OWPPs. Each wind turbine is assumed to be rated 10MW, hence in total 90 wind turbines are to be connected to each OWPPs. As shown in Figure 3.15, the substation is connected to the wind turbines via ten strings of submarine AC cables and each string of cable is connected to nine wind turbines.

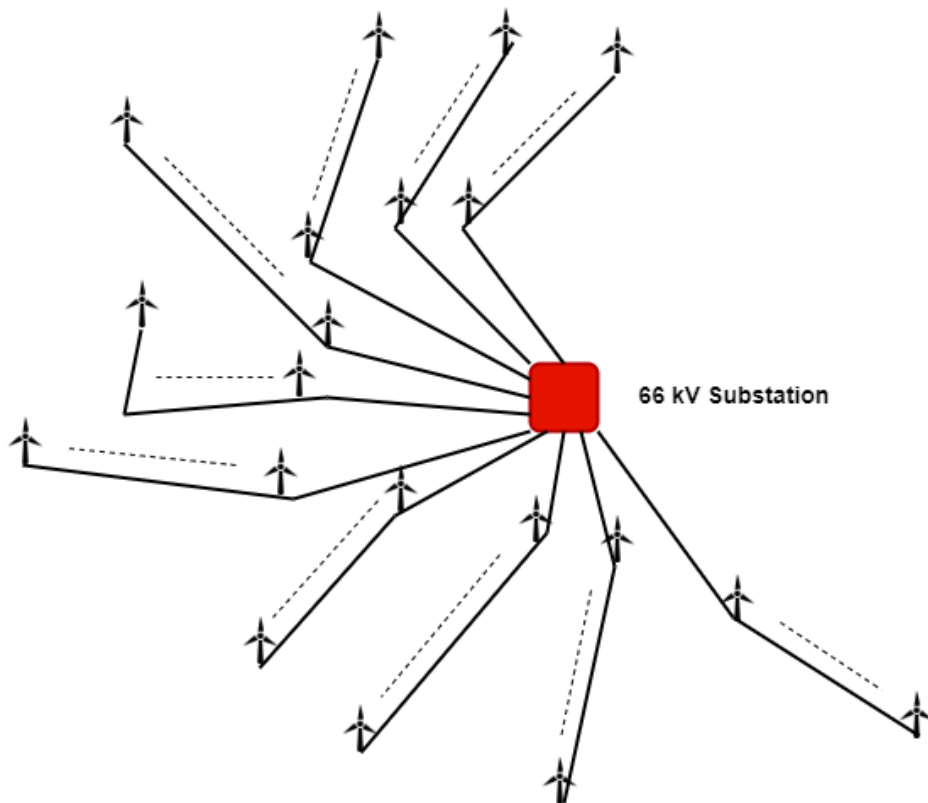


Figure 3.15: OWPPs architecture: Radial connection of wind turbines to the 66 kV substation

A capacitor bank is added to the OWPP to mimic the reactive power demand of the cable, which is used to connect the aggregated wind turbines to the generator, as shown in Figure 3.13. As per [24], 66kV rated submarine cable has capacitance from $0.2\mu F/km$ to $0.3\mu F/km$ and for 900MW OWPP with 10MW rated wind turbines, total cable length of 120km to 160km can be assumed. To imitate the maximum reactive power demand, 160 km of cable length and $0.3\mu F/km$ of cable capacitance is selected as reference ratings for the submarine cable between each wind turbine and the substation. Capacitor bank rating is calculated assuming the AC bus voltage of 66kV as 66MVar.

4

Analysis of point to point link

This section combines the system as described in section 3.2 with the power balance strategies from section 3.1 to inspect the system behavior under steady-state and transient unbalanced conditions. Figure 7.1 in Appendix 7.1.2 shows the PSCAD simulation model of onshore and offshore segments of point-to-point link used during the analysis.

Possible unbalance scenarios considering a radial layout:

- Energization of array cables (upward step change in reactive power)
- Wind generation fluctuations
- Controlled shutting down of one turbine or string
- Sudden loss of turbine or string due to fault
- Fault in the cable connecting OWPP and converter

4.1. Energization of array cables

As mentioned in section 3.3.2, within the OWPP, the wind turbines are connected to the main 66kV substation via submarine cables. The submarine cables are charged before the wind turbines start generation. The string cables connecting wind turbines are energized step-by-step for this simulation, the step is assumed to be two strings (20%) per second, as shown in Figure 3.15. During this process, the wind turbines are not in operation, and converters have to cover the active power losses within the offshore grid equipment. This reactive power is provided by the connected offshore converters, as shown in Figure 4.1.

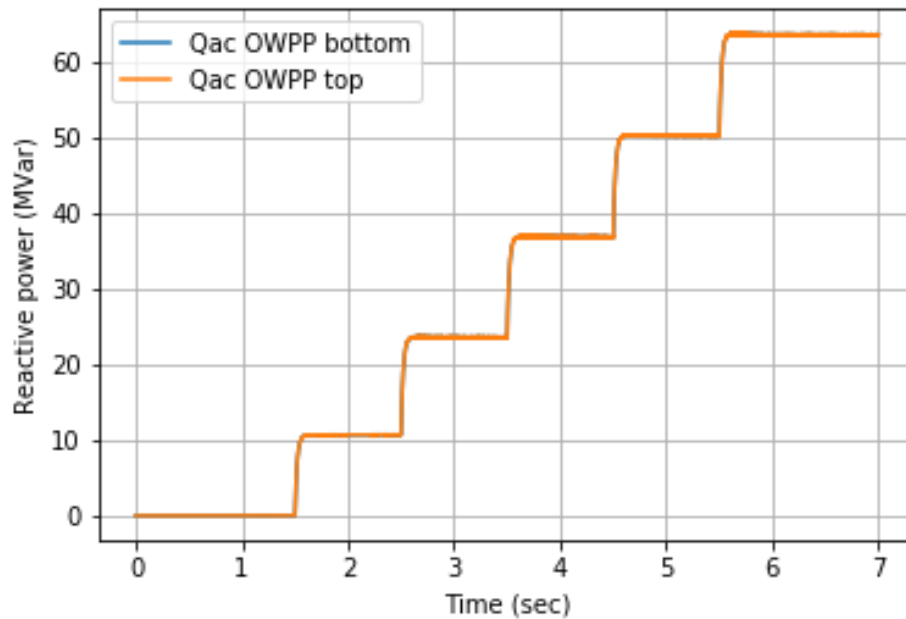
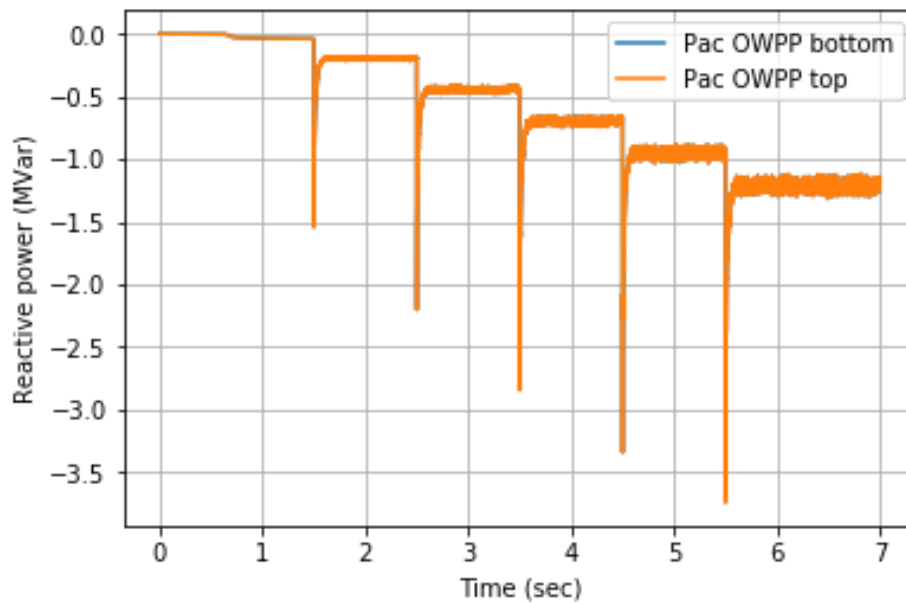


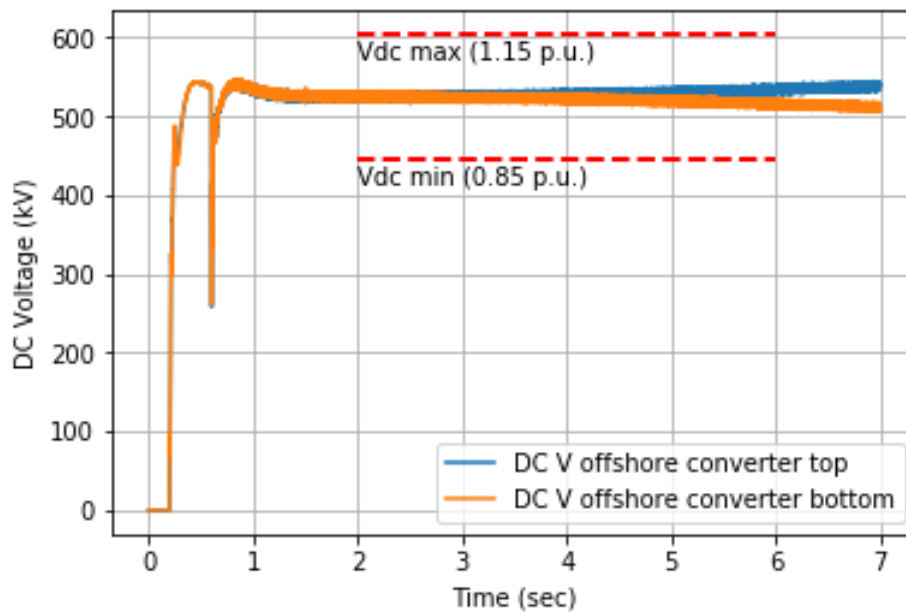
Figure 4.1: Step-energization (reactive power loading) of top and bottom OWPP

4.1.1. Power set points control

Power set points control strategy is able to inject required power to the OWPPs for initial cable energization while maintaining a stable DC voltage, as shown in Figure 4.2. However, as only one converter is controlling power flow and OWPPs are not supplying any power, there is a difference in the offshore converters power loading, which causes 10kV DC voltage unbalance between top and bottom offshore poles. The converter working under island mode has to cover the losses of both converters. This causes a constant power flow through the AC interlink from the island mode operating converter to the converter operating under power control mode. The island mode converter is also able to maintain a stable AC voltage and frequency, as shown in Figure 7.2 in the Appendix 7.2.1.



(a) Active power losses of top and bottom OWPPs and converter

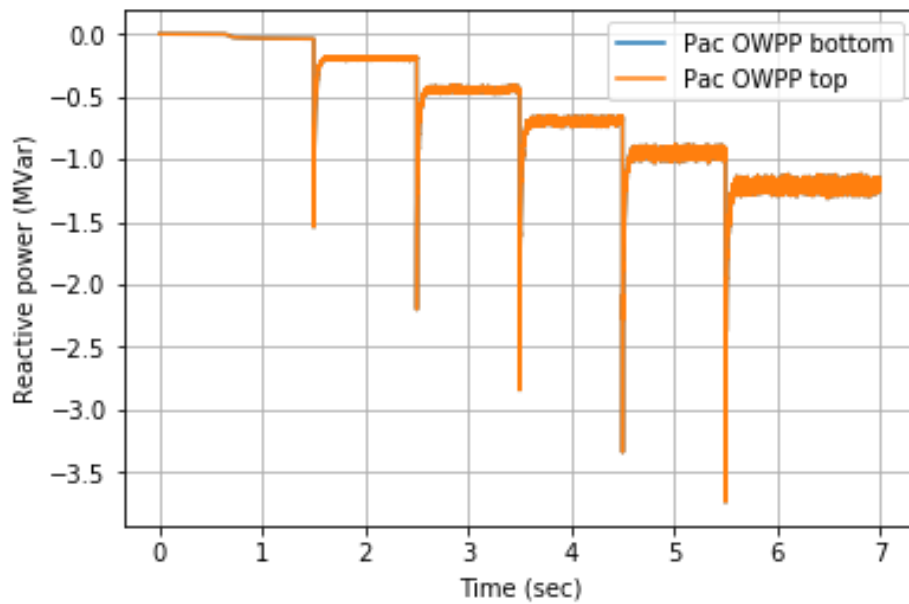


(b) DC voltage of top and bottom offshore poles

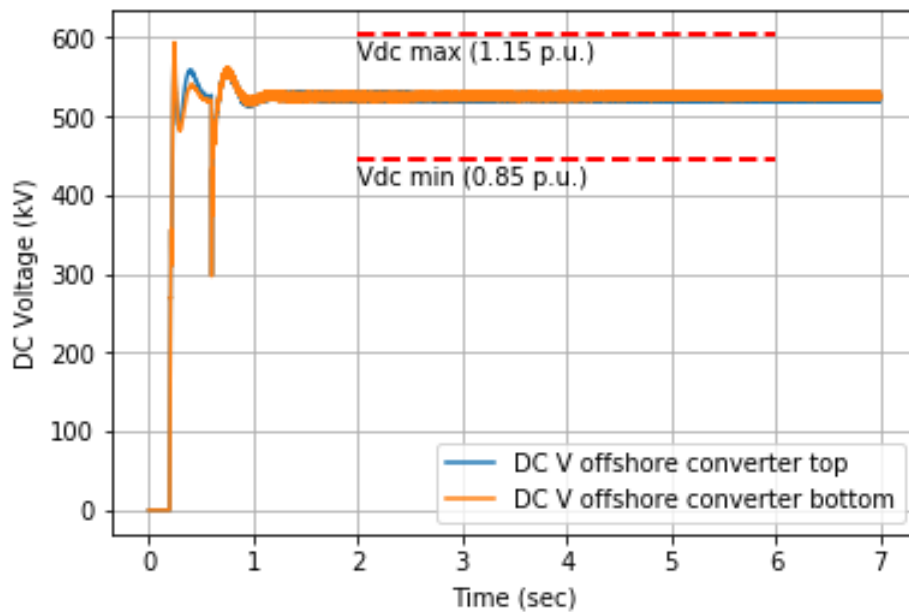
Figure 4.2: Active power losses of the equipment and DC voltages of offshore poles under power set points control while cable energization

4.1.2. Droop control

Under droop control converters are able to inject required power to the OWPPs. As, both the converters are following identical control scheme there remains no irregular unbalance between the DC voltages of the top and bottom offshore poles, as shown in Figure 4.3. Both the island mode converters cover their own active power losses while maintaining a stable AC voltage and frequency, as shown in Figure 7.3 in the Appendix 7.2.1.



(a) Active power losses of top and bottom OWPP and converter



(b) DC voltage of top and bottom offshore poles

Figure 4.3: Active power losses of both equipment and DC voltages of offshore poles under droop control while cable energization

4.2. Wind generation fluctuations

To examine the performance of the control strategies and HVDC link under real-life wind fluctuations, Hornsdale wind farm and Hornsdale wind farm 2 in South Australia are selected for generation references¹.

Both of these wind farms are situated in the same region and have equal power ratings of 102MW . Thus, the Hornsdale wind farms can directly correspond to the two aggregated OWPP in the HVDC link model. The generated power data reference (102MW) is scaled up to the ratings of modelled OWPP (900MW) by multiplying with a constant value of $900/102$, as shown in Figure 4.4.

The selected generation reference data is recorded with a temporal resolution of per 5min basis. A data set of 16hr and 40min is selected which has large amount of generation fluctuations to take a conservative approach. In PSCAD it's difficult to simulate and analyze hourly data of wind fluctuations. Therefore, reference data is sampled with a frequency of 10.0Hz . Thus, each second of simulation time in all the graphical data of section 4.2 represent 50min of real-time wind generation fluctuations. This simulation analysis is also a conservative approach for the control strategies as the time given to the power-balance control loops is three thousand times less compared to real-life fluctuations timings.

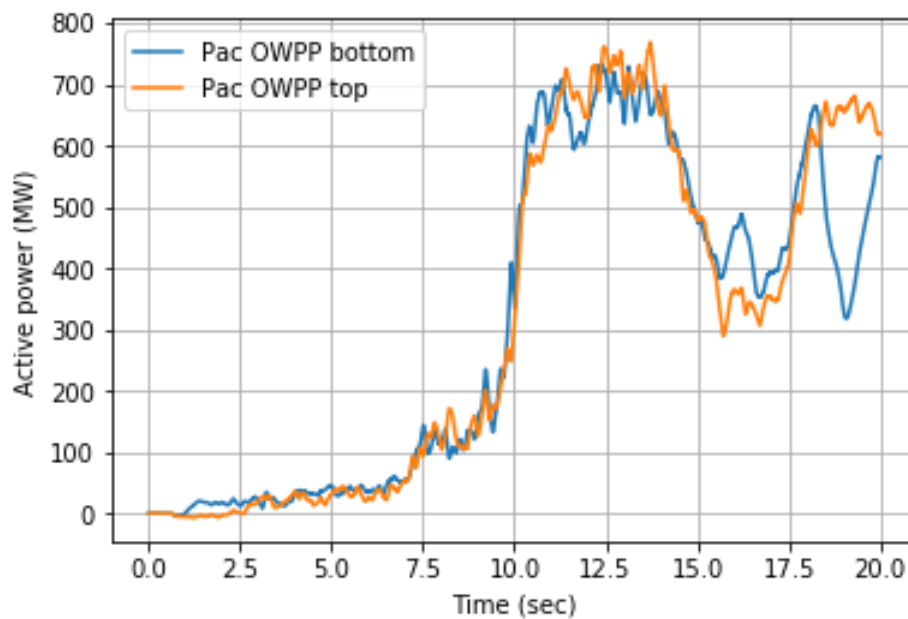


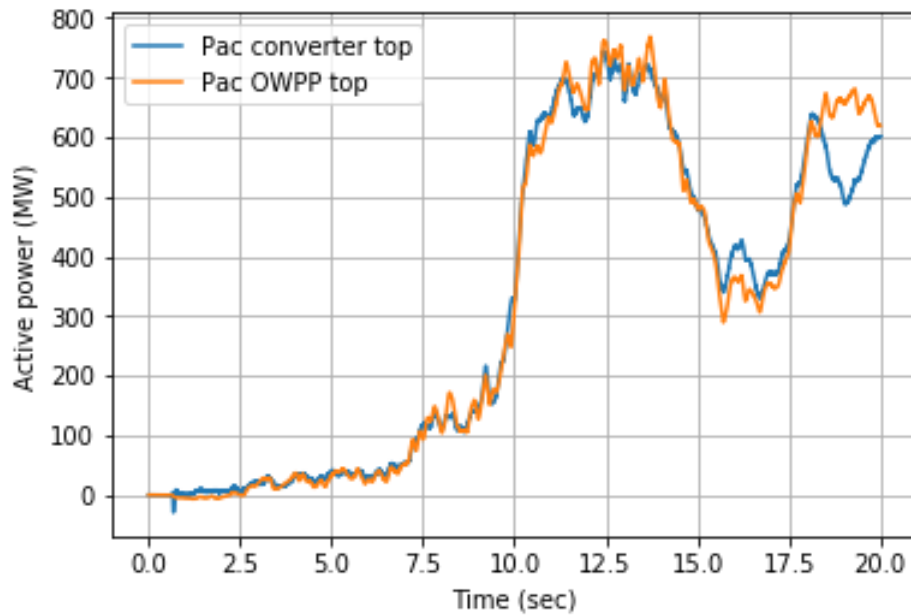
Figure 4.4: OWPP power generation references with wind fluctuations

DC voltage waveforms as shown in Figure 7.4 and 7.5, are well regulated as per the power generation fluctuations. Both offshore and onshore pole DC voltages remain between the maximum and minimum ratings as stated in table 7.1. Refer to Appendix 7.2.2 for other related HVDC-link characteristics under wind fluctuations.

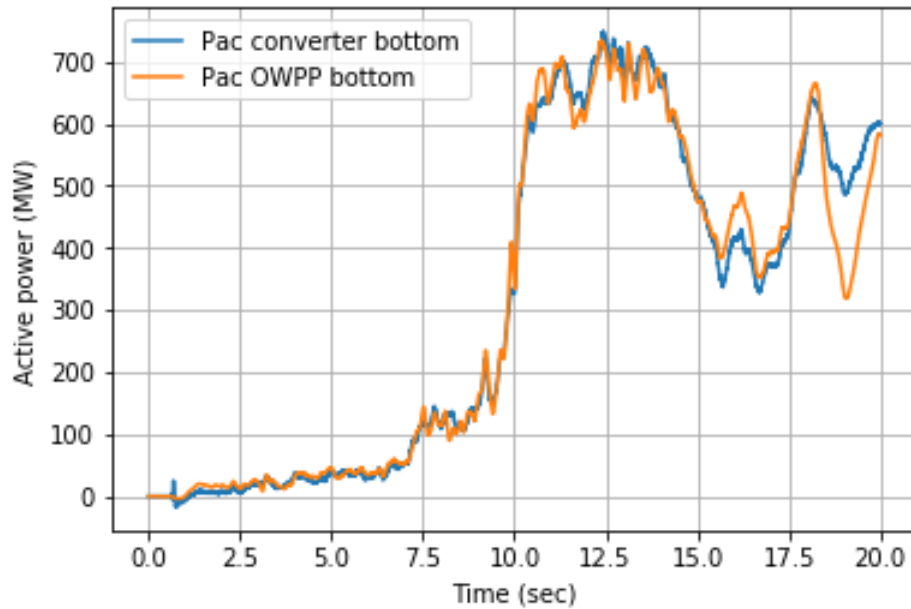
¹Source: Aneroid

4.2.1. Power set points control

Figure 4.5 shows that due to the wind fluctuations, power loading of the OWPP is unequal. However, the power set points based control strategy ensures equal loading of the converters.



(a) Active power loading of top OWPP and converter

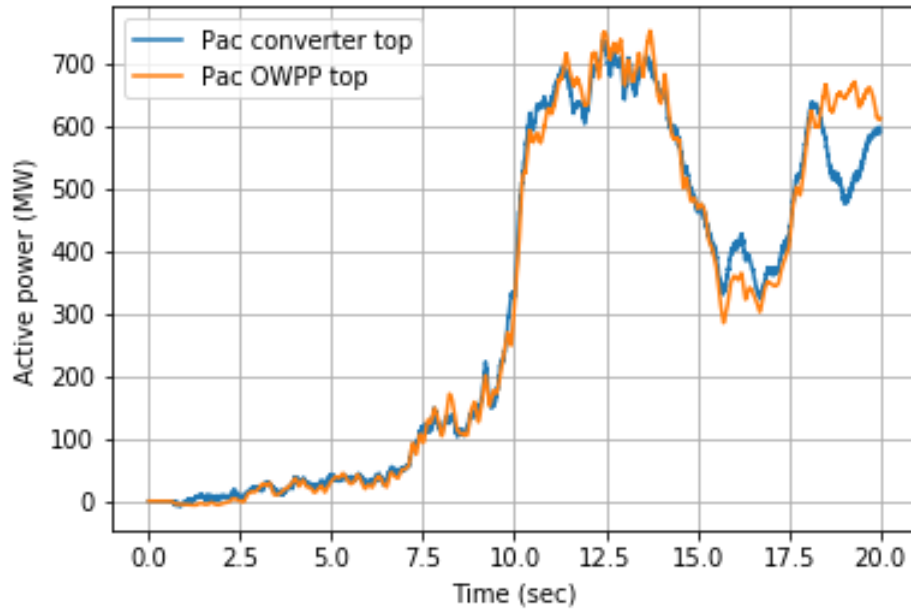


(b) Active power loading of bottom OWPP and converter

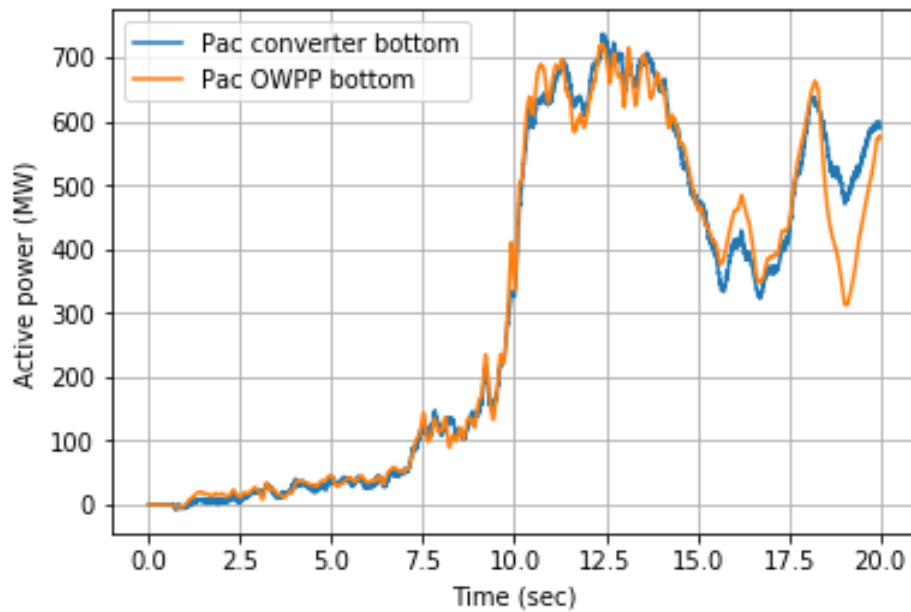
Figure 4.5: Active power loading of both OWPP and converters under power set points control with wind fluctuations

4.2.2. Droop control

From the Figure 4.6 it can be verified that the droop control based control strategy is ensuring the equal loading of the converters during real-life wind fluctuations.



(a) Active power loading of top wind farm and converter



(b) Active power loading of bottom wind farm and converter

Figure 4.6: Active power loading of both OWPP and converters under droop control with wind fluctuations

4.3. Controlled ramp down of wind turbine and string of the OWPP

To follow the onshore grid power demand the OWPPs adjust the power generation by turning the wind turbines on or off. Such variations are done with ramp up or down in a controlled manner so that the stable operation of HVDC link is not influenced. To test the HVDC link under a controlled ramp down scenario, a sequence of operations is designed as shown in table 4.1. Maximum ramp-up rate is limited at 350MW/s to avoid large simulation times as OWPP need to ramp-up 800MW . Maximum ramp-down rate is limited at 90MW/s . Figure 4.7 shows, the active power loading of the top and bottom OWPPs as per the sequence described in table 4.1.

Time (s)	Operation sequence
0.2	Onshore converters De-block
0.6	Offshore converters De-block
1.0	OWPPs in operation (800MW each) with slow ramp up
4.0	Wind turbine (10MW) attached to bottom OWPP controlled ramp down
6.0	Wind turbine string (90MW) attached to bottom OWPP controlled ramp down

Table 4.1: Sequence of operations for controlled ramp-down of OWPP wind turbine and string.

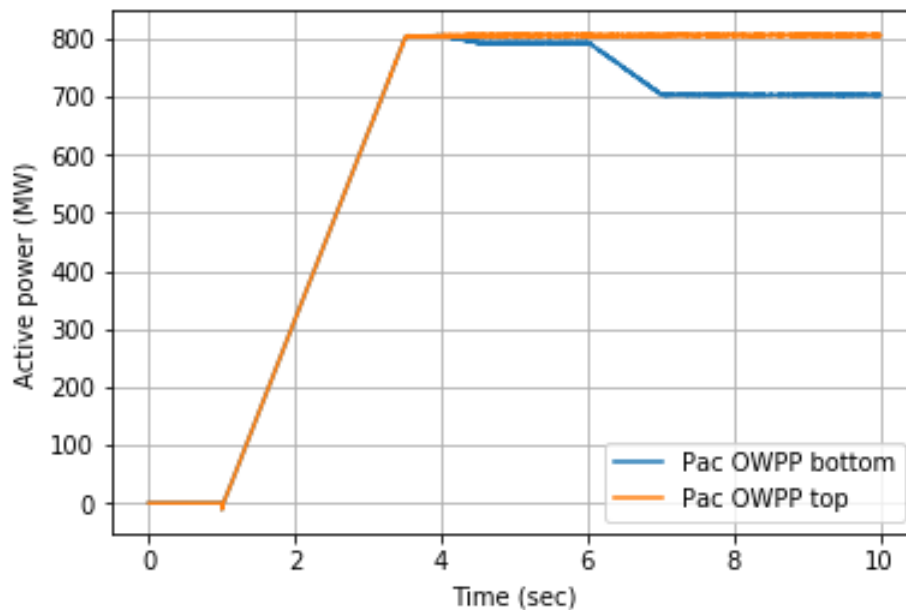
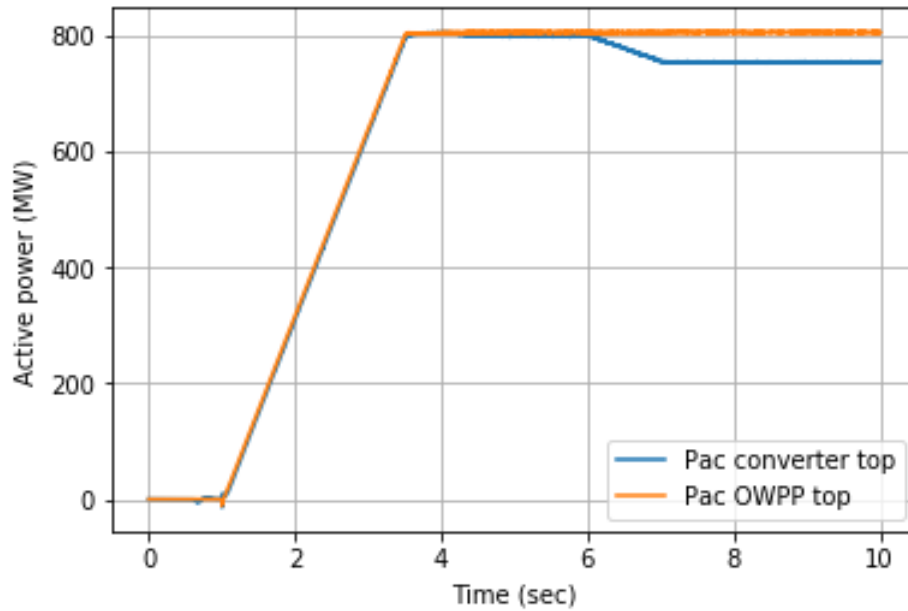


Figure 4.7: Slow ramp down of turbines and active power loading of top and bottom OWPP

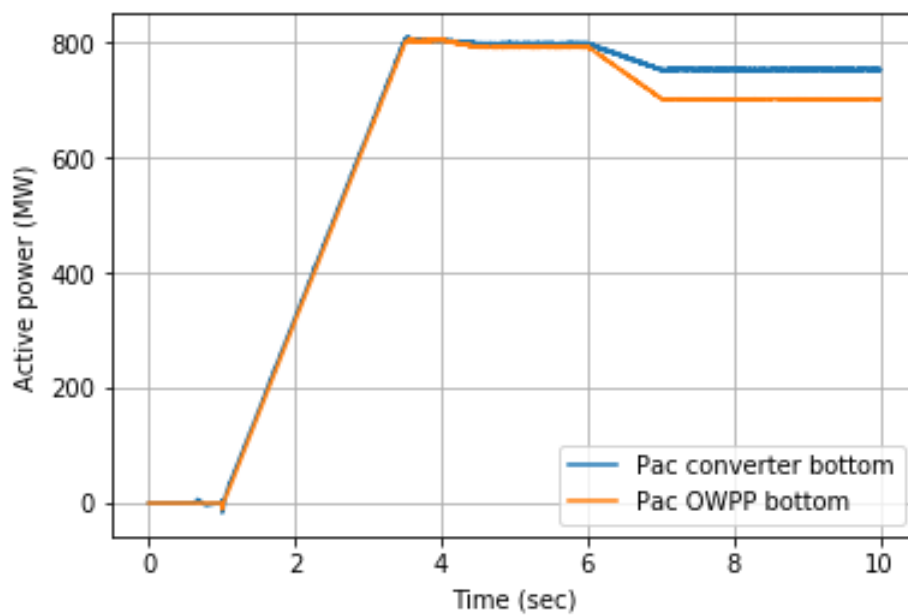
4.3.1. Power set points control

Figure 4.8 shows that, during the controlled ramp down of wind turbines under power set point control strategy the converters are loaded equally. In appendix 7.2.3, the Figure 7.6 shows that the onshore DC voltage is well regulated as per the ramp-up and down of power. The offshore DC voltages of the two poles show unbalance initially, due to the high ramp-up rate but eventually reach to the rated value after the ramp up. DC currents show two peaks, at 0.2s and 0.6s as the converters are de-blocked and the inrush currents flow to charge the SM capacitors and HV cables. Active

and reactive power transferred through the interlink show that the control strategy is balancing the converter loadings.



(a) Active power loading of top OWPP and converter

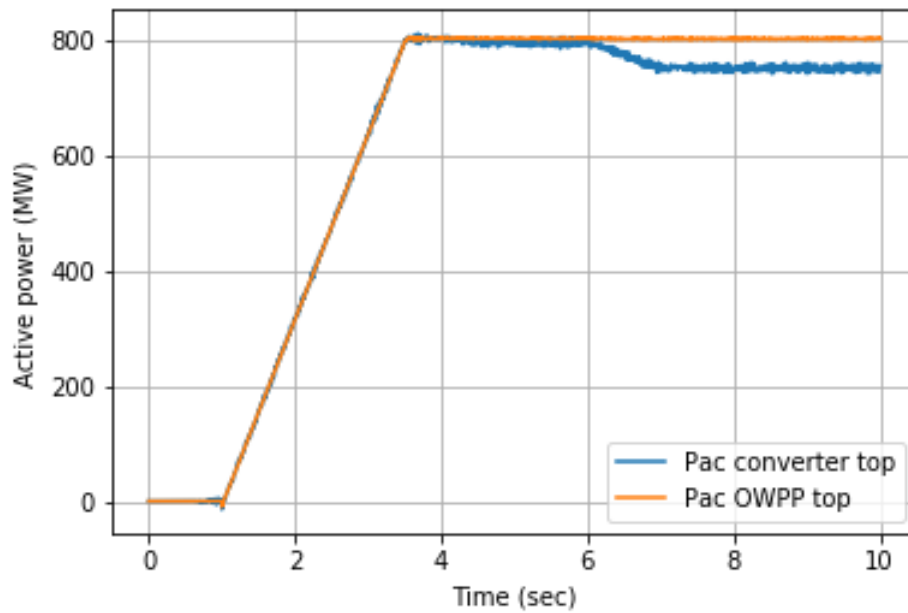


(b) Active power loading of bottom OWPP and converter

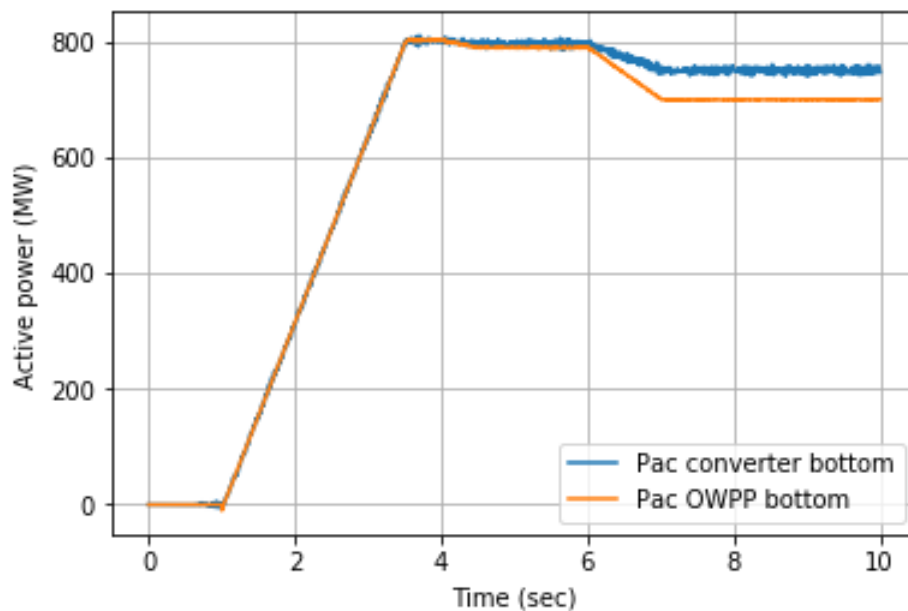
Figure 4.8: Active power loading of both OWPP and converters under power set points control with controlled ramp down of wind turbines

4.3.2. Droop control

Droop control strategy is able to regulate power to ensure equal converter loading of the converters as shown in Figure 4.9. Figure 7.7 from appendix 7.2.3, shows that the onshore and offshore voltages are well regulated without any irregular unbalance between the two poles.



(a) Active power loading of top OWPP and converter



(b) Active power loading of bottom OWPP and converter

Figure 4.9: Active power loading of both OWPP and converters under droop control with controlled ramp down of wind turbines

4.4. Loss of wind turbine and string of the OWPP

The wind turbines connecting submarine cables might have a fault and thus the OWPP loses a wind turbine or whole string of wind turbines. The OWPP is not modelled with individual strings, as shown in Figure 3.15. Hence faults within the OWPP cannot be simulated. It is assumed that the protection equipment will be able to limit fault current and the converter control strategies are tested only under loss of power. To test the HVDC link under a wind turbine loss scenario, a sequence of operations is designed as shown in table 4.2. Maximum ramp-up rate is limited at 350MW/s as in the previous case. Ramp-down is done with an infinite ramp-down rate to simulate instantaneous loss of wind turbines. Figure 4.10 shows, the active power loading of the top and bottom OWPPs as per the sequence described in table 4.2.

Time (s)	Operation sequence
0.2	Onshore converters De-block
0.6	Offshore converters De-block
1.0	OWPPs in operation (800MW each) with slow ramp up
4.0	Wind turbine (10MW) attached to bottom OWPP lost
6.0	Wind turbine string (90MW) attached to bottom OWPP lost
8.0	Three wind turbine strings (270MW) attached to bottom OWPP lost

Table 4.2: Sequence of operations to simulate loss of wind turbines

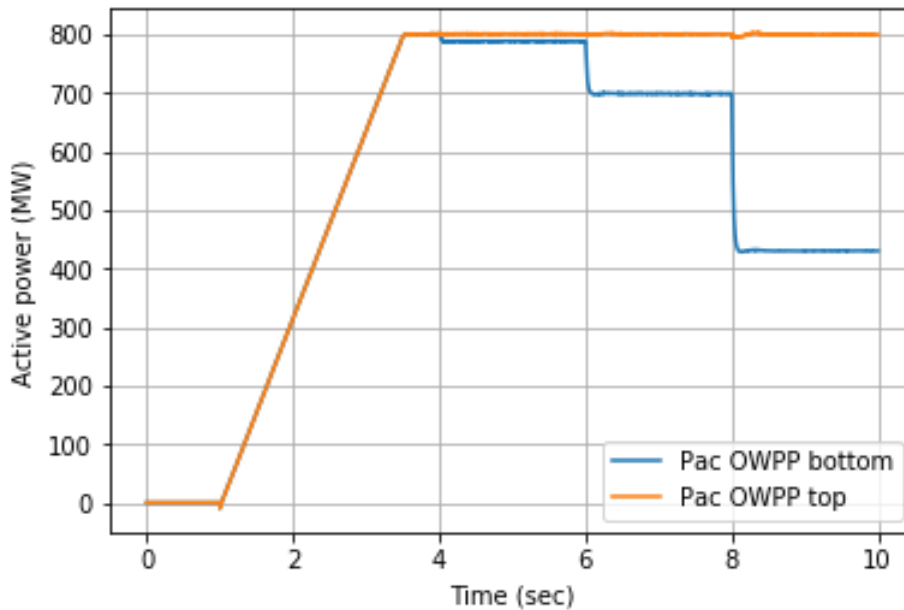
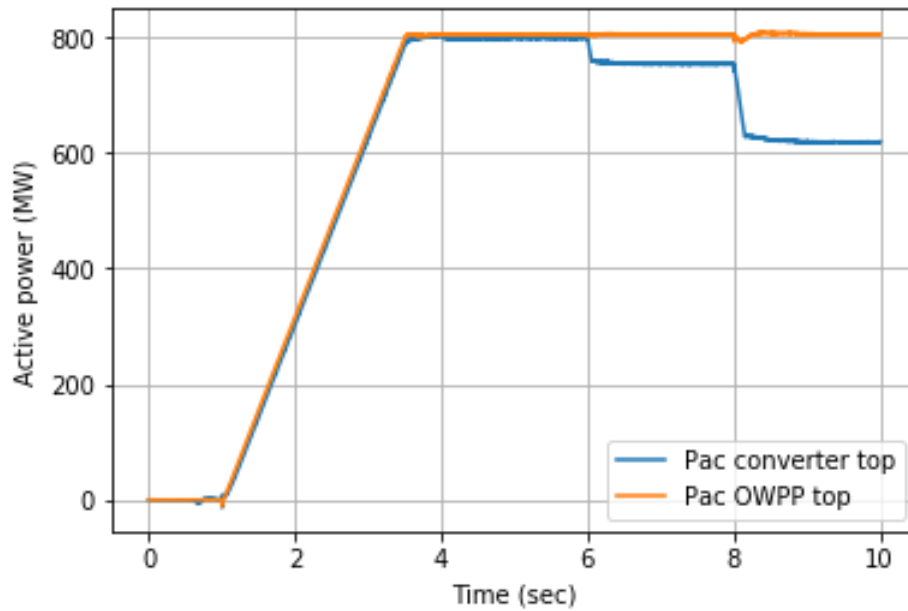


Figure 4.10: Active power loading of top and bottom OWPP under loss of wind turbines

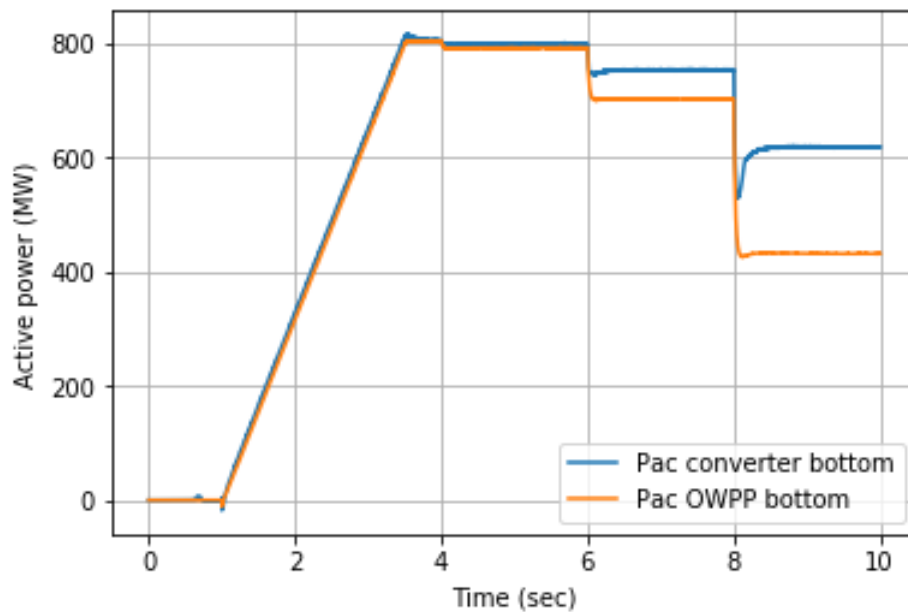
4.4.1. Power set points control

Figure 4.11 shows that, during the loss of wind turbines with power set point control strategy the converters are loaded equally. Figure 7.8 in appendix 7.2.4, shows that the onshore DC voltage is well regulated as per the ramp-up and loss of power. Initial DC voltage unbalance during ramp-up

and behavior of DC currents is similar to previous scenario. Overall, HVDC-link is able to reject disturbances and continue operation without any major DC voltage fluctuations due to the loss of wind turbines.



(a) Active power loading of top OWPP and converter

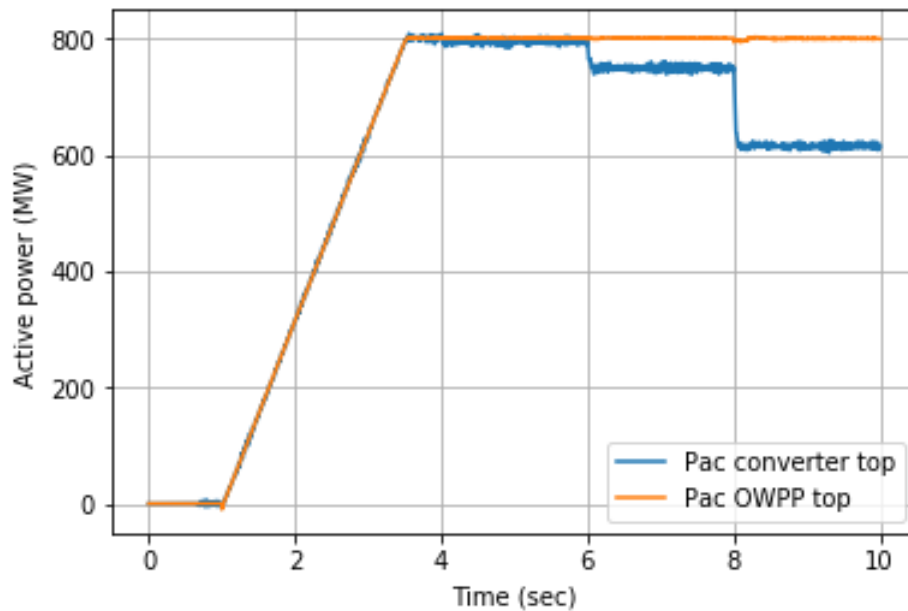


(b) Active power loading of bottom OWPP and converter

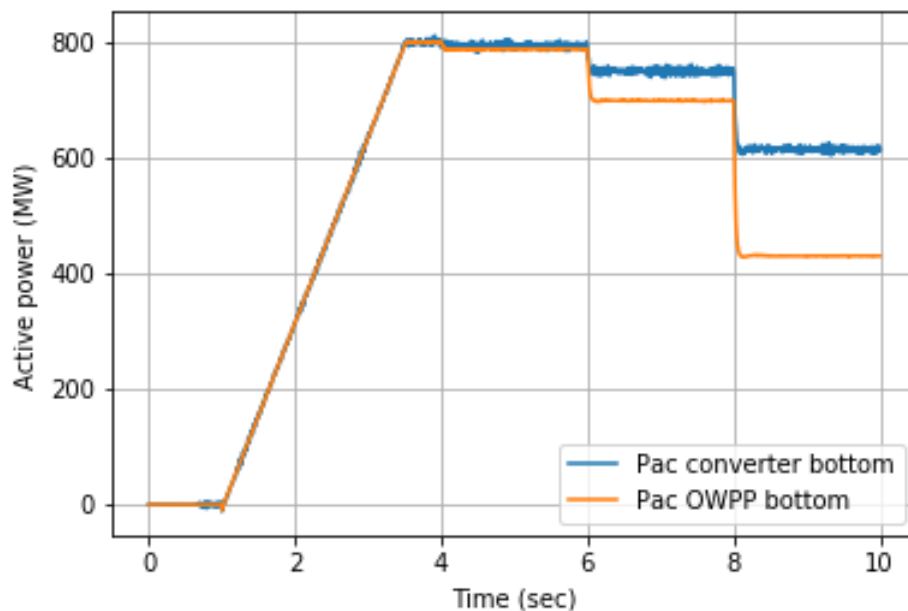
Figure 4.11: Active power loading of both OWPPs and converters with power set points control under loss of wind turbines

4.4.2. Droop control

Under droop control strategy the converters are loaded equally as shown in Figure 4.12. Figure 7.7 in appendix 7.2.4, shows that the onshore and offshore voltages are well regulated without any irregular unbalance between the two poles due to loss of wind turbines.



(a) Active power loading of top OWPP and converter



(b) Active power loading of bottom OWPP and converter

Figure 4.12: Active power loading of both OWPPs and converters with droop control under loss of wind turbines

4.5. Fault in the cable connecting wind farm and converter

The 66kV cable connecting the OWPP and converter, as shown in Figure 3.13, may undergo fault. In such a scenario, the breaker disconnects the faulty cable and connected OWPP from the offshore AC grid until the fault is subsided. As per the grid code applied on the offshore voltage, the converters should be able to maintain certain AC voltage and frequency if the fault is for a short duration. To consider the worst-case scenario only results of three-phase fault are included in this report. During three phase to ground fault the impedance of the faulty cable reduces and the currents from connected equipment in the network starts to flow towards the fault. After, the fault is subsided the converters should return to the rated parameter values and restart the usual operation. Table 4.3 describes the sequence of operation designed to simulate a three-phase fault in the cable between top converter and OWPP.

Time (s)	Operation sequence
0.2	Onshore converters De-block
0.6	Offshore converters De-block
1.0	OWPPs in operation (800MW each) with slow ramp up
4.0	Three phase fault in the cable connecting top OWPP and top converter
4.005	Fault detected and breaker opens
4.1	Fault subsided
4.2	Breaker closes

Table 4.3: Sequence of operations to simulate fault in the cable connecting top OWPP and converter

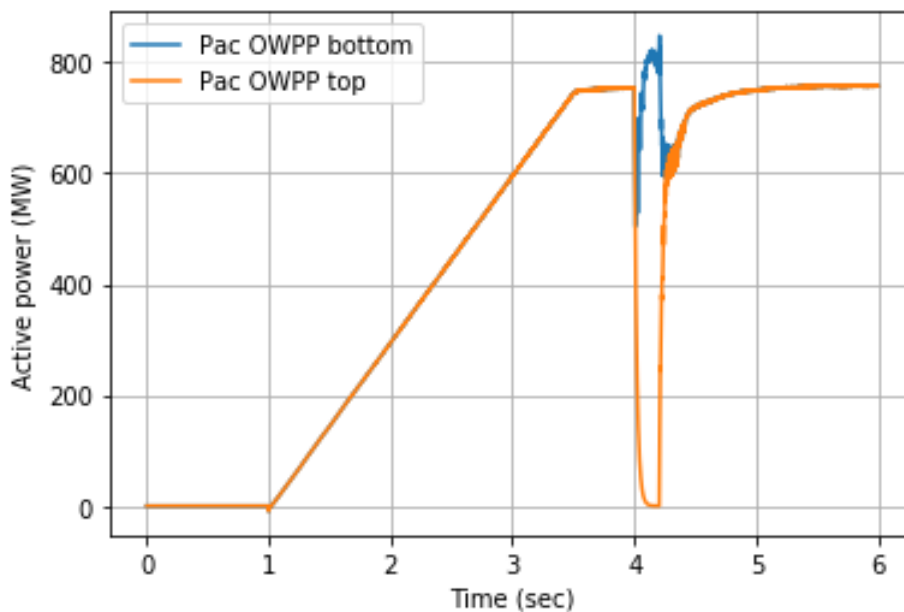
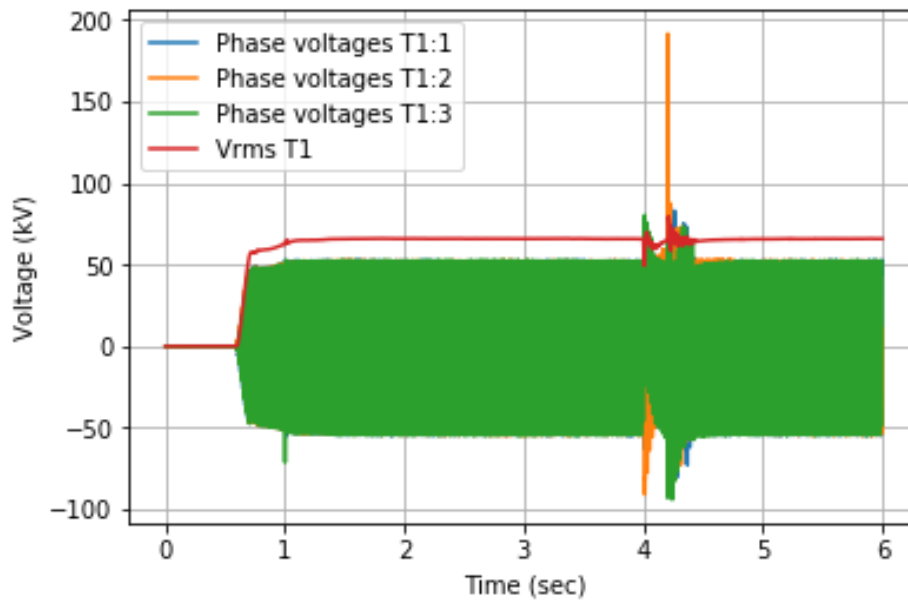


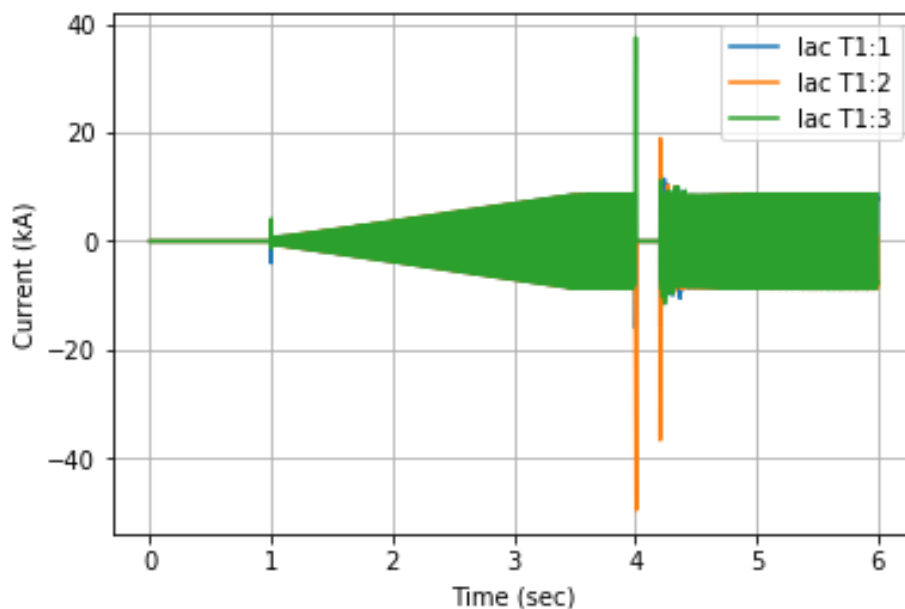
Figure 4.13: Active power loading of top and bottom OWPP under fault in the cable connecting top OWPP and converter

4.5.1. Power set points control

Figure 4.14 shows that, during the fault in the cable connecting top OWPP and converter with power set point control strategy the converters are able to maintain the offshore AC voltage. Figure 7.6 in appendix 7.2.5, shows that the HVDC-link is able to recover and continue usual rated operation after the fault.



(a) Three phase AC and RMS voltage of the offshore Terminal 1 (top)

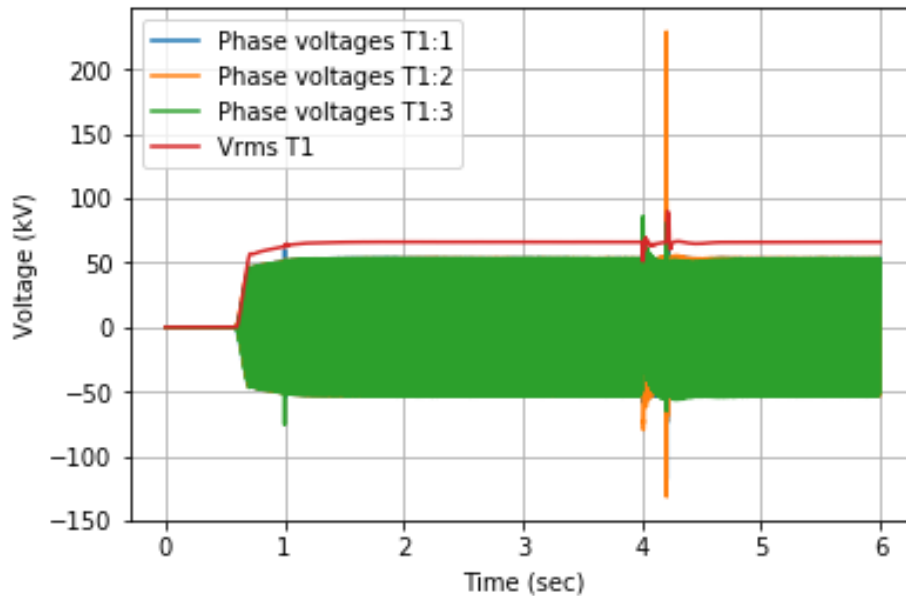


(b) Three phase AC current of the offshore Terminal 1 (top)

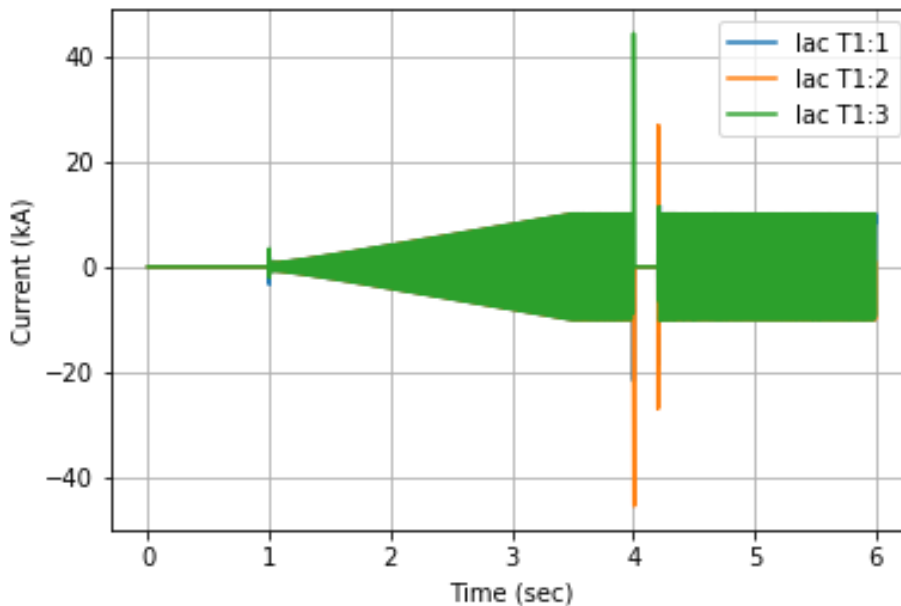
Figure 4.14: Three phase AC voltage and current of offshore Terminal 1 (top) with power set point control under fault in the cable connecting top OWPP and converter

4.5.2. Droop control

Under droop control strategy the converters are able to maintain AC voltage and frequency during fault as shown in Figure 4.15. Figure 7.7 in appendix 7.2.5, shows that the HVDC-link continues the regular operation after the recovery from the fault.



(a) Three phase AC and RMS voltage of the offshore Terminal 1 (top)



(b) Three phase AC current of the offshore Terminal 1 (top)

Figure 4.15: Three phase AC voltage and current of offshore Terminal 1 (top) with droop control under fault in the cable connecting top OWPP and converter

5

Results and discussion

From the results of previous sections in Appendix 7.2, it can be concluded that the control strategies mentioned in section 3.1 are able to regulate the offshore power loading and voltage of the converters without any major fluctuations. Both tested control strategies were able to support the initial reactive power demand of the OWPPs and black-start. Analysis done in section 4.2 shows that the control strategies are able to handle the real-life wind variations.

5.1. Steady-state performance

As the MMC creates the DC voltage artificially, fluctuations of $\pm 2kV$ remain in the steady-state between the top and bottom pole. DC voltage noise influences AC power loading and AC voltage with a small amount of noise.

In the droop control strategy, both converters are working under the island mode scheme, which doesn't have any current limiting and inner current control loop. The active and reactive power loading of the converter depends entirely on the frequency and voltage of the converter, respectively. Hence, noise in the power loading of converters is present due to the fluctuations in DC voltage and control related discrepancies within the converter. Using an offshore AC filter helps to reduce the noise in steady-state reactive power loading but increases the ground current from the offshore AC filter.

However, in Power set point control strategy, as one of the converters is constantly balancing the power with the inner current control loop, the power can be controlled with improved accuracy, and this reduces noise. Absence of an inner current control loop affects the controller performance in tracking and maintaining the steady power loading of the converter.

Table 5.1 summarizes the major observations from the analysis of the HVDC-link during steady-state operation.

Parameter	Power set point control	Droop control
Pac offshore	Converters are loaded equally in steady-state with minimal noise ($\pm 0.5 MW$).	Converters are loaded equally in steady-state with a small amount of noise ($\pm 1.0 MW$).
Qac offshore	Converters are loaded equally in steady-state with minimal noise ($\pm 0.5 MVar$).	Converters are loaded equally in steady-state but with large noise ($\pm 3.0 MVar$).
DC voltage offshore	No unbalance, during steady-state.	No unbalance, during steady-state.
DC voltage onshore	Uninfluenced by the control strategy, maintained at the rated value by onshore converters.	Uninfluenced by the control strategy, maintained at the rated value by onshore converters.
DC current	Balanced between both poles uninfluenced by the control strategy. Magnitude depends only on the active power.	Balanced between both poles uninfluenced by the control strategy. Magnitude depends only on the active power.
Vac offshore (RMS)	Remains constant	Remains constant with small noise
Frequency offshore	Remains constant.	Remains constant.
Iac offshore	Controlled by OWPP only.	Controlled by OWPP only.

Table 5.1: Summary of performance of the control strategies under steady-state operation.

5.2. Dynamic state performance

Both the control strategies are able to reach a new balanced steady-state due to sudden power difference. However, converters go through slight unbalance during the transient state with the power set points control strategy as modifying the state of operation of both inner and outer control loops causes delay. Due to this lagging behavior, the power set points controlled offshore converters will always have slight overshoot/undershoot in power loading depending upon the unbalance. Droop control strategy instantaneously balances power without regulating currents and controlling power indirectly via AC frequency and voltage without any significant delay.

Table 5.1 summarizes the major observations from the analysis of the HVDC-link during the dynamic operation.

Parameter	Power set point control	Droop control
Pac offshore	Initial loading unbalance during transient states due to lagging power control.	No loading unbalance during transient states, due to rapid P/freq control.
Qac offshore	Initial loading unbalance during transient states due to lagging power control.	No loading unbalance during transient states, due to rapid Q/Vac control.
DC voltage offshore	Unbalance between pole voltages, present during high ramp-up/ ramp-down rates.	No unbalance between poles voltages, during ramp-up or ramp-down, due to fast control action.
DC voltage onshore	Well regulated by the onshore converters, as per the sudden changes in power loading of poles.	Well regulated by the onshore converters, as per the sudden changes in the power loading of poles.
DC current	Remain balanced.	Remain balanced.
Vac offshore	Remain constant.	Regulated as per the Qac loading of converters.
Frequency offshore	Remain constant.	Regulated as per the Pac loading of converters
Iac offshore	Controlled only the OWPP.	Controlled only by the OWPP.

Table 5.2: Summary of performance of the control strategies under dynamic operation.

From the analysis done in section 4.3, it can be concluded that during the controlled ramp-up or ramp-down of power through the OWPP the rate must be limited up to $90\text{MW}/\text{s}$ to avoid any DC voltage unbalance between poles. That means, for the assumed OWPP structure, the strings must be activated at the rate of one string (9 wind turbines) per second (or lower) per OWPP. This maximum rate of $90\text{MW}/\text{s}$ considers maximum power output from each of the wind turbines which considering the real-life variable wind speeds is a conservative assumption. In real-life, the OWPP power capacity is ramped up or down with far lower rates with changes made in order of minutes. Hence, it can be concluded that both control strategies will be able to maintain stable behavior under controlled modifications in power generation by the OWPP in a similar HVDC-link.

During, the sudden loss of power analysis in section 4.4 under both control strategies, the offshore pole voltages did not have any significant overvoltage ($> 10\text{kV}$) with the loss of a wind turbine (10MW) or string (90MW). However, under the loss of three strings (270MW) with power set point control strategy, the poles go through an unbalance with overshoot up to 550kV in one pole and undershoot up to 490kV in the other pole for 0.5s . This unbalance is not present in case of droop control strategy where both the poles go through a disturbance of 10kV for 0.5s . While in both cases, the offshore AC voltage was well regulated, with an undervoltage up to 65kV for 0.5s . Thus, it can be concluded that in order to sustain operation during the loss of more than three wind turbine strings (270MW) in one of the OWPP, the droop control strategy is preferable. The cable ratings need not be altered as the overvoltages are well under rated 1.15pu limit.

The dynamic performance of the converters is directly influenced by the amount of unbalance in the converter loading and controller outer-loop tuned bandwidths. For example, during the loss of power within one of the OWPP, there exists an unbalance between the converter power loadings. As DC currents can't be unequal, the direct impact is over the offshore pole DC voltages. The impact of this scenario over onshore DC voltages depends directly upon the PI controller tuning of onshore DC voltage controllers. If the PI tuning parameters of the offshore power controller/droop controller are optimally tuned, then the offshore pole loading will be balanced again. The speed and performance of the system to reach a new steady-state depends upon the controller bandwidths. However, the time taken to reach the new steady-state is depending on the amount of power unbalance.

5.3. Maximum mismatch and Fault

From the analysis done in section 4.4 it can be concluded that if the sudden mismatch in the loading of the converters is below the limit of $270\text{MW}/\text{s}$ the DC voltage maximum deviation in the offshore top and bottom poles remains between the 1.1pu and 0.9pu rating for 0.5s . Thus, the HVDC link can continue operation as per the new steady-state without any major DC overvoltages or overcurrents.

Under a fault, converters are required to control voltage and limit overcurrents. As mentioned in the section 2.6 the island mode control doesn't have any current control loop and uses virtual impedance to reduce AC voltage magnitude to limit the overcurrents. AC overcurrent up to 48kA exists in case of a fault in the cable connecting top OWPP and converter under the Droop control strategy. While in case of Power set point control strategy the peak overcurrent remains lower as shown in the section 4.5.

Due to the current limiter in the Power controlling (top) converter in Power set point control strategy, the currents can be limited more effectively. However, as both offshore converters are working under island mode in case of Droop control strategy, it suffers from higher overcurrents peak during a fault.

5.4. Power set point control vs Droop control strategy

Both designed control strategies are able to handle the given analysis cases and sustain the stable operation of the point-to-point HVDC-link. Although both of them also have drawbacks and benefits in terms of performance over each other when compared.

The power set point control strategy will require external communication between poles to calculate reference power set points for the controllers. External communication might cause slight communication delay, which will result in higher rise times compared to the droop control strategy. Power set point has inherent behavior of initial loading unbalance in case of sudden variations in OWPP power generation as both offshore converters are following different control strategies (power control and grid-forming control). But, the stable steady-state performance of the power set point control is a big benefit over droop control strategy.

Droop control strategy is able to shift to the new power loading instantaneously and thus has a better dynamic performance. However, as the active power loading is dependent directly over the frequency and DC voltage of the pole, noise in DC voltage influences the converter power loading in steady state. The absence of the inner current loop gives faster dynamics but decreases the control performance. Noise in offshore AC voltage induces noise in converter reactive power loading. Thus, the droop control strategy has inherent noise in the converter active and reactive power loadings. To avoid noise in the active power loading number of SM in the converters can be increased to smooth the DC voltage but, small noise up to $2kV$ will always be present. To avoid noise in reactive power loading, AC filters can be used offshore, which will result in the ground current. Both of these solutions will be expensive and require higher maintenance.

The power set-point control strategy shows no unbalance in DC voltages of the two poles when the ramp up/down rate is controlled under the set limit ($90MW/s$). In case of the sudden loss of power up to $270MW$ in one of the OWPPs, there is unbalance in DC voltages for only $0.5s$ within the set minimum and maximum DC voltage limits. Eventually, the system comes to a steady-state and has a stable operation in an acceptable time. Considering, the real-life wind fluctuations and possible power loss scenarios, power set point control strategy is the preferred control strategy for a similar HVDC-link.

6

Conclusion

This research aimed to find out the advantages of operating a Bipole HVDC link with an offshore AC interlink. The AC interlink can be attached to the offshore Bipole poles in both point-to-point and multiterminal links but, due to simplicity, only point-to-point link is analyzed. The primary benefit of an AC interlink in a point-to-point configuration is the ability to operate under DMR fault (Rigid Bipole) under the converter control strategies.

Two converter control strategies were proposed, Power set point control and Droop control to ensure equal loading of the offshore converters with the help of AC interlink in a Rigid Bipole configuration. Under Power set point control, the top and bottom offshore converters follow different control strategies controlling power balance and AC voltage. While in Droop control, both of the converters work as a slack bus sharing the active and reactive power loading as per the droop characteristics. Rigid Bipole point-to-point HVDC link was modelled with 900MW aggregated OWPPs in PSCAD.

After testing both of the control strategies under various possible scenarios, observations were recorded for dynamic and steady-state performances. Due to the absence of current control in the Droop control strategy and each offshore converter controlling different parameters in the Power set point control strategy, there are some inherent characteristics for both of the control strategies, as reported in section 5. These characteristics and observations depend upon the initial power unbalance and converter tuning. Due to the stable steady-state performance and fast dynamic performance the Power set point control strategy should be the preferred choice for an AC interlink control scheme.

The results show the consequences of the AC interlink based control schemes over the ratings of the power equipment, which are under the acceptable range. However, as the complexity of the model is not detailed enough for fast transients, extensive research needs to be done in order to substantiate the impact of the control strategies in real-life faults and transients. The modelled HVDC link doesn't include the protective equipment and unbalanced three-phase system control schemes.

Overall, this thesis presents a basic guideline to increase the Levelized cost of operation of Bipole HVDC links by attaching the offshore poles to the point of common coupling and designing suitable control strategies. The results show that the control strategies can be applied under various real-life scenarios with slight overvoltages within the acceptable range. Further research is

required to support the findings of this work for fast transients in a more detailed model.

6.1. Scope of future work

The OWPPs in this thesis are modelled as voltage-controlled instantaneous current sources. This way, the OWPP reacts to the power changes instantaneously without any lag. However, in real-life, each wind turbine has its own grid feeding converter connected to the turbine's generators. These converters control the power flow through the turbine, and hence the power variations are not instantaneous and have their own dynamic characteristics. To include the dynamics of the aggregated OWPP, active and reactive power control loops can be added to the current sources.

The OWPP can also be modelled as per the USTRAT or IEC (IEC 61400-27) wind farm standards with different run modes (start-up, run), converters and control strategies. Thus, the project can be extended to research about how the real-life OWPP dynamics will affect the dynamics of the control strategies and interlink power balance dynamics. With the complete model of the OWPP faults within the aggregated OWPP can also be tested which are modelled as just loss of power in this thesis work.

The converters are modelled as an arm-level average model, which can be further extended to investigate the impact of converter control strategies over the IGBTs and capacitors within the MMC. Faults within the arm of the MMC can also be tested with a higher detail converter model. In this thesis, only fault situation in the cable connecting the OWPP and offshore converter is examined. As the DC breakers can be added on the DC side of the poles and HVDC cable faults can also be tested. Since Half-bridge topology cannot block a DC fault, DC breakers will help to reduce fault currents. Other protective equipment such as surge arrestors and negative sequence current control scheme, can be added to the simulation model to have a more realistic fault response scenario.

HVDC-link remains connected to a strong onshore grid in the complete analysis. Thus, in the case of offshore power variations and faults, the onshore grid remains at a stable frequency and AC voltage. It will be interesting to observe how the dynamics of the control strategy change in case a similar HVDC-link is connected to a moderate or weak grid.

The above-mentioned points are related to increasing the complexity of a point-to-point HVDC link, but this analysis can be extended to a multiterminal connection. A bipolar multiterminal connection can be modelled and tested in the presence of an offshore AC interlink, as described in section 1.

7

Appendix

7.1. Appendix A

7.1.1. HVDC point to point link ratings

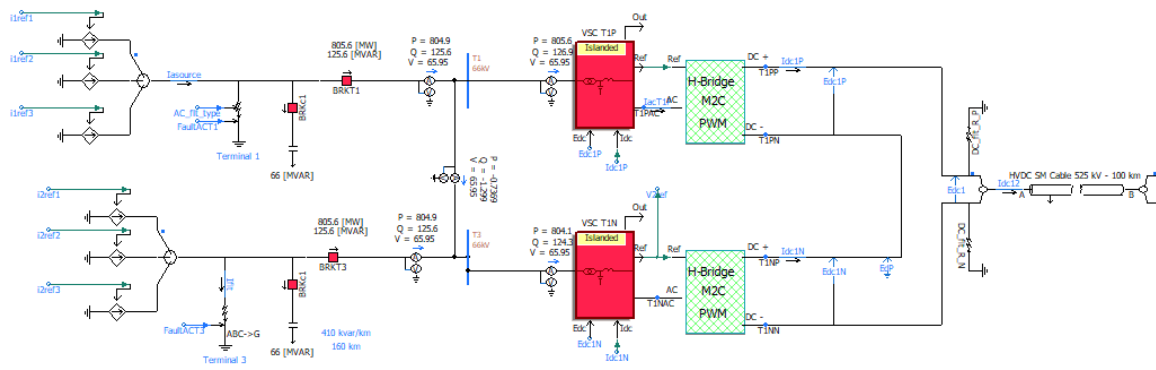
Parameter	Value
OWPP rating	900 MW
Converter rating	1 GW
Offshore AC bus voltage	66 kV
Pole DC voltage	525 kV
AC system Frequency	50 Hz
Onshore strong grid rating	10 GW
DC chopper rating	1 GW
Max DC voltage ¹	1.15 p.u.
Min DC voltage ²	0.85 p.u.
OWPP Reactive power requirement	66 MVar
Offshore transformer voltage rating	66/250 kV
Onshore transformer voltage rating	230/250 kV
Transformer leakage reactance (Xt)	0.1 p.u.
Converter submodule capacitor	15000 uF
Arm Reactor	50 mH
Number of SM in PWM	175
Total SM per arm	200
Simulation time step	250 us
Plot time step	250 us

Table 7.1: Ratings of the equipment used in the HVDC link modelling

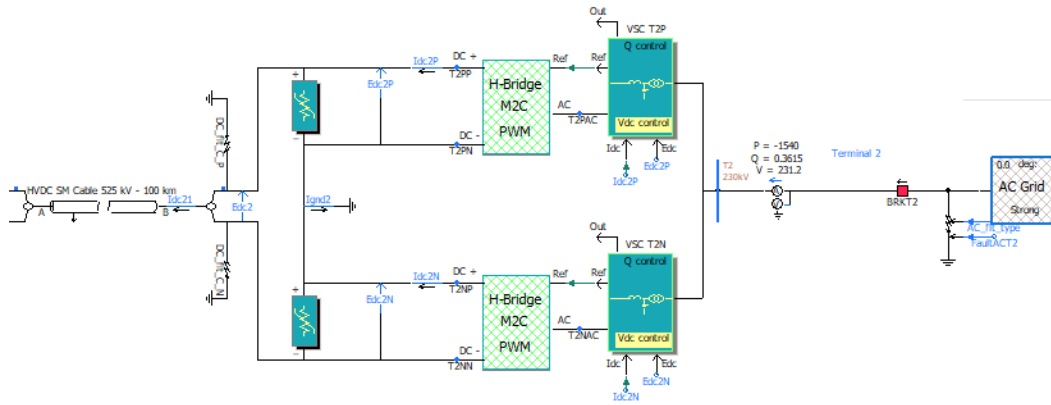
²ENTOSE

³DC stress: $V_{dc}/2 > V_{ac}$

7.1.2. PSCAD model HVDC point to point link



(a) Offshore segment with Terminal 1 and 3

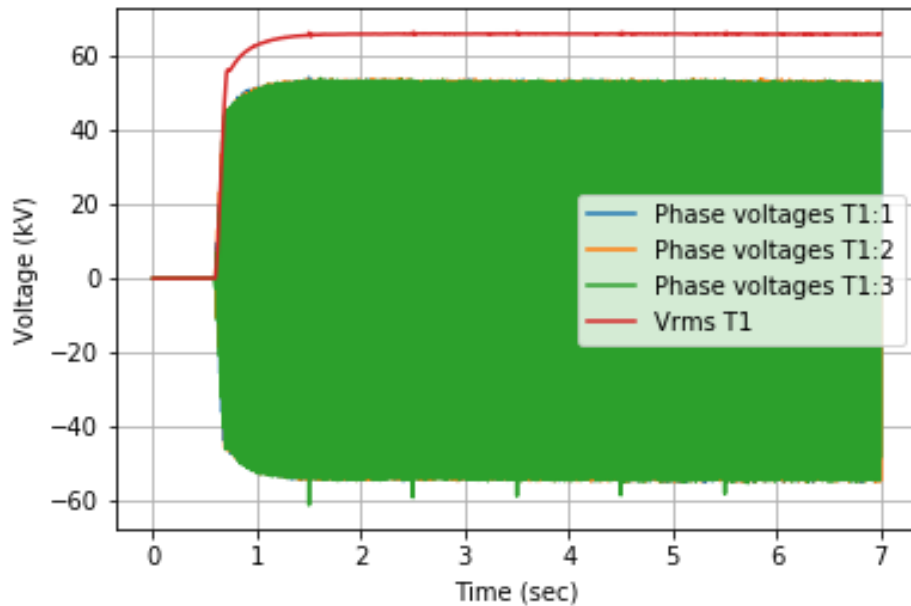


(b) Onshore segment with Terminal 2

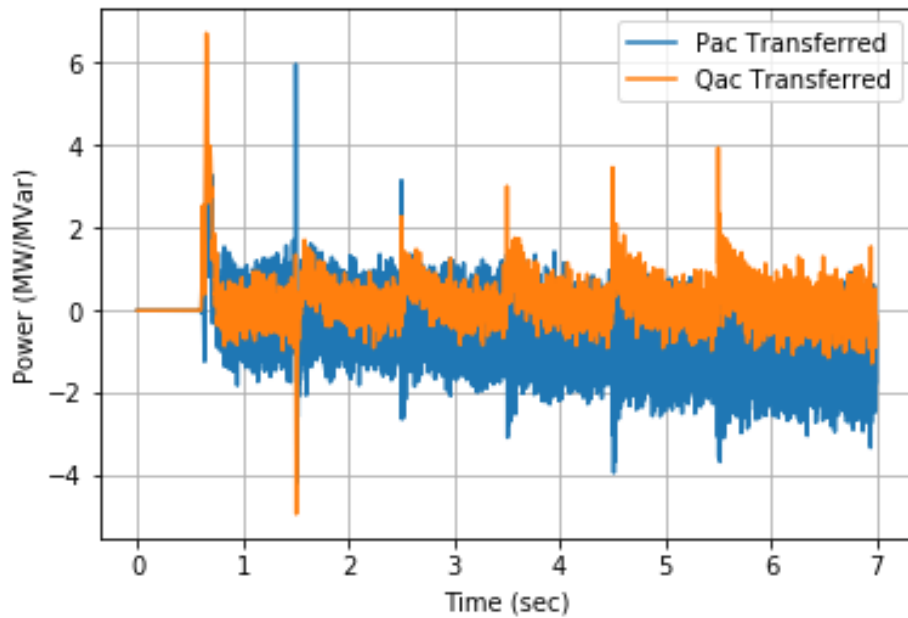
Figure 7.1: Designed PSCAD simulation model of the HVDC point to point link

7.2. Appendix B

7.2.1. Results: Energization of array cables

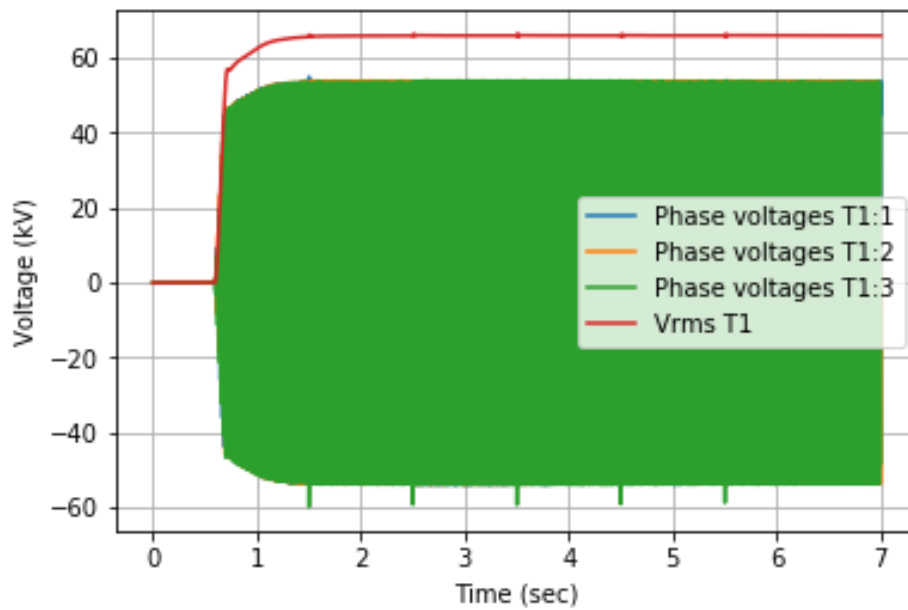


(a) Three phase AC and RMS voltage of the offshore Terminal 1 (top)

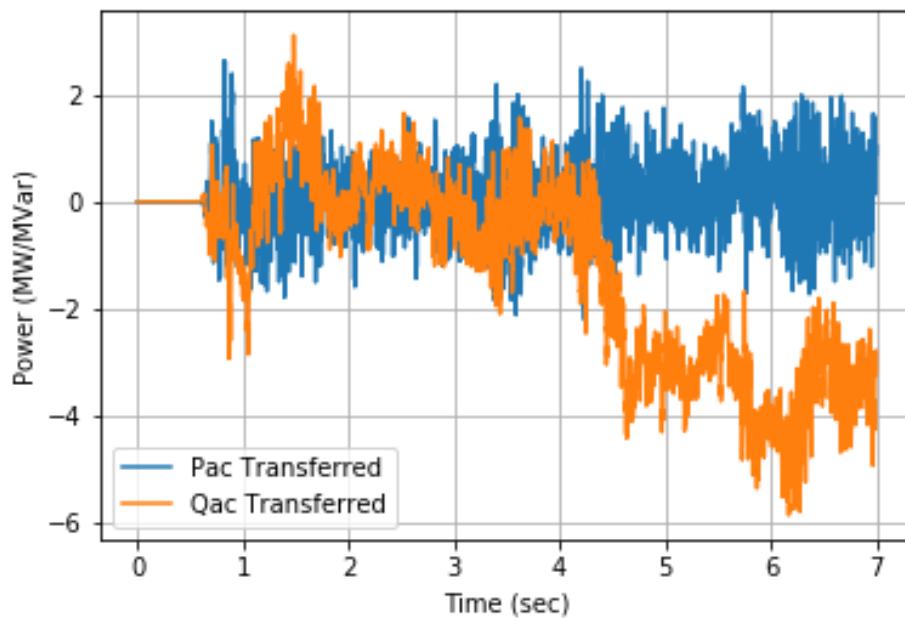


(b) Active and Reactive power transferred between top and bottom poles

Figure 7.2: HVDC-link characteristics under energization of array cables with power set points control



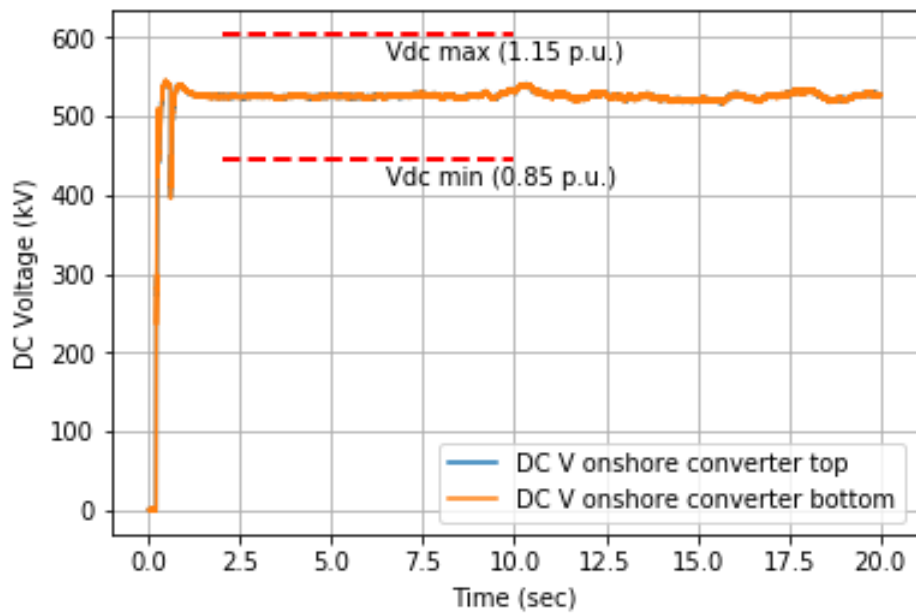
(a) Three phase AC and RMS voltage of the offshore Terminal 1 (top)



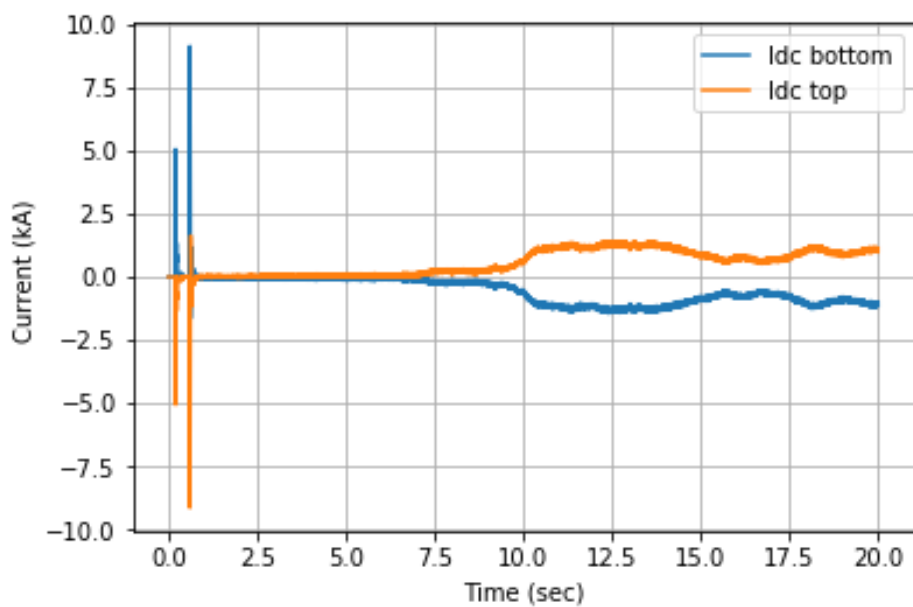
(b) Active and Reactive power transferred between top and bottom poles

Figure 7.3: HVDC-link characteristics under energization of array cables with droop control

7.2.2. Results: wind fluctuations

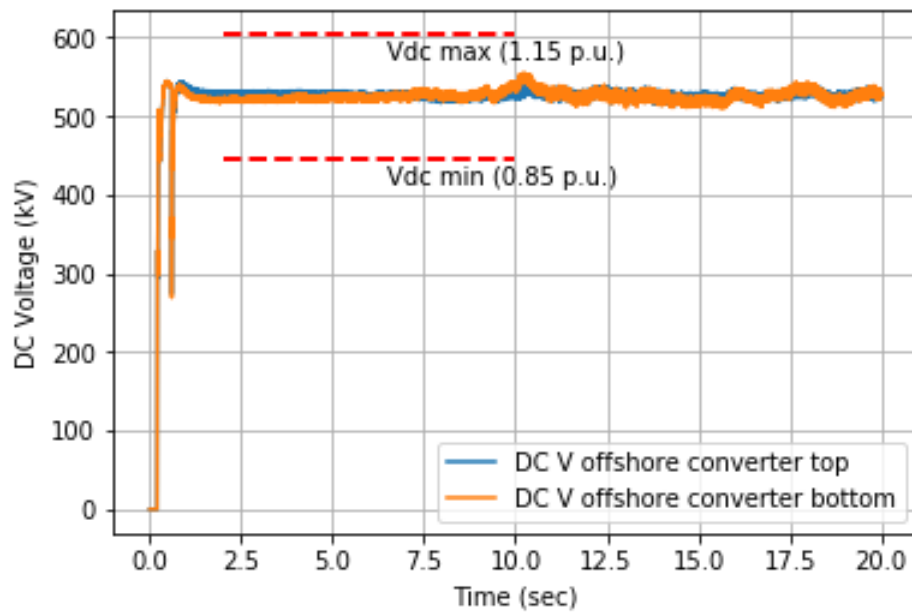


(a) DC voltage of top and bottom onshore poles

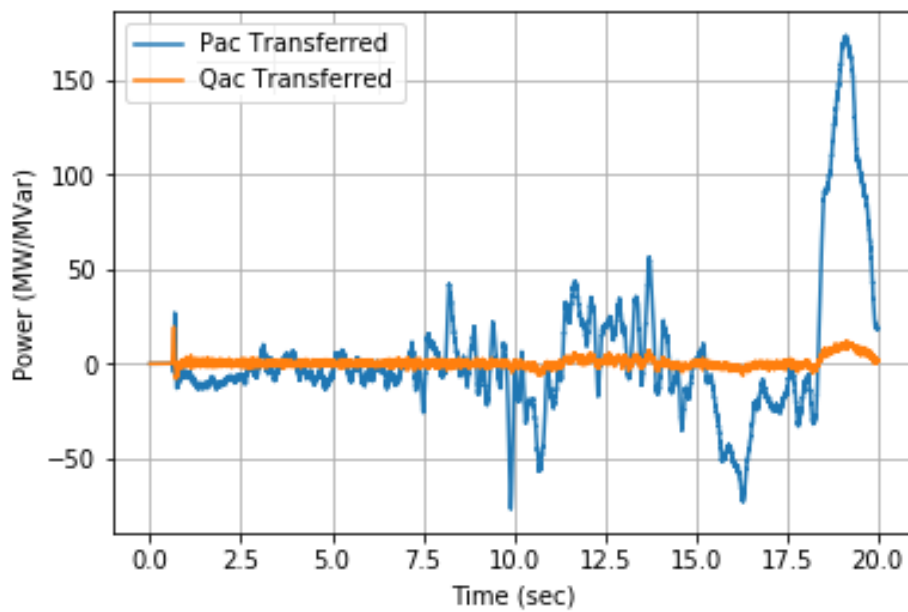


(b) DC currents of top and bottom poles

Figure 7.4: HVDC-link characteristics under wind fluctuations with power set points control

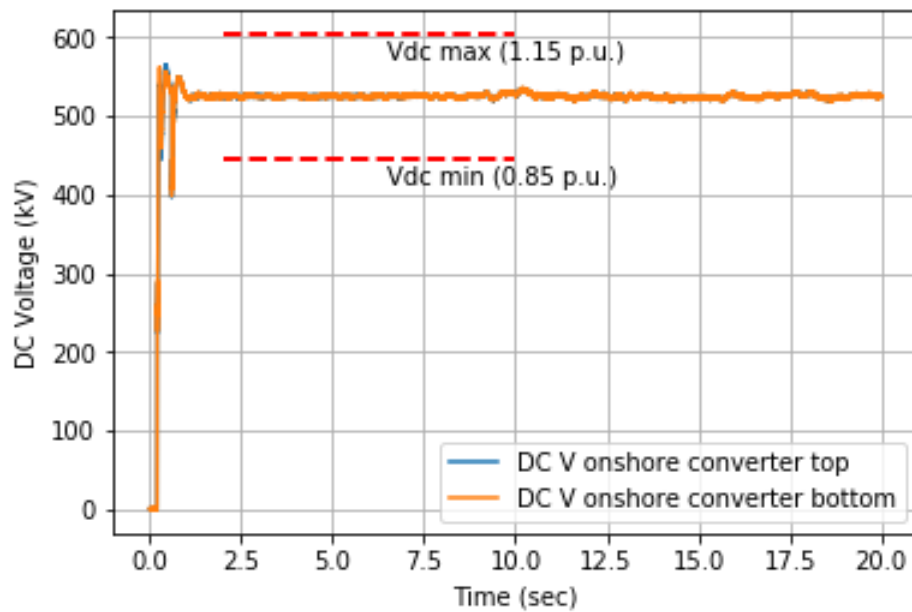


(c) DC voltage of top and bottom offshore poles

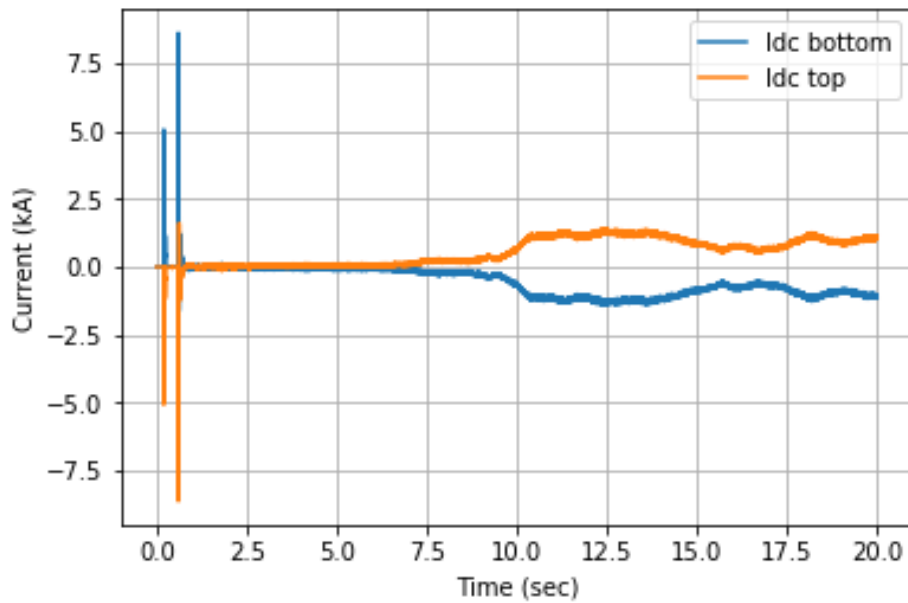


(d) Active and Reactive power transferred between top and bottom poles

Figure 7.4: HVDC-link characteristics under wind fluctuations with power set points control

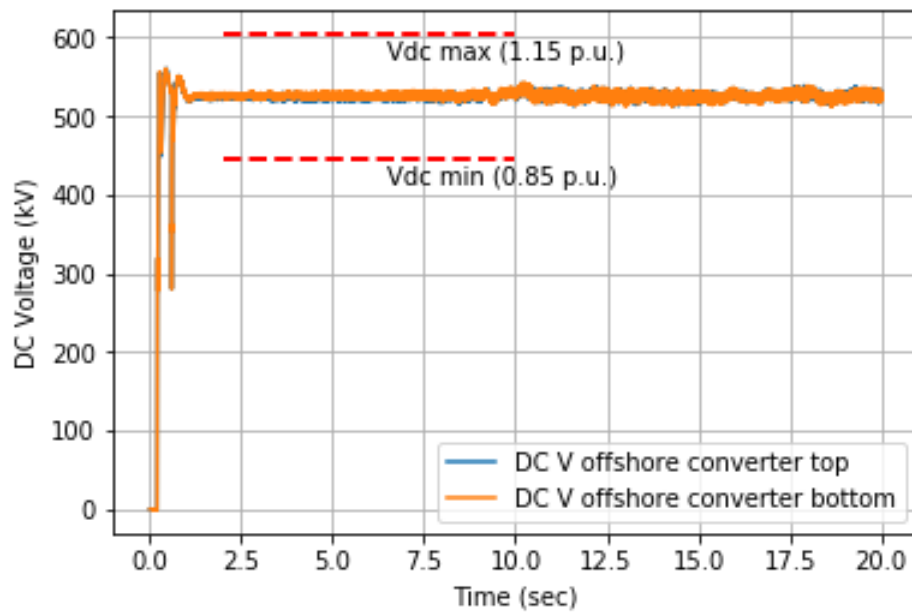


(a) DC voltage of top and bottom onshore poles

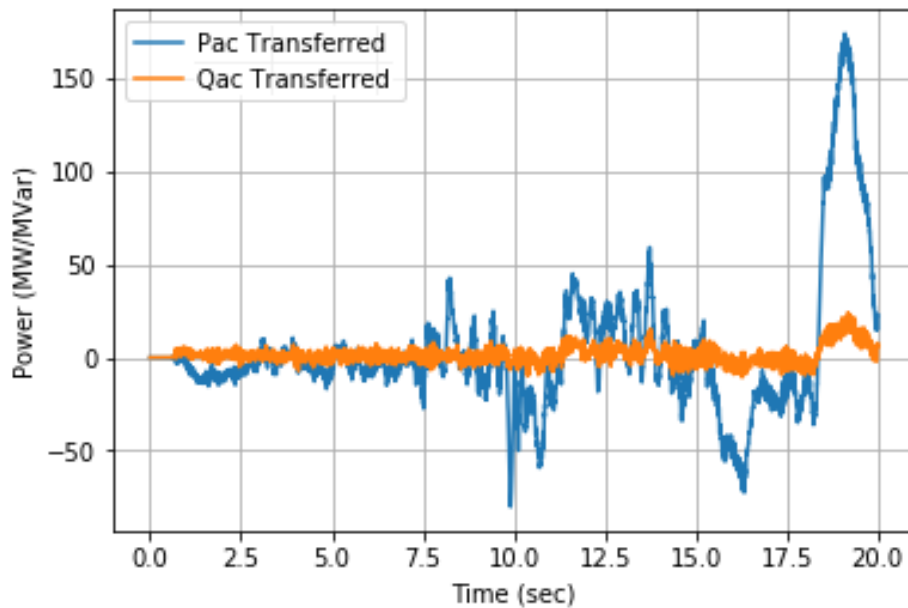


(b) DC currents of top and bottom poles

Figure 7.5: HVDC-link characteristics under wind fluctuations with droop control



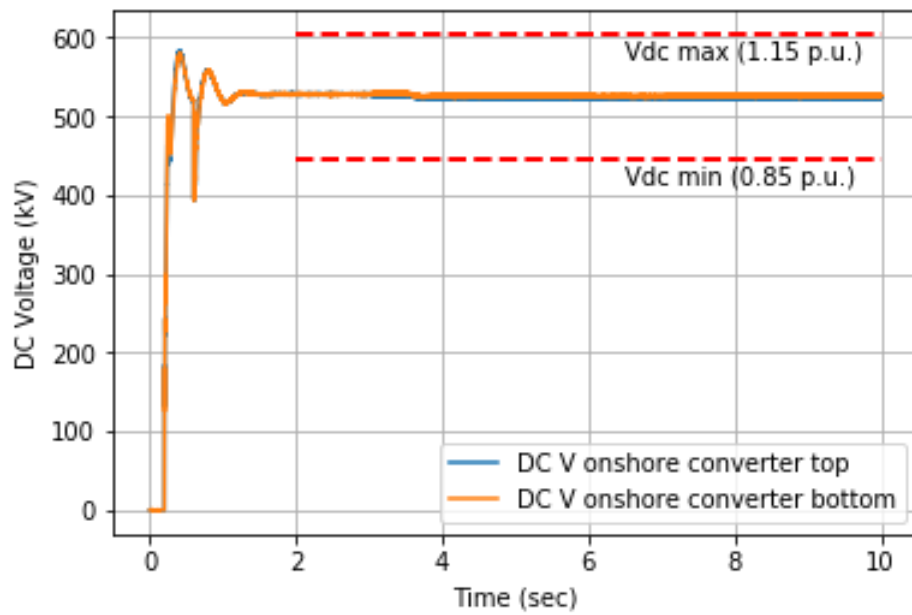
(c) DC voltage of top and bottom offshore poles



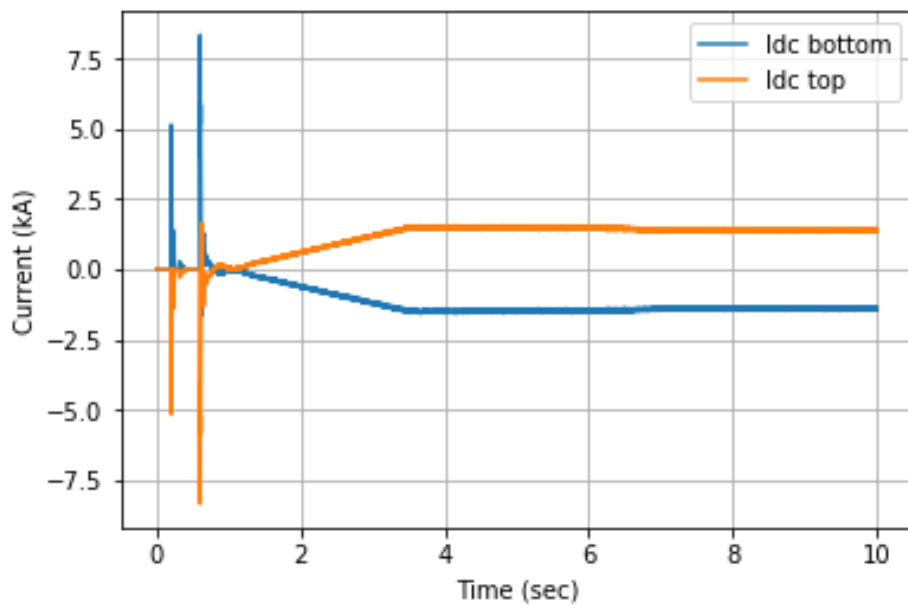
(d) Active and Reactive power transferred between top and bottom poles

Figure 7.5: HVDC-link characteristics under wind fluctuations with droop control

7.2.3. Results: Controlled ramp down of wind turbines

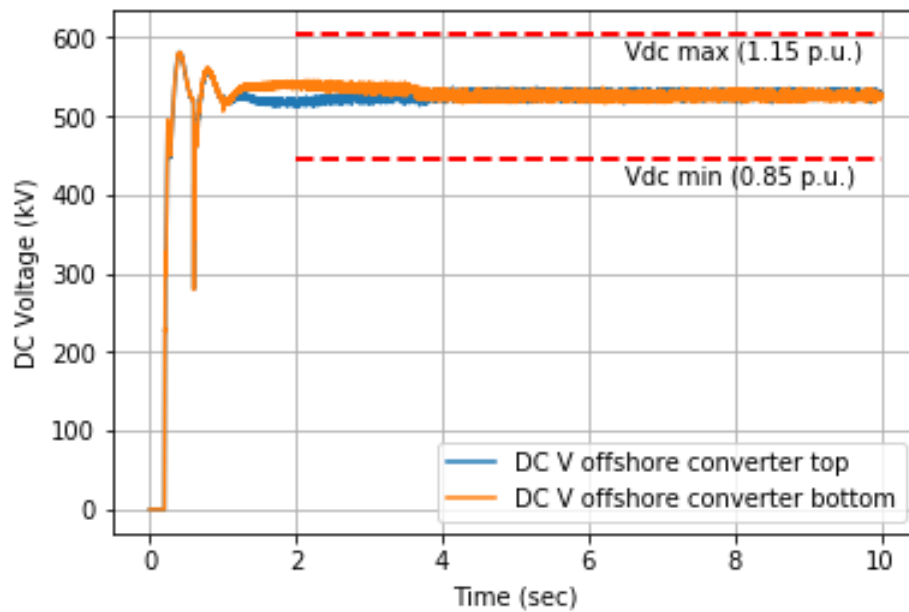


(a) DC voltage of top and bottom onshore poles

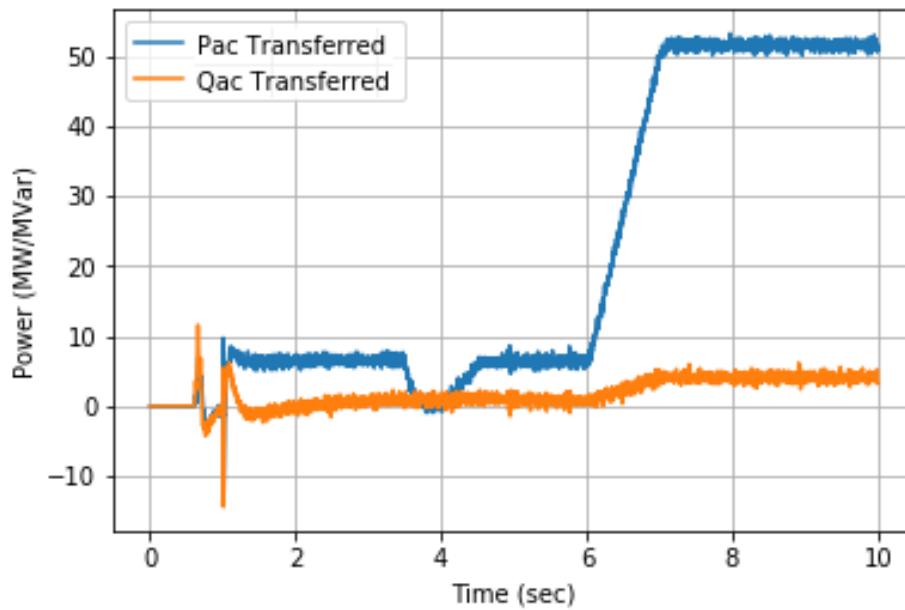


(b) DC currents of top and bottom poles

Figure 7.6: HVDC-link characteristics under controlled ramp down of wind turbines with power set points control

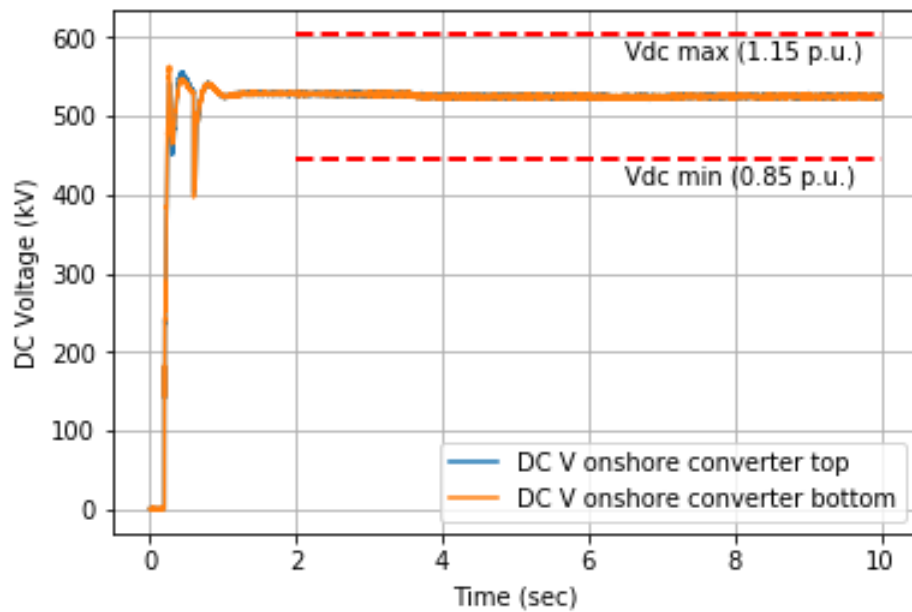


(c) DC voltage of top and bottom offshore poles

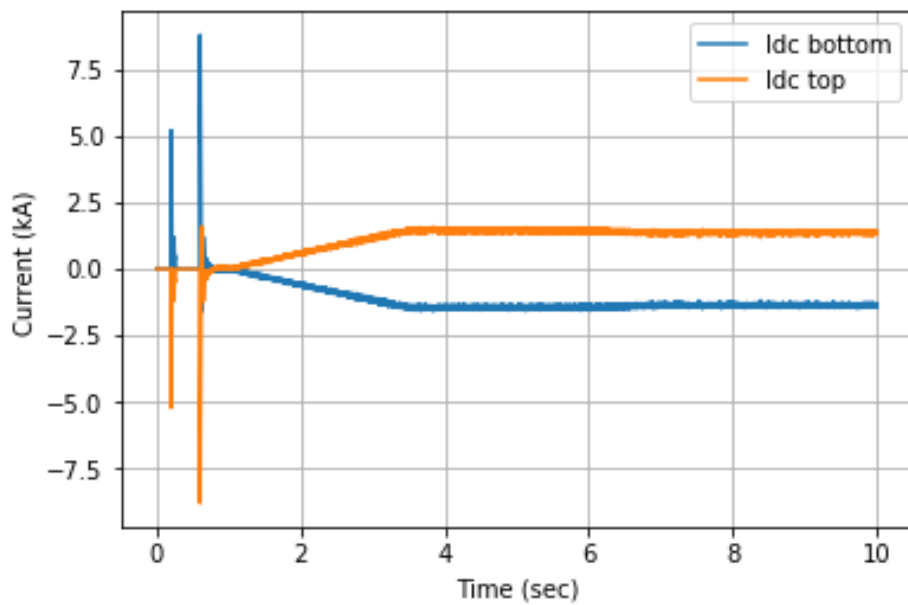


(d) Active and Reactive power transferred between top and bottom poles

Figure 7.6: HVDC-link characteristics under controlled ramp down of wind turbines with power set points control

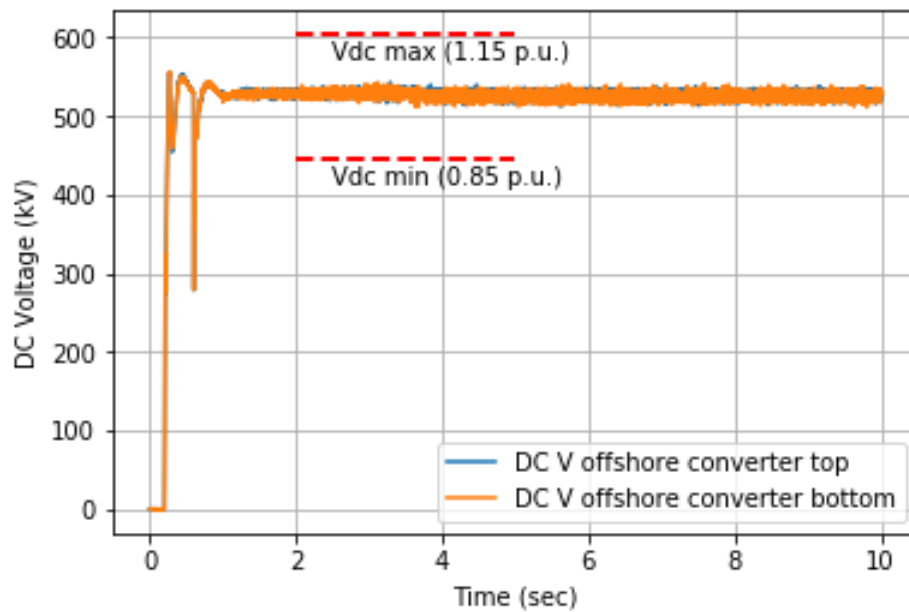


(a) DC voltage of top and bottom onshore poles

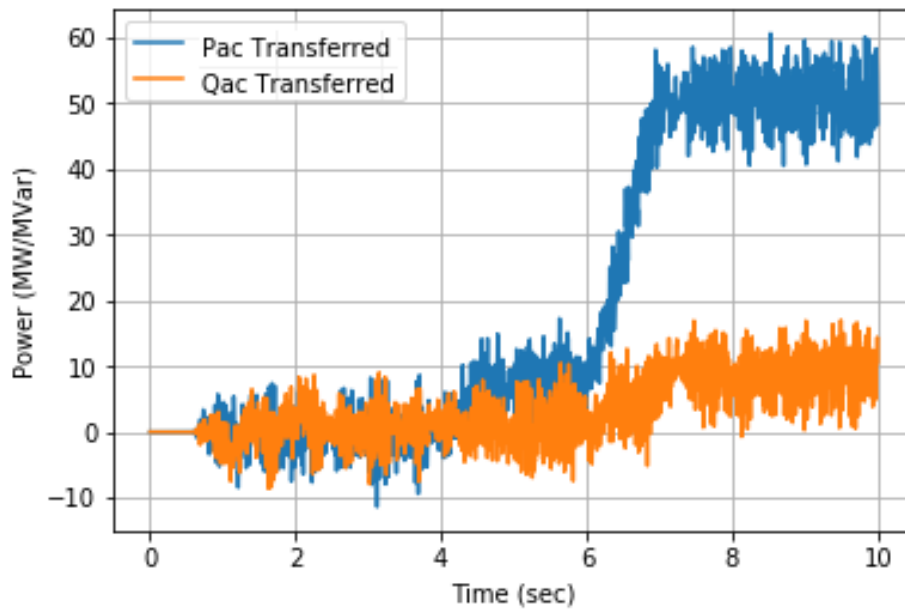


(b) DC currents of top and bottom poles

Figure 7.7: HVDC-link characteristics under controlled ramp down of wind turbines with droop control



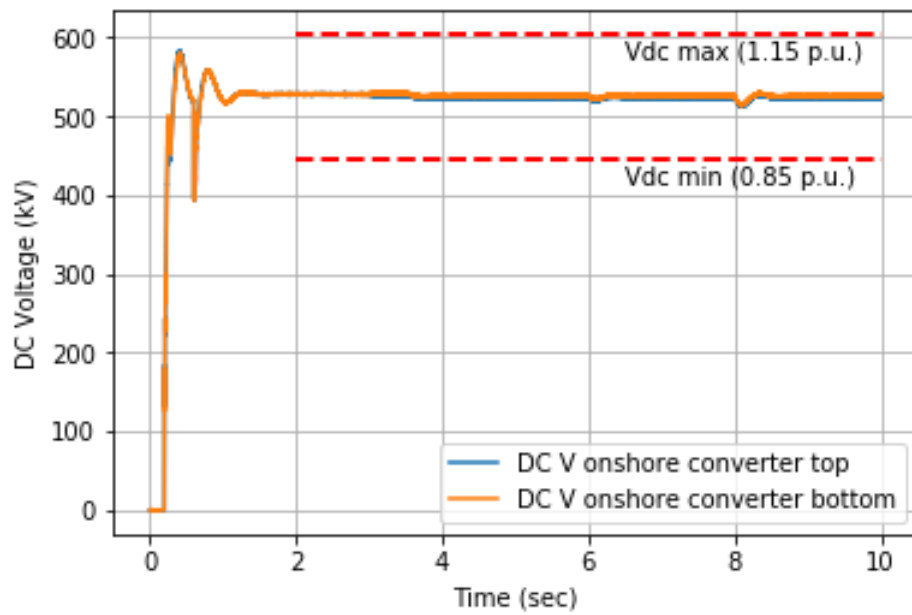
(c) DC voltage of top and bottom offshore poles



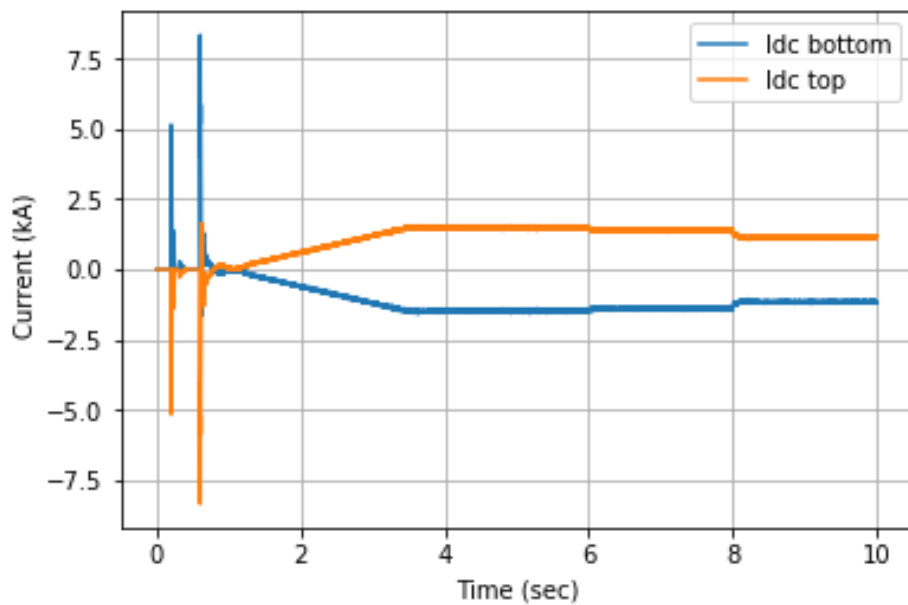
(d) Active and Reactive power transferred between top and bottom poles

Figure 7.7: HVDC-link characteristics under controlled ramp down of wind turbines with droop control

7.2.4. Results: Loss of wind turbines

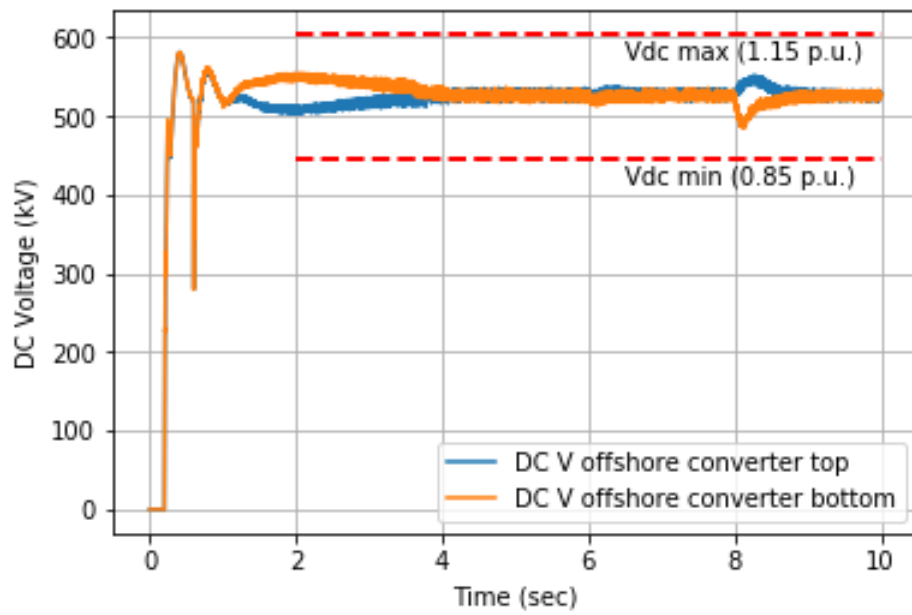


(a) DC voltage of top and bottom onshore poles

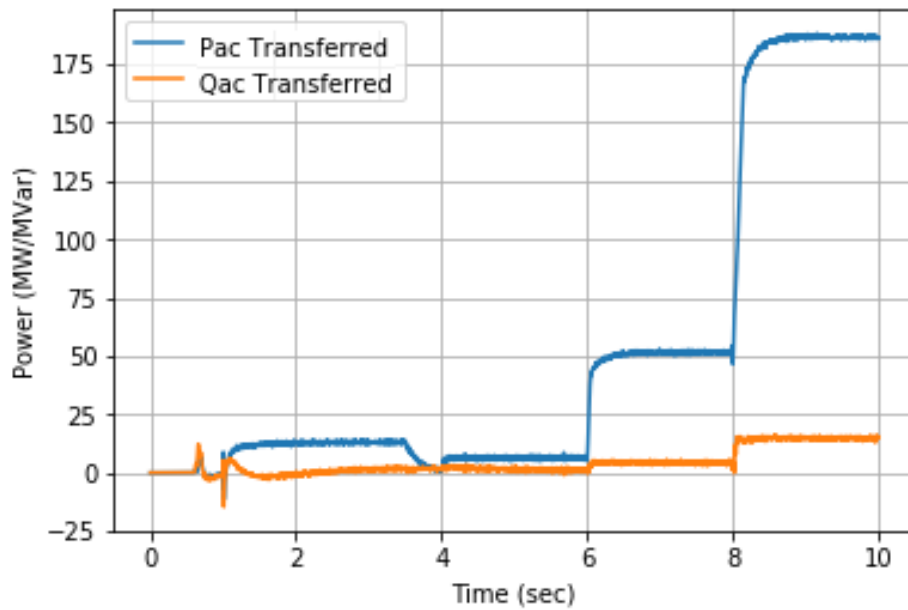


(b) DC currents of top and bottom poles

Figure 7.8: HVDC-link characteristics under loss of wind turbines with power set points control

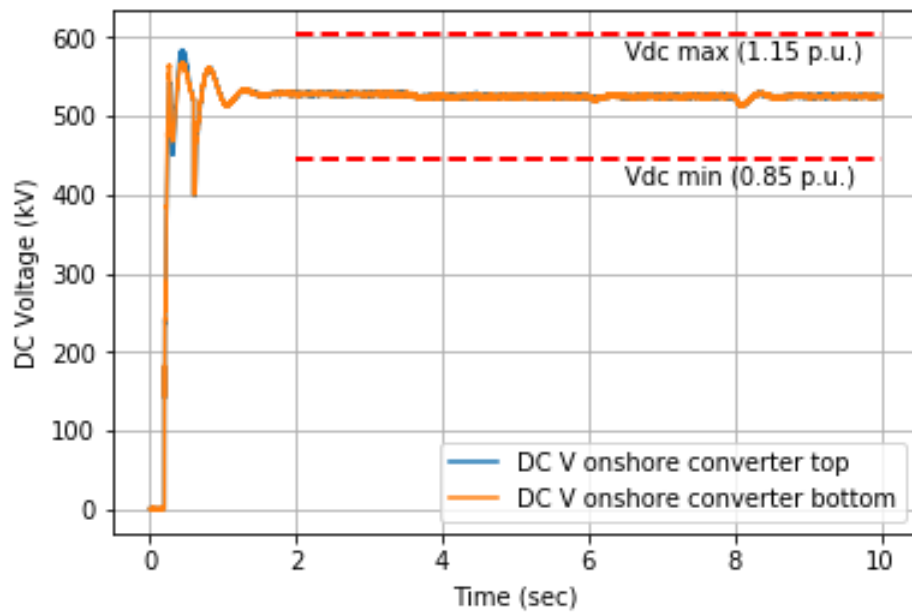


(c) DC voltage of top and bottom offshore poles

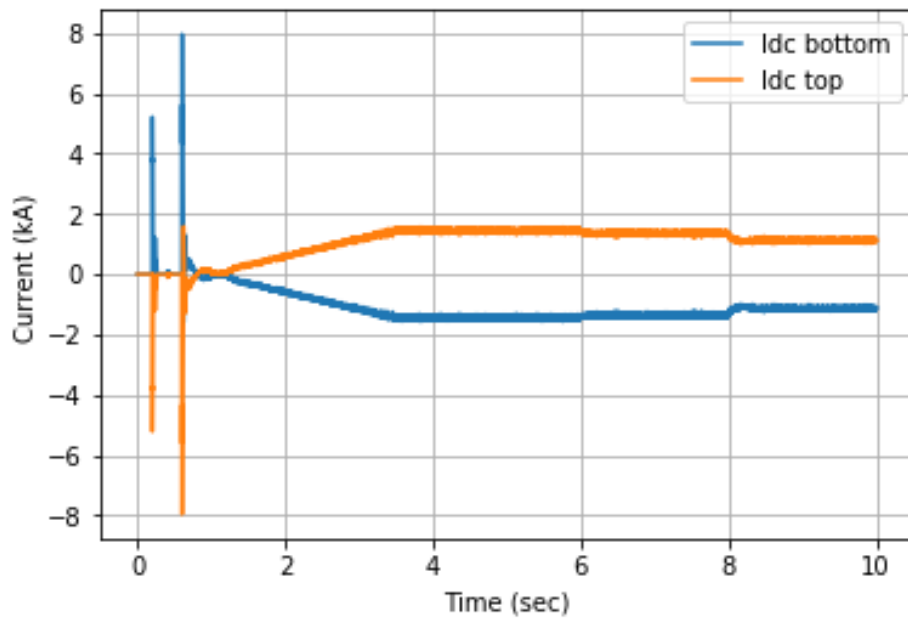


(d) Active and Reactive power transferred between top and bottom poles

Figure 7.8: HVDC-link characteristics under loss of wind turbines with power set points control

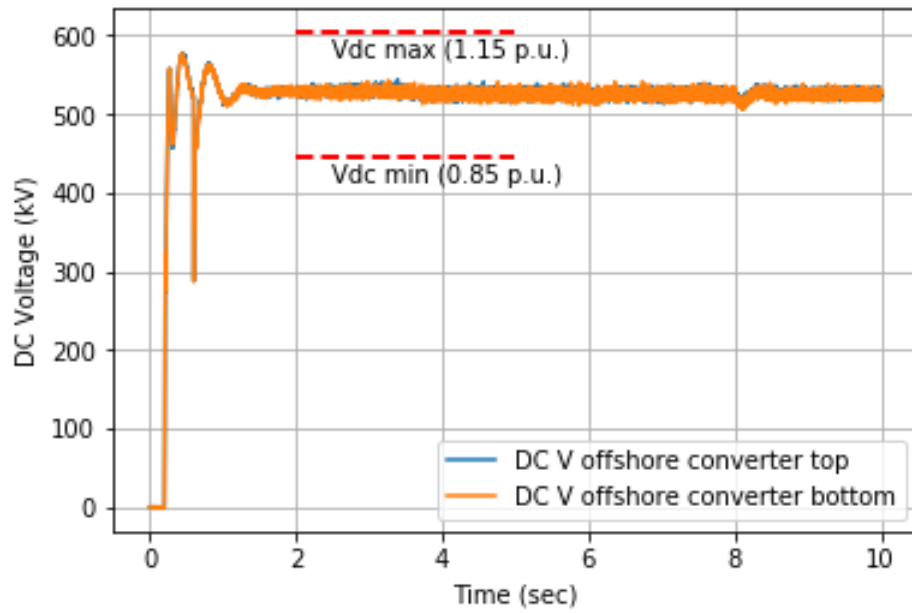


(a) DC voltage of top and bottom onshore poles

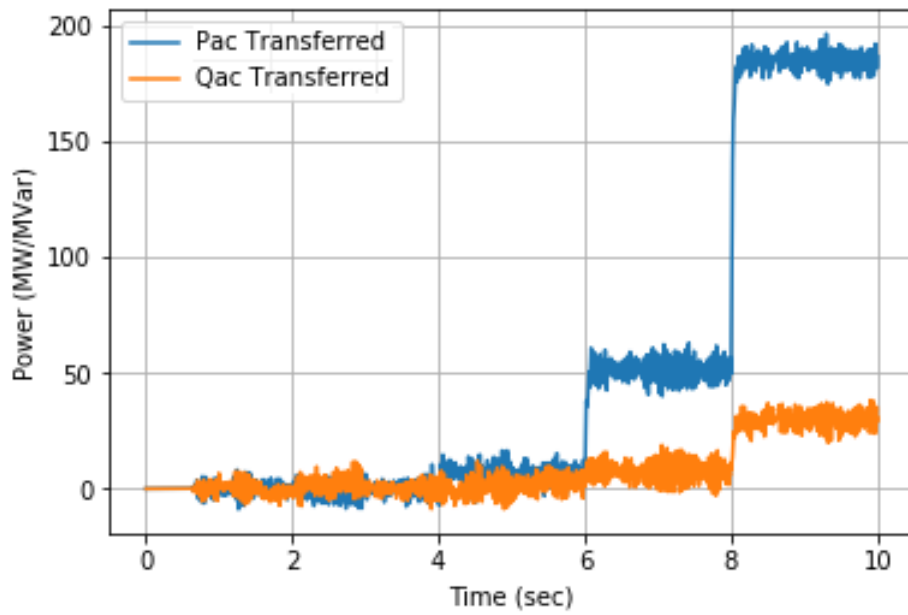


(b) DC currents of top and bottom poles

Figure 7.9: HVDC-link characteristics under loss of wind turbines with droop control



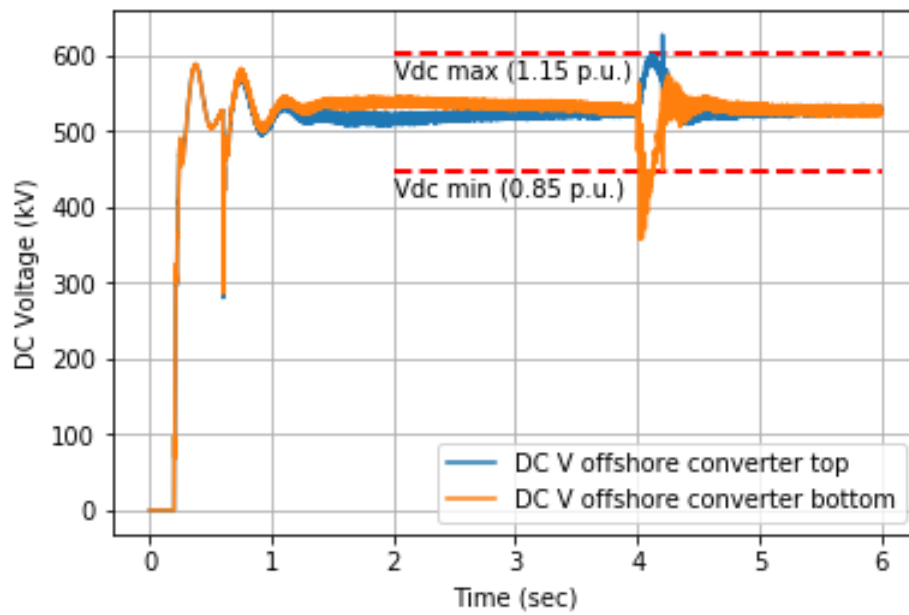
(c) DC voltage of top and bottom offshore poles



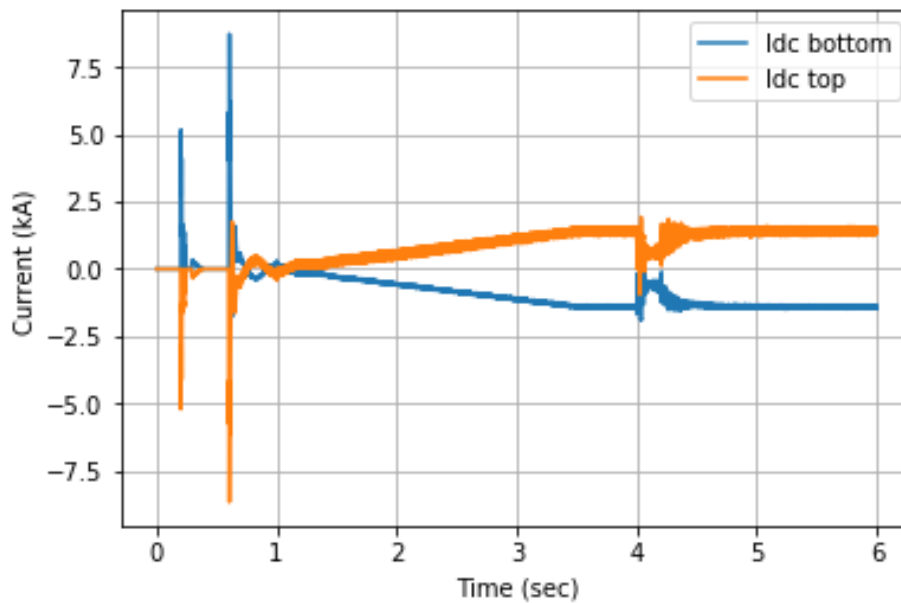
(d) Active and Reactive power transferred between top and bottom poles

Figure 7.9: HVDC-link characteristics under loss of wind turbines with droop control

7.2.5. Results: Fault in the cable connecting wind farm and converter

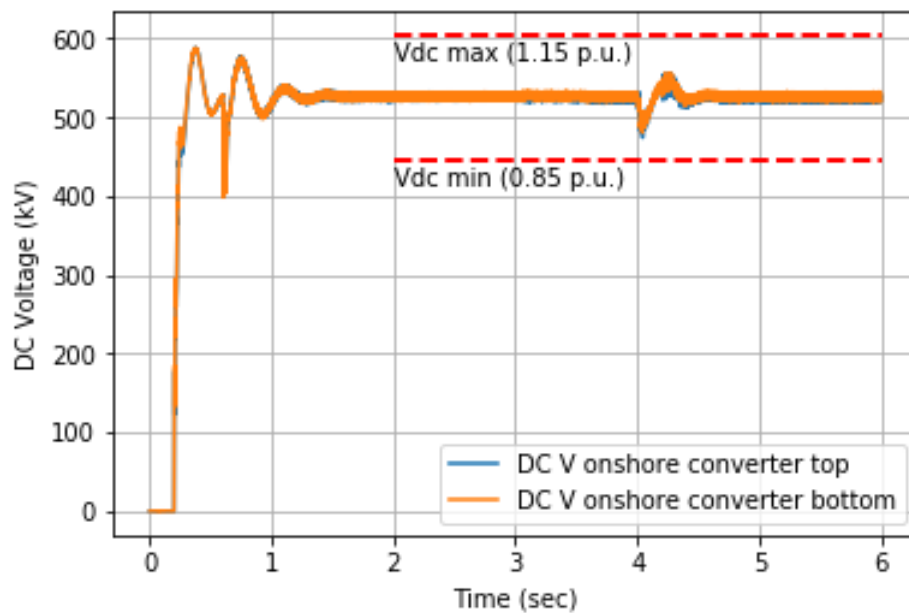


(a) DC voltage of top and bottom onshore poles

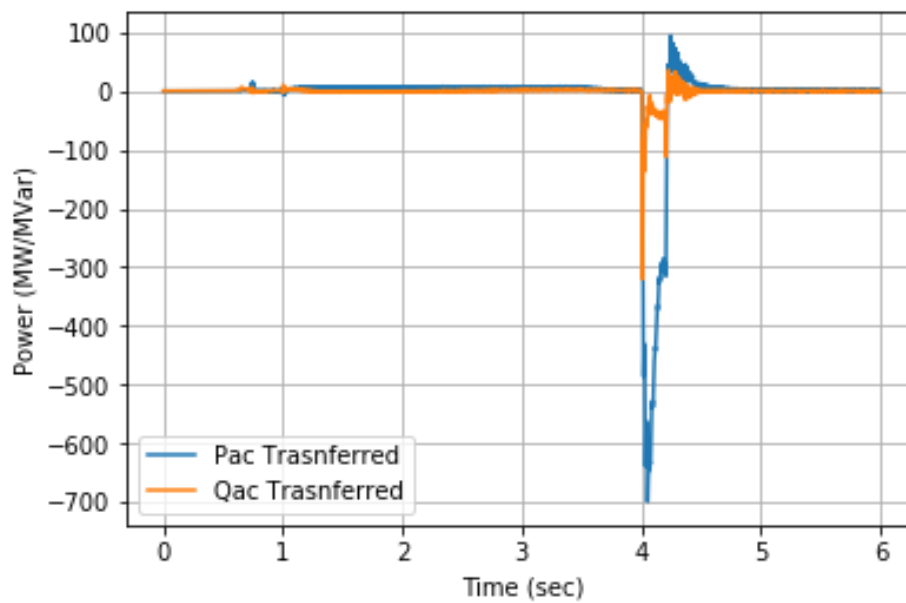


(b) DC currents of top and bottom poles

Figure 7.10: HVDC-link characteristics under fault in the cable connecting top OWPP and converter with power set points control

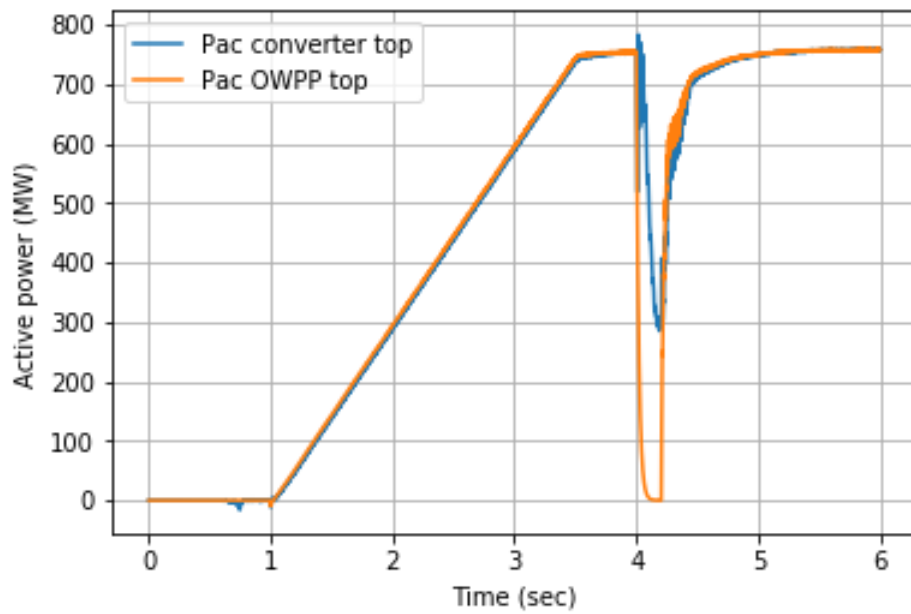


(c) DC voltage of top and bottom offshore poles

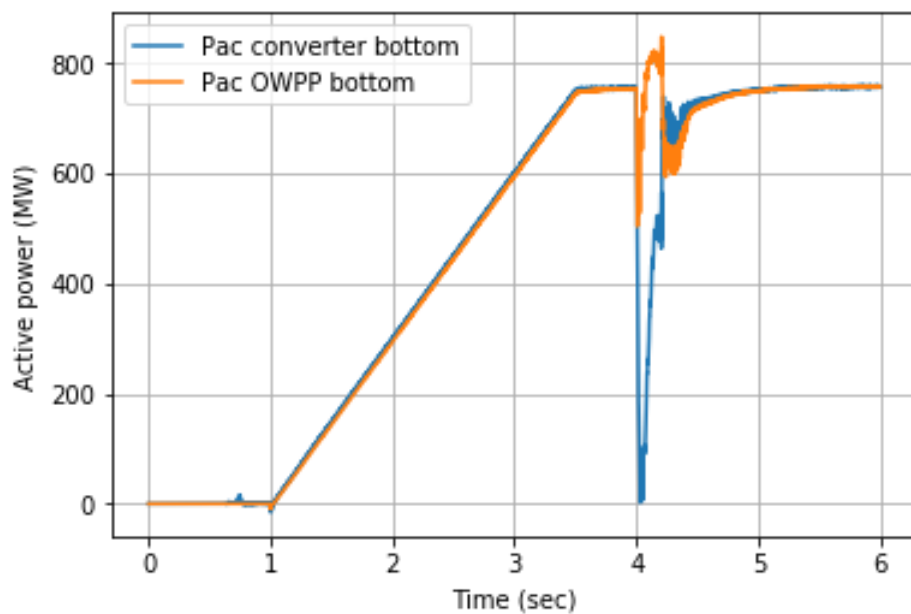


(d) Active and Reactive power transferred between top and bottom poles

Figure 7.10: HVDC-link characteristics under fault in the cable connecting top OWPP and converter with power set points control

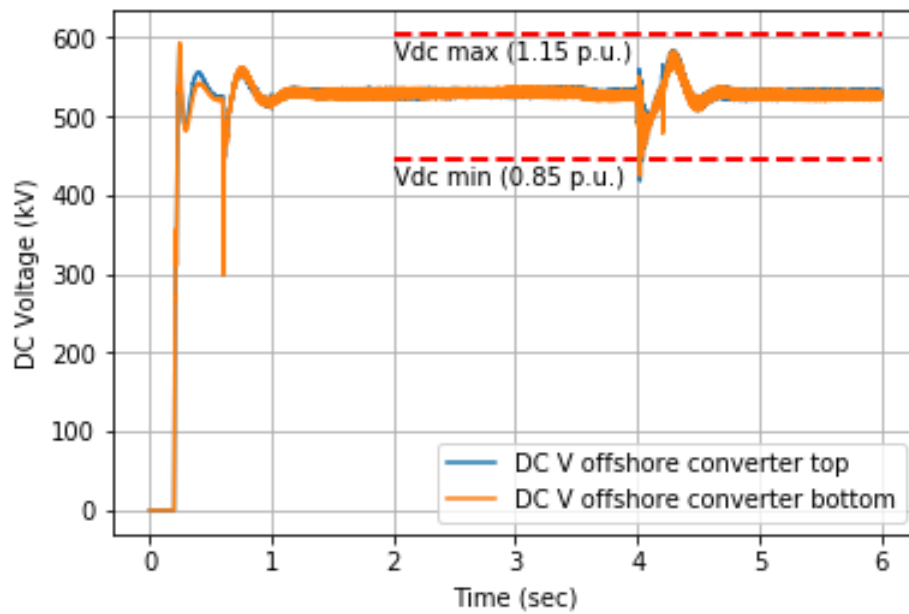


(e) Active power loading of top OWPP and converter

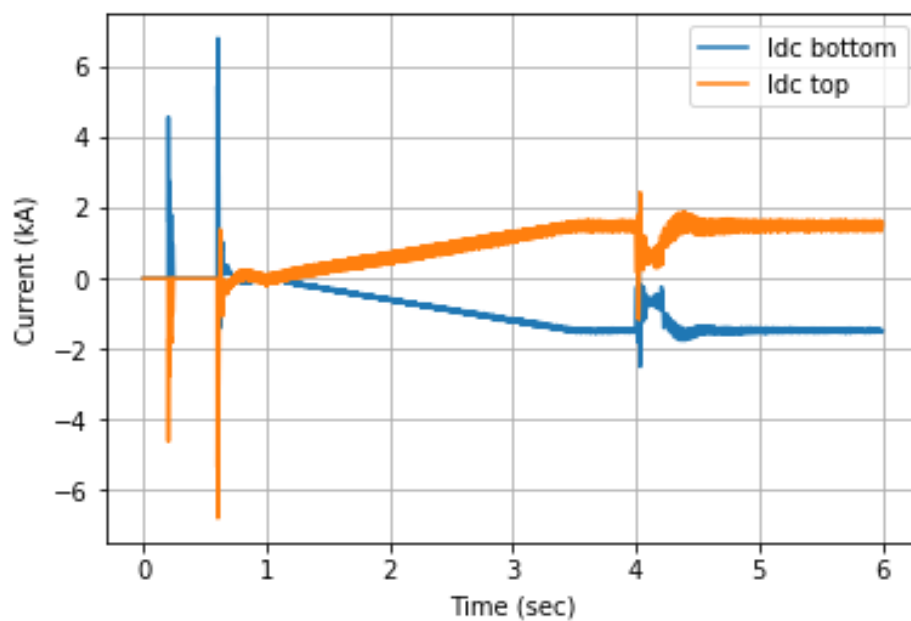


(f) Active power loading of bottom OWPP and converter

Figure 7.10: HVDC-link characteristics under fault in the cable connecting top OWPP and converter with power set points control

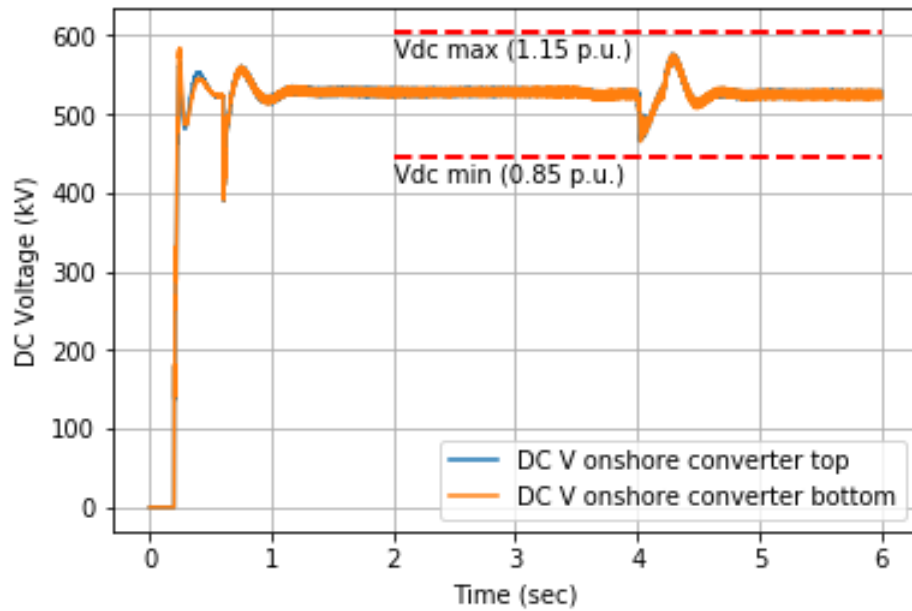


(a) DC voltage of top and bottom onshore poles

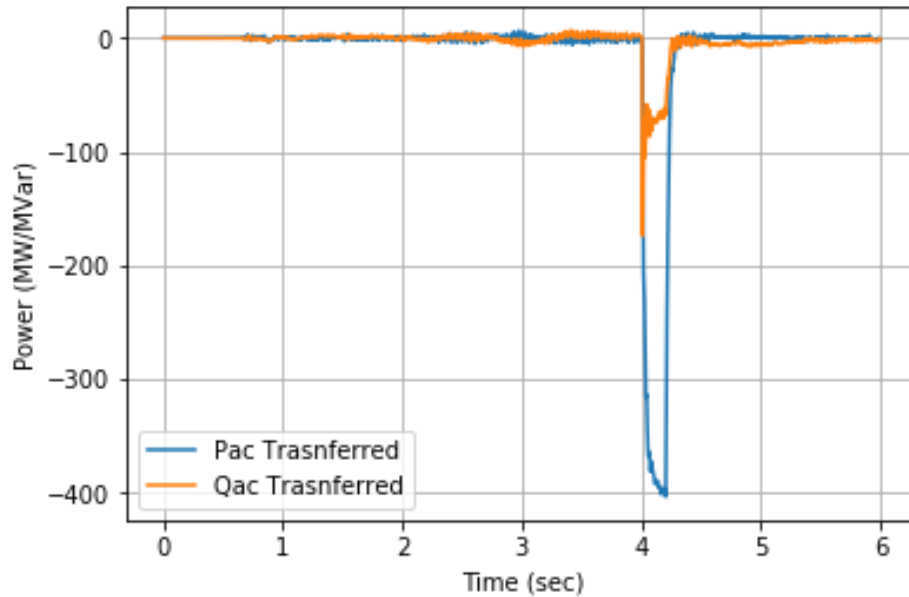


(b) DC currents of top and bottom poles

Figure 7.11: HVDC-link characteristics under fault in the cable connecting top OWPP and converter with droop control

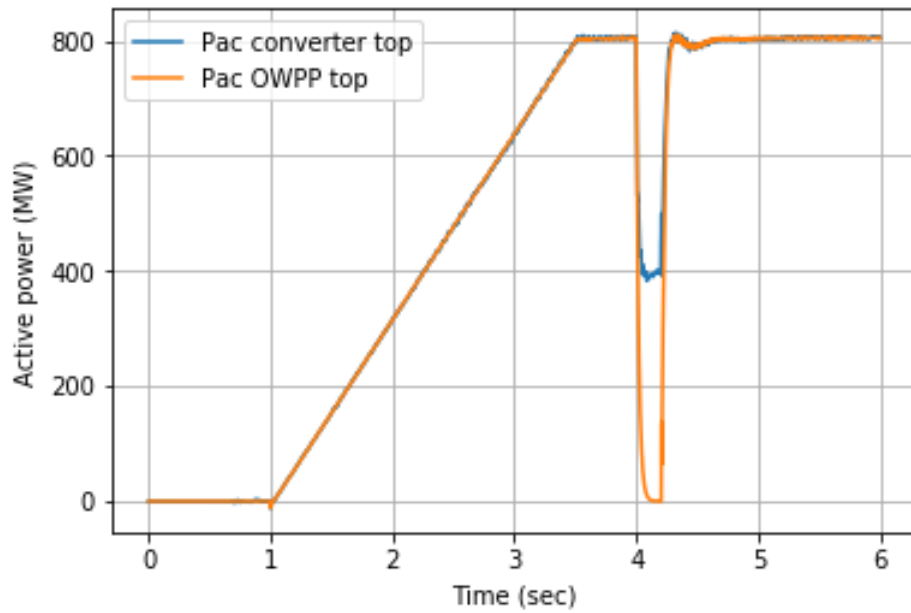


(c) DC voltage of top and bottom offshore poles

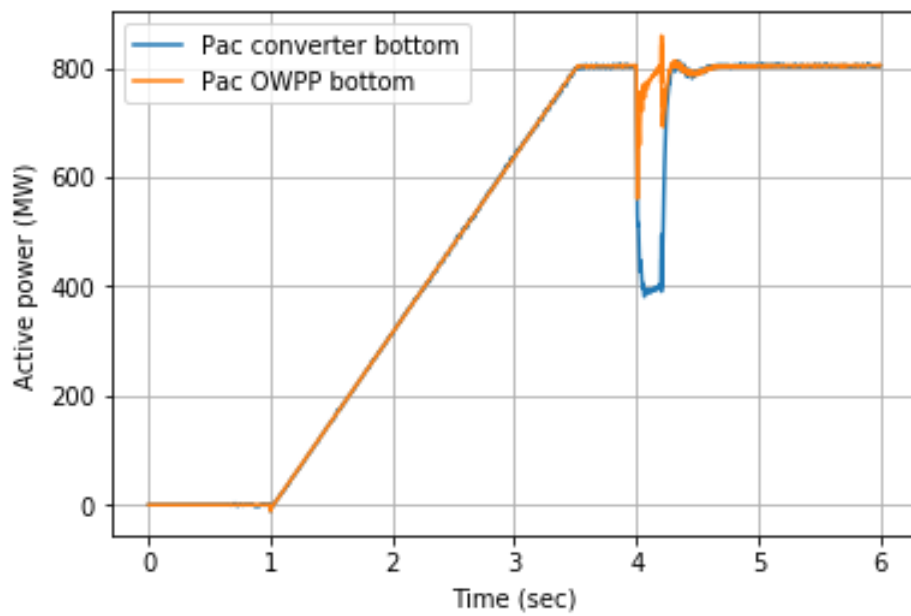


(d) Active and Reactive power transferred between top and bottom poles

Figure 7.11: HVDC-link characteristics under fault in the cable connecting top OWPP and converter with droop control



(e) Active power loading of top OWPP and converter



(f) Active power loading of bottom OWPP and converter

Figure 7.11: HVDC-link characteristics under fault in the cable connecting top OWPP and converter with droop control

Bibliography

- [1] J.-Y. Son and K. Ma, "Wind energy systems," *Proceedings of the IEEE*, vol. 105, no. 11, pp. 2116–2131, Nov. 2017. [Online]. Available: <https://doi.org/10.1109/jproc.2017.2695485>
- [2] M. P. Bahrman and B. K. Johnson, "The abcs of hvdc transmission technologies," *IEEE Power and Energy Magazine*, vol. 5, no. 2, pp. 32–44, 2007.
- [3] O. H. M. Callavik, P. Lundberg, "Nordlink pioneering vsc-hvdc interconnector between norway and germany," 03 2015.
- [4] C. Hirsching, M. Goertz, S. Wenig, S. Beckler, M. Suriyah, and T. Leibfried, "On control and balancing of mmc-hvdc links in rigid bipolar configuration," in *15th IET International Conference on AC and DC Power Transmission (ACDC 2019)*, 2019, pp. 1–6.
- [5] K. Sharifabadi, *Design, control and application of modular multilevel converters for HVDC transmission systems*. Chichester, West Sussex, United Kingdom: John Wiley & Sons, Inc, 2016.
- [6] N. Flourentzou, V. Agelidis, and G. Demetriades, "VSC-based HVDC power transmission systems: An overview," *IEEE Transactions on Power Electronics*, vol. 24, no. 3, pp. 592–602, Mar. 2009. [Online]. Available: <https://doi.org/10.1109/tpel.2008.2008441>
- [7] D. M. Larruskain, I. Zamora, O. Abarategui, and A. Iturregi, "VSC-HVDC configurations for converting AC distribution lines into DC lines," *International Journal of Electrical Power & Energy Systems*, vol. 54, pp. 589–597, Jan. 2014. [Online]. Available: <https://doi.org/10.1016/j.ijepes.2013.08.005>
- [8] N. Flourentzou, V. G. Agelidis, and G. D. Demetriades, "Vsc-based hvdc power transmission systems: An overview," *IEEE Transactions on Power Electronics*, vol. 24, no. 3, pp. 592–602, 2009.
- [9] S. D. Boeck, P. Tielens, W. Leterme, and D. V. Hertem, "Configurations and earthing of HVDC grids," in *2013 IEEE Power & Energy Society General Meeting*. IEEE, 2013. [Online]. Available: <https://doi.org/10.1109/pesmg.2013.6672808>
- [10] J. Rocabert, A. Luna, F. Blaabjerg, and P. Rodríguez, "Control of power converters in ac microgrids," *IEEE Transactions on Power Electronics*, vol. 27, no. 11, pp. 4734–4749, 2012.
- [11] O. Oni, K. Mbangula, and I. Davidson, "A review of lcc-hvdc and vsc-hvdc technologies and applications," *Transactions on Environment and Electrical Engineering*, vol. 1, 09 2016.
- [12] J. N. Sakamuri, Göksu, A. Bidadfar, O. Saborío-Romano, A. Jain, and N. A. Cutululis, "Black start by hvdc-connected offshore wind power plants," vol. 1, pp. 7045–7050, Oct 2019.
- [13] A. Gkountaras, S. Dieckerhoff, and T. Sezi, "Evaluation of current limiting methods for grid forming inverters in medium voltage microgrids," in *2015 IEEE Energy Conversion Congress and Exposition (ECCE)*, 2015, pp. 1223–1230.

- [14] E. Prieto-Araujo, F. D. Bianchi, A. Junyent-Ferre, and O. Gomis-Bellmunt, "Methodology for droop control dynamic analysis of multiterminal VSC-HVDC grids for offshore wind farms," *IEEE Transactions on Power Delivery*, vol. 26, no. 4, pp. 2476–2485, Oct. 2011. [Online]. Available: <https://doi.org/10.1109/tpwr.2011.2144625>
- [15] W. Wang, M. Barnes, and O. Marjanovic, "Droop control modelling and analysis of multi-terminal vsc-hvdc for offshore wind farms," in *10th IET International Conference on AC and DC Power Transmission (ACDC 2012)*, Dec 2012, pp. 1–6.
- [16] R. E. Torres-Olguin, A. R. Årdal, H. Støylen, A. G. Endegnanew, K. Ljøkelsøy, and J. O. Tande, "Experimental verification of a voltage droop control for grid integration of offshore wind farms using multi-terminal HVDC," *Energy Procedia*, vol. 53, pp. 104–113, 2014. [Online]. Available: <https://doi.org/10.1016/j.egypro.2014.07.219>
- [17] T. Vrana, L. Zeni, and O. Fosso, "Active power control with undead-band voltage frequency droop for hvdc converters in large meshed dc grids," 08 2011.
- [18] C. Bajracharya, M. Molinas, J. Suul, and T. Undeland, "Understanding of tuning techniques of converter controllers for vsc-hvdc," 06 2008.
- [19] *Guide for the development of models for HVDC converters in a HVDC grid, TB604*. Paris: CIGRE, 2014.
- [20] M. C. Chandorkar, D. M. Divan, and R. Adapa, "Control of parallel connected inverters in standalone ac supply systems," *IEEE Transactions on Industry Applications*, vol. 29, no. 1, pp. 136–143, 1993.
- [21] A. ENGLER, "Applicability of droops in low voltage grids," *Int. Journal of Distributed Energy Resources*, 2005. [Online]. Available: <https://ci.nii.ac.jp/naid/10024343414/en/>
- [22] G. J. Anders, *Rating of Electric Power Cables: Ampacity Computations for Transmission, Distribution, and Industrial Applications*. McGraw-Hill Professional, nov 1997.
- [23] S. Lumbreras and A. Ramos, "Offshore wind farm electrical design: A review," *Wind Energy*, vol. 16, pp. –473, 04 2013.
- [24] Tennet, "66 kv systems for offshore wind farms," *DNV GL – Report No. 113799-UKBR-R02*, 03 2015.